HYDROGEOLOGICAL INVESTIGATION OF THE CHRISTCHURCH CITY AQUIFER

A thesis submitted in partial fulfilment of the

requirements for the degree of

Master of Science in Environmental Science

in the University of Canterbury

by Logan Brian McLean

University of Canterbury

2018

ACKNOWLEDGEMENTS

Firstly, I would like to thank my supervisors Dr Lee Burbery and Dr Leanne Morgan. Your assistance throughout the project ranging from commenting on my writing, to the more technical aspects was appreciated. Groundwater modelling was new to me when I started this project, and I now feel significantly upskilled in this subject.

Thank you to all the technical staff. In particular, Phillip Abraham for assisting with the slug tests, and for staying composed when the battery in the Hilux went flat out at the site. Also, thanks to Nicole van de Weerd and Siale Faitotonu for access to the lab and teaching me how to conduct a particle size distribution.

I would also like to thank Suellen Knopick and the Waterways Centre for Freshwater Management for hosting me while I undertook the research.

Finally, thanks to my parents Scott and Anne for your support throughout my studies, and for flying me home every few months for a break from student life.

ABSTRACT

The Christchurch City aquifer is a coastal groundwater system, consisting of a sequence of terrestrial and marine hydro-stratigraphic units. It is recharged from the west, by groundwater and surface-water that passes through agricultural land before reaching the groundwater reserves beneath Christchurch or discharging into coastal springs. Critical understanding of the aquifer system's hydrogeological properties can help develop an understanding of potential groundwater flow, and aid in the effective management and utilisation of this groundwater resource.

The principal aim of this thesis is to establish a vertical profile of hydraulic conductivity in an extension to the Christchurch City aquifer system about Kaiapoi by utilising an array of multi-tier wells installed across two sites. Additionally, this thesis will incorporate an examination of model complexity by evaluating the range of methods used to achieve the principal aim.

Initially, aquifer sediments extracted from boreholes at the field sites were analysed for particle size distribution. A range of empirical models were then applied to the data to obtain hydraulic conductivity estimates. The results showed great variation between the range of empirical models, signifying the large margins of error associated with the modelling approach. This method produced the least reliable results in this study.

Following this, slug tests were conducted on the multi-tier wells at both sites. Analytical and numerical models were applied to the slug test data to obtain hydraulic conductivity estimates. These two modelling approaches yielded similar results. However, the numerical model results are considered more reliable as the method requires the least amount of assumptions and simplifications and allows a more accurate representation of the wells construction and boundary conditions.

Overall, variation in hydraulic conductivity both vertically and horizontally between the two sites illustrated the heterogeneous nature of the aquifer system. Additionally, the system was found to be highly conductive.

TABLE OF CONTENTS

LIST OF TABLES

LIST OF FIGURES

Chapter 1. INTRODUCTION

1.1 Project background

The Canterbury region is located on the South Island of New Zealand, stretching between the main divide of the Southern Alps and the east coast. Christchurch is the second largest city in New Zealand, and provincial capital of Canterbury region. Fertile soils and flat topography across the Canterbury Plains have encouraged large scale agricultural intensification, resulting in what is now a highly productive agricultural region. Canterbury hosts approximately two thirds of all irrigated land in New Zealand (Dark et al., 2017). Much of the required irrigation water is sourced from rivers and is supplied to farms via large distribution systems. Nonetheless, groundwater has become the preferred choice for public and agricultural supply due to its good quality, reliability and availability across the region (Brown & Weeber, 2002). The Greater Christchurch area (Figure 1-1), represents an urban – rural environment, where water resources are shared by farmers, as well as the dense population of the coastal city. Surface-water and groundwater flows eastwards from the foothills to the coast, passing first through agricultural land before reaching Christchurch. Thus, any resulting contamination of the water system from agriculture can propagate downstream to affect water quality in spring-fed lowland streams and possibly the groundwater resource for Christchurch city.

Figure 1-1. Greater Christchurch area in the South Island of New Zealand

It is estimated that approximately 97% of liquid freshwater potentially available for human use is in the form of groundwater (Sarath Prasanth et al., 2012). Although groundwater is a large resource, it is a vulnerable one. Groundwater flows at very slow rates in comparison to rivers and streams. The velocities are orders of magnitude less. Because of this, contaminants do not simply flush away, and instead can remain in the system for long periods of time. Nitrate contamination is a major water quality issue occurring in regions of intensive agriculture (Trevis, 2012). As defined by the Ministry of Health (2008) drinking water standards, nitrate has a maximum acceptable value (MAV) of 50 mg/L. This equates to 11.3 mg/L nitrate-nitrogen, which refers to the mass of nitrogen in the

nitrate anion. In 2016, 7% of wells measured in the Canterbury annual groundwater quality survey had nitrate levels exceeding the MAV (Hanson, 2016).

The Ashley-Waimakariri Plains are located within the Greater Christchurch area, bound by the Ashley River to the north, and the Waimakariri River to the south. Land-use within this 105,000 ha area is predominantly agricultural, resulting in a significant nitrate input to the groundwater system (Dodson et al., 2012). Groundwater in this area is used for potable water supply and irrigation, and also sustains flows in many lowland spring-fed streams. Regionally low levels of nitrate have been identified in the water in the discharge zone of the plains near the coast (Figure 1-2). This is peculiar given the intensive agriculture occurring upstream. There are two possible explanations for this anomaly:

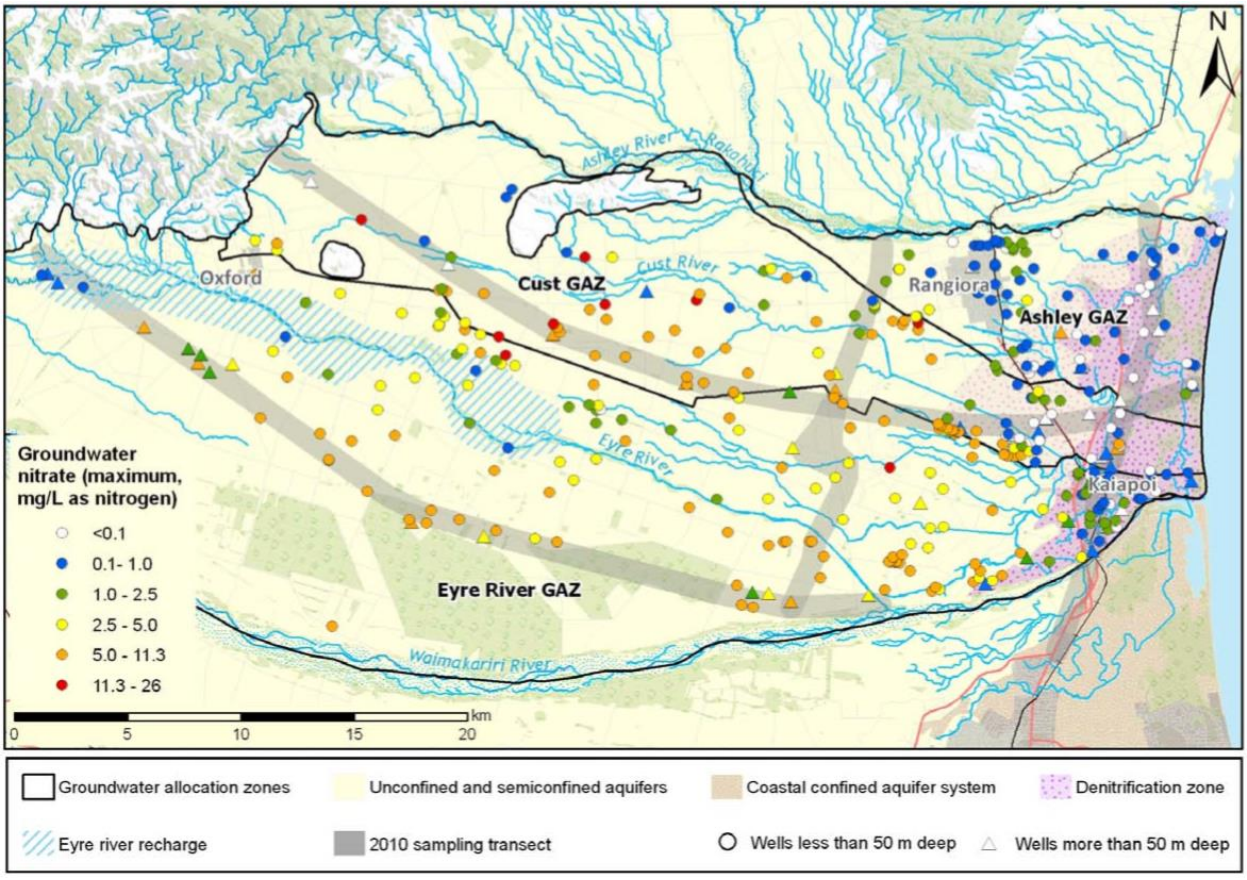

Figure 1-2. Maximum nitrate concentrations expressed as nitrate-nitrogen in groundwater in the Ashley-Waimakariri Plains (Dodson et al., 2012)

1. The water at this location entered the groundwater system prior to the beginning of agricultural intensification in the region, thus avoiding nitrate contamination.
2. The geology in the area is facilitating nitrate reduction reactions, naturally attenuating nitrate in the groundwater.

The latter hypothesis is supported by the prevalence of organic peaty material, which may support microbiological ecosystems involved in denitrification processes. Scientific study of the hydrogeological properties of this groundwater system is required to better understand the fate and transport of nitrate in the coastal spring-fed system north of Christchurch, which is essentially an extension of the Christchurch City aquifer. In particular, the aquifer parameter hydraulic conductivity (K), is one of the most important and useful hydrogeological parameters for groundwater flow/transport investigations (Kasenow & Röhrich, 2001). It is a measure of the rate at which a geologic material can transmit a fluid under a hydraulic gradient (Fetter, 2000), and has dimensions of L/T. The value of hydraulic conductivity is used in equations that govern groundwater flow and velocity. Additionally, aquifer parameters such as transmissivity depend on it.

1.2 Christchurch City aquifer

The Christchurch City aquifer refers to the aquifer system beneath Christchurch including the portion of the Coastal Confined Aquifer System north of Banks Peninsula (Figure 1-3). The coastal area between the Waimakariri River and the Ashley River is included as it represents a natural extension to the aquifer system i.e. the sub-surface geology between Banks Peninsula and the Ashley River was formed from the same depositional processes (Dodson et al., 2012).

The occurrence of groundwater in an aquifer system is dependent on both the depositional, and post-depositional processes that alter the physical form of the grains or the structure of the bedding (Brown & Weeber, 2002). The following literature review

describes the depositional history of the Christchurch City aquifer, and the implications for groundwater flow.

Figure 1-3. Location of the Coastal Confined Aquifer System and the study area

1.2.1 Depositional history

The geological units of concern in the Christchurch City aquifer were all deposited within the Quaternary period (≤ 2.59 Ma BP (Cohen et al., 2013)). The majority of this material is glacial outwash gravel, derived from the mountain catchments to the west (Talbot et al., 1986). Nearer the coast, where this study is being conducted, minor wedges of marine and estuarine units lain during inter-glacial periods intercept the terrestrial gravels (Brown & Weeber, 2002; Talbot et al., 1986; Wilson, 1976). These wedges consist mostly of clay, silt, and sand of lower permeability than the outwash gravel. The low permeability units effectively act to confine the groundwater in the various gravel strata. The result is a succession of aquitards and aquifers, named the “Christchurch artesian system” by Brown & Weeber (2002). The shallowest units within this sequence were named by Suggate (1958). At the top of this sequence is the confining Christchurch Formation, followed by the Riccarton Gravel aquifer, the Bromley Formation, and then the Linwood Gravel aquifer (Figure 1-4). Further inland, the Riccarton Gravel aquifer is unconfined due to the absence of the Christchurch Formation, and is overlain by alluvial sediments known as the Springston Formation aquifer.

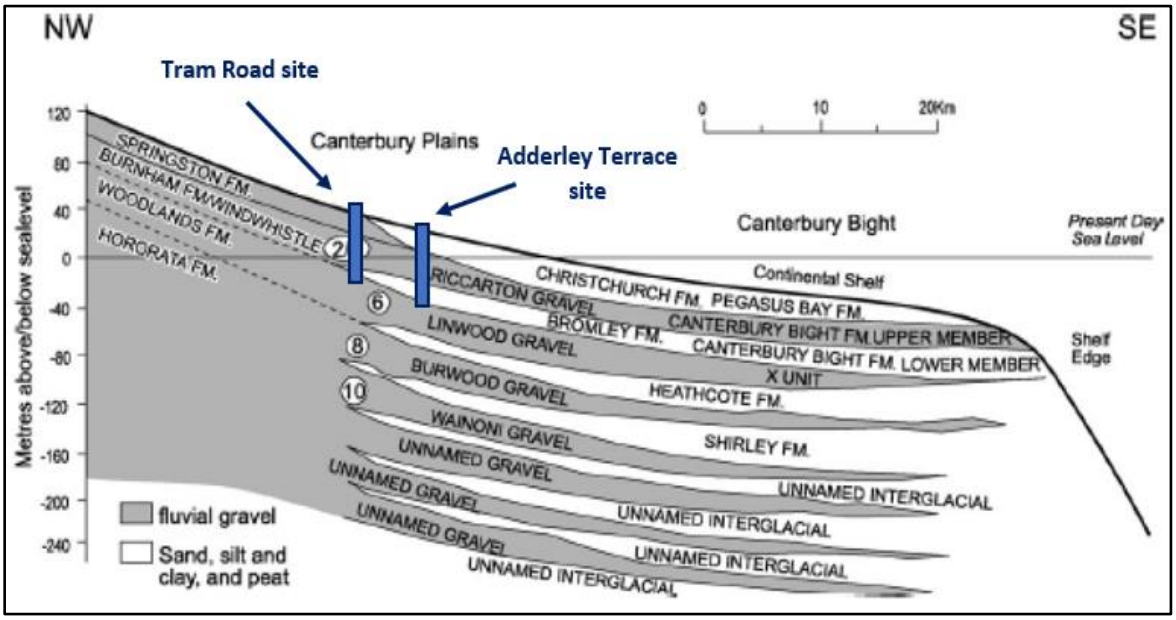

Figure 1-4. Cross section through Central Canterbury at the coast, illustrating the aquifer-aquitard sequence and approximate locations of multi-tier well sites (adapted from Browne & Naish, 2003; after Brown & Weeber, 1992)

This depositional pattern of the study area can be attributed to the glacial-interglacial cycles that occurred during the Quaternary (Brown & Weeber, 2002; Suggate, 1958; Talbot et al., 1986; Wilson, 1976). During glacial periods, the sea level was much lower than the present elevation, with the coastline extending approximately 95 km further east (Talbot et al., 1986). Large alpine rivers transported and deposited Torlesse quartzofeldspathic (greywacke) sediments from the Southern Alps into a basin to the east (Brown & Weeber, 2002). Additionally, tectonic uplift in the west and basin subsidence in the east resulted in inland river entrenchment and aggradation further downstream. During interglacial periods, the sea level rose and migrated westward. The environment was dominated by scrubs, swamps and estuaries, resulting in the deposition of silts, sands, and peat (Talbot et al., 1986). Warmer climate during the interglacial periods allowed for the growth of vegetation at higher altitudes, reducing the rate of erosion. Rivers responded to the lack of debris by entrenching into the floodplains and depositing the sediments downstream (Brown & Weeber, 2002). Therefore, increased erosion and sedimentation is attributed to glacial periods. Subsequent entrenchment and reworking of the fluvial deposits occurs within post-glacial and interglacial periods. The inland extent of the marine deposits represents the historical coastline location. Glacial-interglacial cycles (Figure 1-5) have been repeated many times, leading to the formation of the present-day stratigraphy.

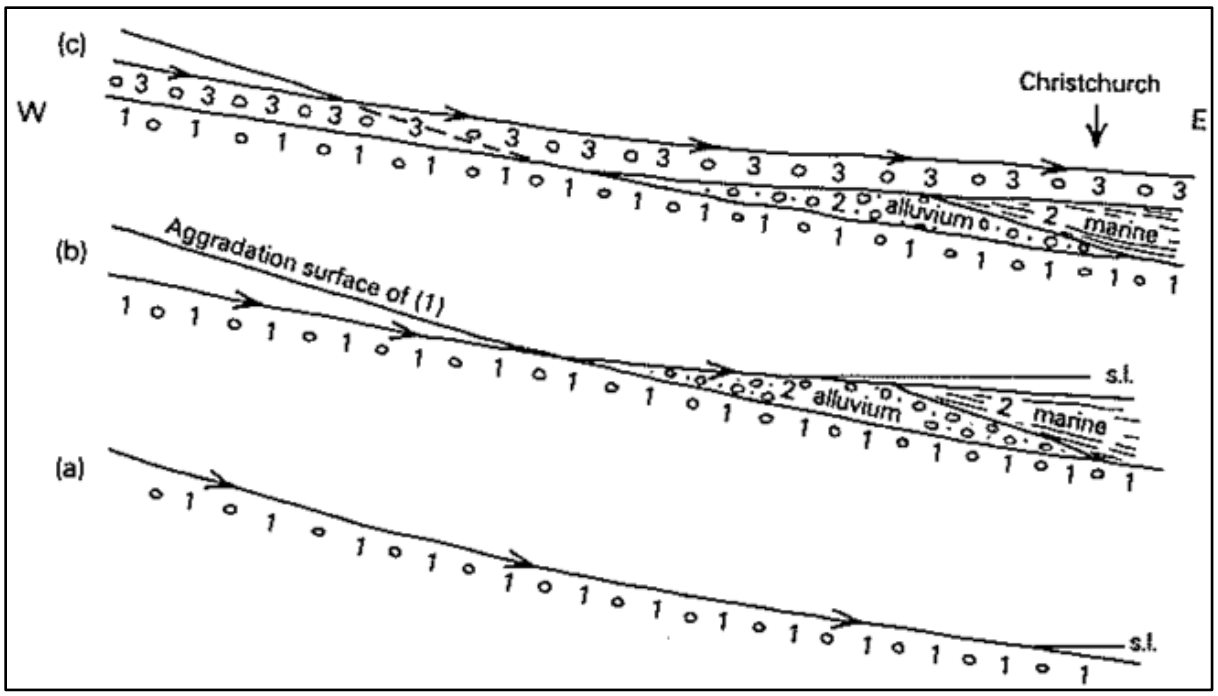

Figure 1-5. Cross sections representing depositional processes through glacial-interglacial cycles (Wilson, 1976).

a) Glacial period: glacial outwash (1) is eroded from the foothills and deposited down to a historically low sea level.

b) Interglacial period: inland river entrenchment and subsequent aggradation downstream resulting in alluvium deposits (2). As the sea level rises, and transgresses westwards, estuarine and marine deposits form on top.

c) Glacial period: as the coastline transgresses eastwards, more glacial outwash (3) is deposited across the plains on top of existing terrestrial, estuarine and marine deposits.

1.2.2. Hydrogeological setting

It is evident from the literature that the fluvial nature of the Plains highly influences groundwater flow paths as the rivers form buried channel conduits and provide a significant source of recharge to the groundwater system. Due to proximity to the study area, the Waimakariri River is the major braided river responsible for deposition of the bulk of outwash material that forms the sub-surface geology in the Christchurch City

aquifer system. A study by Stewart (2012) using oxygen isotopes has discovered that the Waimakariri River is the primary source of recharge for the Christchurch groundwater system, although it is not evident that the river recharges the groundwater system to the north (Dodson et al., 2012). It is also noted that old channels formed by this river are of very high permeability, and act as preferential pathways for groundwater. Brown & Weeber (2002) describe the area on the river profile where river recharge is most likely. This can occur between the intersection point and the knick point; the zone of minimal erosion. The intersection point is the location on the river profile where the river channel intersects with the land surface and a change from entrenchment to aggradation occurs (Hooke, 1967). The knick point is the upper-most point of coastal erosion in the river profile (Brown & Weeber, 2002). Within the zone of minimal erosion is a stretch of riverbed that allows seepage into buried river channels connected to aquifers. In addition, river recharge can occur within the entrenching channel if the river bed intersects a permeable channel.

The depositional processes that formed the Christchurch aquifer system have resulted in heterogeneous hydrogeological properties. Stewart (2012) describes the groundwater flow behaviour as highly variable over short distances. The river systems have contributed significantly to this heterogeneity, as a result of buried channel conduits and the reworking of gravel deposits. The upstream entrenchment and downstream deposition of this material alters the particle size distribution of the deposit (Stewart, 2012). Talbot et al. (1986) agree, also stating that the coastal deposits are of a higher degree of sorting than the inland deposits, which can increase permeability.

Heterogeneity is also present in the coastal confining units. Talbot et al. (1986) noted that gravel channels resulting from river flood events have been mapped within the top coastal confining unit; the Christchurch Formation. It is suggested that these should exist within deeper confining units, thus, vertical leakage between aquifers is likely. This is supported by Stewart (2012), and Wilson (1976) who states that the leakage would occur upwards due to the artesian conditions.

1.3 Study site

In 2016, two sets of multi-tier well clusters were drilled into the top 40 m of the aquifer system. The most inland site is located on Tram Road in Clarkville, with the other on Adderley Terrace in Kaiapoi (Figure 1-4). Each site contains a cluster of five wells that screen discrete sections of the hydro-stratigraphic units. These wells provide a useful means for examining the difference in hydrogeological and biogeochemical properties of the various hydro-stratigraphic units that make up the stratified Christchurch aquifer system.

The Tram Road site is situated adjacent to the Kaiapoi River, on the periphery of the coastal confined aquifer system, and represents the coastal extent of the Springston Formation alluvial gravel aquifer. The boreholes also penetrate the Riccarton Gravel, the Bromley Formation and the top of the Linwood Gravel, which are present at both sites. The top two geological units form one single aquifer unit. The Adderley Terrace site is situated adjacent to the Kaiapoi River further downstream, within the coastal confined aquifer system. Here, the Springston Formation is absent, and the Riccarton Gravel aquifer is confined by the Christchurch Formation. This confining unit pinches out at some point between the two sites. The sites including the well clusters are displayed in Figures 1-6a and 1-6b.

The Institute of Environmental Science and Research Limited have logged sediments from each of the boreholes, which are filed in the local regional council (Environment Canterbury) well database. These bore logs provide geological descriptions of the sediments which offer supporting material in the characterisation of the local aquifer system and offer initial insight into potential groundwater flow properties. The deepest bore log from each site is located in Appendix A. Environment Canterbury uses a naming system for all wells filed in their database. However, the well ID's referred to in this thesis differ. Table 1-1 correlates these well ID's to the Environment Canterbury well ID's and the hydro-stratigraphic units that they screen. The wells were drilled so that they screen similar depths at each site. Wells of corresponding screen depths are paired together in the table.

Figure 1-6a. Multi-tier well cluster at Tram Road, Clarkville

Figure 1-6b. Multi-tier well cluster at Adderley Terrace, Kaiapoi

Table 1-1. Well ID's and details of screened sections. Site elevation is 9.16 m and 2.65 m above mean sea level for Tram Road and Adderley Terrace respectively.

Tram Road					**Adderley Terrace**			
Well ID	ECAN Well ID	Hydro-stratigraphic unit targeted	Screen depth (m bgl)		Well ID	ECAN Well ID	Hydro-stratigraphic unit targeted	Screen depth (m bgl)
NB3	BW24/0344	Springston Formation	2 – 3		AT5	BW24/0341	Christchurch Formation	1.5 – 2.5
NB4	BW24/0345	Contact: Springston Formation / Riccarton Gravel	7.8 – 8.3		AT4	BW24/0340	Top of Riccarton Gravel	8.4 – 8.9
NB2	BW24/0343	Riccarton Gravel	19.7 – 20.2		AT3	BW24/0339	Riccarton Gravel	25.1 – 25.6
NB5	BW24/0346	Base of Bromley Formation/top of Linwood Gravel	33 – 33.5		AT2	BW24/0338	Base of Bromley Formation / top of Linwood Gravel	33.4 – 33.9
NB1	BW24/0342	Linwood Gravel	38.5 - 39		AT1	BW24/0337	Linwood Gravel	35 – 35.5

1.3.1 Well construction

Sonic drilling, a technique which utilises a vibrating and rotating drill head, was used to drill the 125 mm diameter boreholes. This method allows for accurate sediment core retrieval. The wells were constructed with 50 mm diameter PVC pipes, with slotted screen lengths of 0.5 m for all wells except NB3 and AT5 (Figure 1-7). These wells screen the water table and have 1 m screen lengths. The annulus between the well screen and the edge of the borehole was infilled with 2 mm diameter sand filter pack and topped with a 1 mm diameter blinding sand and bentonite grout seal. The filter pack extended from 100 m below the well screen to 100 m above it.

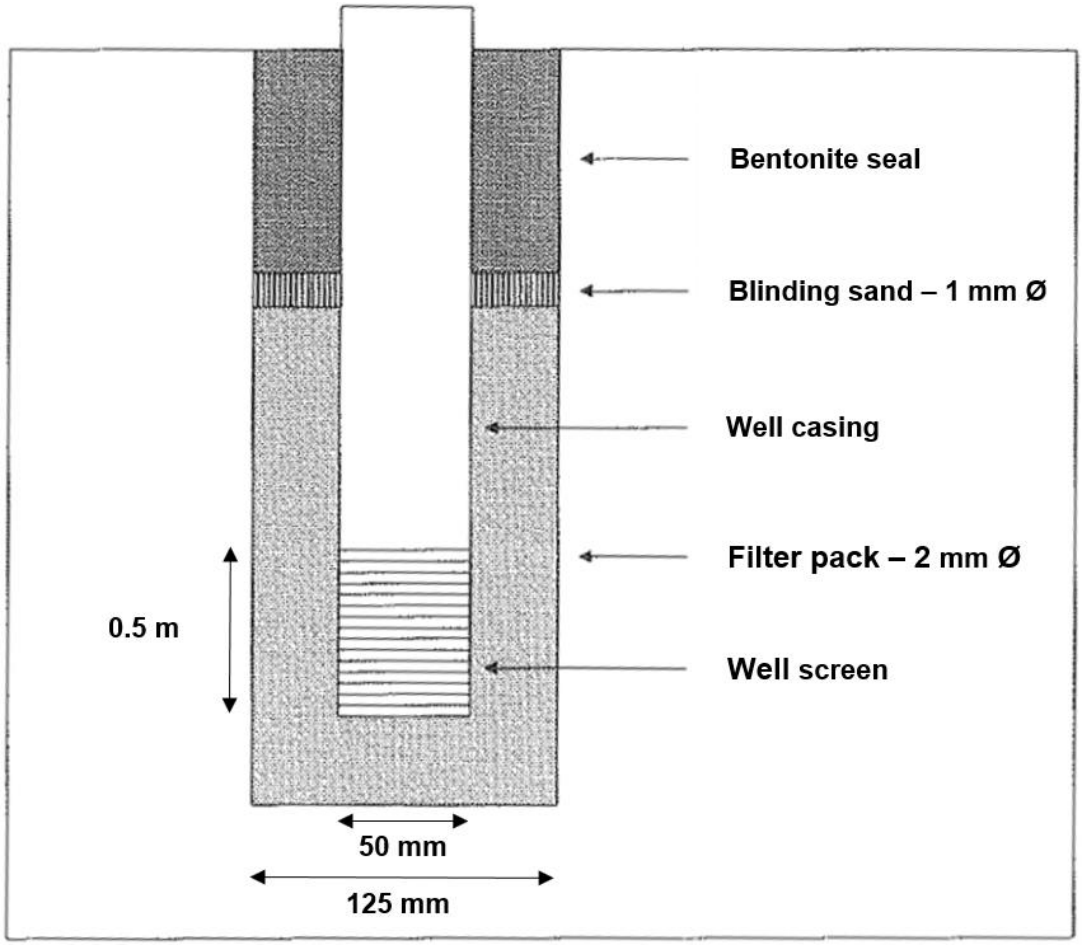

Figure 1-7. Cross section illustrating well construction components. Note. Diagram not to scale.

1.4 Research aim and objectives

This thesis makes use of the multi-tier well arrays installed at Tram Road and Adderley Terrace. The aim is to establish a vertical hydrogeological profile of the top 40 m of the aquifer system north of Christchurch, by making hydraulic conductivity estimates, using a range of methods. Such knowledge is useful for developing an improved understanding of potential groundwater movement through the extension of the Christchurch City aquifer system at and near Kaiapoi. In the future, this might constrain groundwater flow/transport models of the local system and assist with contaminant studies. A goal is to apply different methods to estimate hydraulic conductivity to cater for uncertainty in the various approaches. The methods used to estimate hydraulic conductivity will be compared and evaluated to provide recommendations based on reliability and viability to the study. Additionally, this thesis will incorporate an examination of model complexity as applicable to single-well test methods for examining hydraulic conductivity. The objectives of the thesis are as follows:

1) Conduct a particle size distribution analysis of bulk sediment samples taken from screened sections of wells.
2) Determine hydraulic conductivity estimates based on empirical modelling of particle size distribution data.
3) Conduct direct in-situ slug tests on multi-tier wells.
4) Determine hydraulic conductivity estimates based on analytical modelling of slug test data.
5) Determine hydraulic conductivity estimates based on numerical modelling of slug test data.

Chapter 2. PARTICLE SIZE ANALYSIS

2.1 Introduction

Empirical relationships have been established between a materials particle size distribution and hydraulic conductivity. Thus, the availability of sediment cores from both the Tram Road and Adderley Terrace sites meant that there was an opportunity to gain initial hydraulic conductivity estimates. The sediment cores were extracted from the two second deepest boreholes, NB5 and AT2, which screen the base of the Bromley Formation. Representative samples were extracted from these sediment cores at depths that correspond to the well screen depths of each surrounding well in the cluster. Hydraulic conductivity estimates obtained from empirical models will assist in achieving the aim of the thesis i.e. to create a vertical profile hydraulic conductivity in an extension to the Christchurch City aquifer and evaluate the different methods used to achieve this.

There are a range of empirical models that have been evaluated by various authors. The results of which are often compared with those obtained from hydraulic tests such as slug tests and pump tests (Svensson, 2014). Within this literature review, selected studies will be analysed to determine the propriety of using particle size analysis to estimate hydraulic conductivity. Additionally, areas of contention will be identified.

2.1.1 Benefits and limitations of using particle size distribution analysis to estimate hydraulic conductivity

In-situ hydraulic tests such as slug tests and pumping tests are common methods used for the determination of hydraulic conductivity. However, these tests can be expensive and impractical (Eggleston & Rojstaczer, 2001). Particle size distribution analysis and subsequent application of empirical models is often used as an alternative method due to its economic advantage, and non-reliance on knowledge of aquifer geometry and hydraulic boundaries (Cheong et al., 2008; Odong, 2007). The particle size distribution of a sample is also easily achieved in the laboratory.

Empirical models that relate particle size distribution to hydraulic conductivity include many assumptions and simplifications. The most limiting factor is thought to be the disturbance of the sample, such that all sediment structure is destroyed (Pucko & Verbovškev, 2015). As well as particle size distribution, hydraulic conductivity is dependent on other parameters such as cementation, sediment stratification, and low weight percentage fines (Eggleston & Rojstaczer, 2001). These factors are often not expressed within the various models. Additionally, due to the disturbance of the sample, values derived from these equations reflect neither the vertical nor horizontal component of hydraulic conductivity (Cheong et al., 2008). The physical size of aquifer sediment samples used to analyse particle size distribution are small, so it is difficult to obtain a sample that is representative of a heterogeneous unit. Therefore, this method only determines properties of a very small volume of aquifer, whereas measurements derived from field tests permit measurement over a much larger scale (Schultz & Ruppel, 2002), thus encapsulating some heterogeneity.

2.1.2 Review of empirical models

It is widely accepted that each empirical model has its limitations, and that most methods are only suitable for a range of grain sizes (e.g., Hazen, 1892, Kozeny-Carman, 1927, 1937, Beyer, 1964). However, there are some areas of contention as to which method is the most accurate. Rosas et al. (2014) conducted a study to analyse the application of various empirical formulae to different depositional environments. Before the samples were divided into groups based on depositional environment and lithology, very poor correlation was established between grain-size derived hydraulic conductivity and measured hydraulic conductivity. After grouping, it was discovered that some methods exhibit good correlations with specific depositional environments, enforcing the fact that some methods are only suitable for a specific range of grain sizes. Kasenow and Röhrich (2001) describe the commonly used empirical models of Hazen (1893), Kozeny (1927), Sauerbrei (1932), Beyer (1964), and the United States Bureau of Reclamation (USBR, 1978) and state the applicability of each to grain size ranges. They suggest that the Hazen formula is applicable to a range of grain sizes, as long as it is a uniformly graded sample, an opinion shared by (Odong, 2007). It is also stated that Kozeny's equation (1927) should be applied to coarse grained sands. This is supported by Cheong et al. (2008). The Sauerbrei equation is applicable to sand and sandy clay of grain sizes of 0.5 mm or less. The conclusion of the study by Odong (2007) was that the Kozeny-Carman equation (a modification of the Kozeny equation (1927)), provides the best all round estimation of permeability. However, it was also concluded that the Beyer method which can be used for a range of sand grain sizes, provides the best estimation for a highly heterogeneous sample, and that the USBR method is inaccurate. The inaccuracy of the USBR method is widely agreed upon throughout the literature (Pucko & Verbovškev, 2015). The application of particle-size analysis for determining the hydraulic conductivity of gravel yields high margins of error (Rosas et al., 2014). Pucko & Verbovškev (2015) believe that the Slichter method (1905) is the only valid method for application to gravels. However, Odong (2007) states that this method is inaccurate and underestimates hydraulic conductivity values. All empirical models mentioned are summarised in Table 2-1.

Table 2-1. Summary of empirical models for determining hydraulic conductivity from particle size distribution

	Domain of applicability	Incorporates porosity	Summary
Hazen (1893)	Fine sand – gravel, uniform samples	Yes	Widely used due to simplicity
Slichter (1905)	Fine sand - gravel	Yes	Specialises in gravel samples
Kozeny-Carman (1927, 1937)	Silt – gravel, uniform samples	Yes	Widely considered most accurate method
Sauerbrei (1932)	Sandy clay - clay	Yes	Specialises in fine grained samples
Beyer (1964)	Fine – coarse sand, heterogeneous samples	No	Considered best for heterogeneous samples
USBR (1978)	Medium sand, uniform samples	No	Widely considered inaccurate

2.2 Methods and materials

Nine bulk sediment samples were analysed for particle size distribution. Each sample consisted of between 1.5 – 3.0 kg of sediment extracted from one representative sediment core from each site. The samples were taken at depths corresponding to the screen depths of the surrounding wells. NB1, which screens the Linwood Gravel aquifer at the Tram Road site was the only sample not tested as it was unavailable. Determination of particle size distribution was carried out in a laboratory using the procedures described in NZS 4402; Methods of testing soils for engineering purposes (Standards Association of New Zealand, 1986) as guidance. The testing was divided into three stages. Firstly, wet sieving was undertaken on the samples to remove any mud stuck to the grains, and to separate the very fine material from the coarse grains. Secondly, the coarse material was dry sieved to determine its particle size distribution. Finally, the fine material underwent particle size distribution analysis via the hydrometer method. The equipment required to conduct the particle size distribution analysis is listed in Appendix B.

2.2.1 Wet sieving

Procedure:

a) Each sample was weighed in its container.

b) Due to cohesion of samples, water was added to each sample to separate the grains.

c) After 4 h, the gravel was removed from the samples and set aside. This was to protect the sieve.

d) The rest of the samples were transferred into 75 µm sieves with a catch pan attached. Water was added when necessary to help separate grains and assist the fine material

through the sieve. The gravel was washed over the sieve to remove any mud stuck to the grains, and then set aside again.

e) The sieve was agitated so that the samples moved over the sieve mesh in an irregular motion for at least 2 min. The motion was continually varied to allow the individual grains to pass through the sieve where possible.

f) Anything passing through the sieve into the catch pan was considered as ‘fines.’ This material was set aside for the hydrometer test. Any material remaining on the 75 µm sieve was considered as ‘coarse’ and was placed in a metal bowl with the rest of the gravel.

g) The coarse material was oven-dried at 104 ˚C overnight.

2.2.2 Dry sieving

After the coarse material had been oven-dried, dry sieving was undertaken to acquire the samples particle size distribution.

Procedure:

a) The coarse material was weighed with the bowl.

b) Two stacks of sieves were set up so that the sieve meshes decreased in size towards the bottom. The first stack consisted of sieves ranging from 64 mm to 2.36 mm (Figure 2-1). The second stack consisted of sieves from 1.18 mm down to 63 µm. Each stack had a catch pan attached.

c) The oven-drying process caused the grains to bind together again. Before the sieving process began these grains were separated.

d) The coarse material was transferred to the first sieve stack. The stack was agitated in an irregular motion for at least 2 min. On sieves coarser than 16 mm, individual grains were tested where necessary to see if they fell through. For finer sieves, grains were not forced through the mesh.

e) Once satisfied that the grains had been separated properly, the sample retained in each sieve was weighed.

f) The bowl containing each sample was weighed before the sample was placed back in its bowl.

Figure 2-1. Sample of coarse material ready for dry sieving through the first sieve stack

Calculations:

a) Initially, the percentage of material (of the total sample mass) retained in each test sieve was calculated. The sum of these percentages was subtracted from 100 to calculate the loss during testing. This did not exceed 1% for any sample which is an acceptable loss (Standards Association of New Zealand, 1986).

b) For each sieve the cumulative percentage of the total mass passing that sieve was calculated.

2.2.3 Hydrometer method

The fine material that was removed during the wet sieving process was then used for the hydrometer analysis. This process is required for silt and clay that is too small for sieve analysis. Particle size percentages were calculated using Stokes law, which governs the rate at which particles fall out of suspension. Testing was undertaken in two lots due to the large number of samples. Initially, the four samples from Tram Road were tested, followed by the five samples from Adderley Terrace.

Procedure:

Determination of sample water content:

a) The mass of the fine material was weighed in its container.

b) The fine material had been sitting for a while and had mostly fallen out of suspension. This was scraped off the bottom of the container and stirred with the overlying water until it was evenly mixed.

c) A scoop of this sample (~ 50 g) was taken and placed in a metal aluminium tray. This sub-sample was weighed and oven-dried at 104 ˚C overnight.

d) The oven-dried sample was then reweighed to calculate water content.

Test Preparation:

e) Approximately 30 g of sediment was required for the hydrometer test. The fine material samples consisted mostly of water, so the sub-sample was taken based on its observed water content. Sub-sample sizes ranging from 50 g to 150 g were measured out and placed in 250 ml beakers.

f) Sodium hexametaphosphate solution was made by mixing 40 g of sodium hexametaphosphate with 1 L of deionised water.

g) 125 ml of sodium hexametaphosphate solution was added to each beaker and allowed to soak overnight. This solution is a dispersing agent used for separating grains.

h) 125 ml of sodium hexametaphosphate solution was added to 875 ml of deionised water in a 1 L graduated cylinder. The hydrometer was placed in the cylinder and allowed to float freely. Once the hydrometer had settled, a density measurement of the solution was taken (ρ_c [ML^{-3}]).

i) Another 1 L graduated cylinder was set up containing 1 L of deionised water. This was for the hydrometer to float in between measurements and when it was not in use.

j) A 1 L graduated cylinder and a stop watch was set up for each sample being tested (Figure 2-2).

k) The sample in the beaker was poured into the mechanical mixer cup using the squirt bottle to help transfer all grains. The cup was then filled up to about half way and mixed for 1 min.

l) The contents were then transferred into its test cylinder and filled up to the 1 L mark with deionised water. The bung was placed on securely and the cylinder was inverted

constantly for 1 min. Approximately 90 inversions were sufficient to ensure full and even suspension of the sample. The stop watch was started once the inversions were complete and the test tube had been placed on the bench. The bung was carefully removed.

Running the test:

The stop watch activation signalled the start of the test. Hydrometer readings were taken after 2 min, 5 min, 15 min, 30 min, 1 h, 4 h and 24 h.

m) The hydrometer was removed from its cylinder of water approximately 1 min before the reading was due to be taken. It was lowered into the test cylinder slowly to avoid sediment disturbance. Once the hydrometer had become steady, ensuring that it was floating freely and not resting on the cylinder wall, the reading was taken from the bottom of the meniscus. The hydrometer was then slowly removed from the test cylinder and placed back in the cylinder of water.

n) After every reading the thermometer was used to record the temperature in the test cylinder.

n) Each test was repeated in a staggered format, such that a new test started every 10 min.

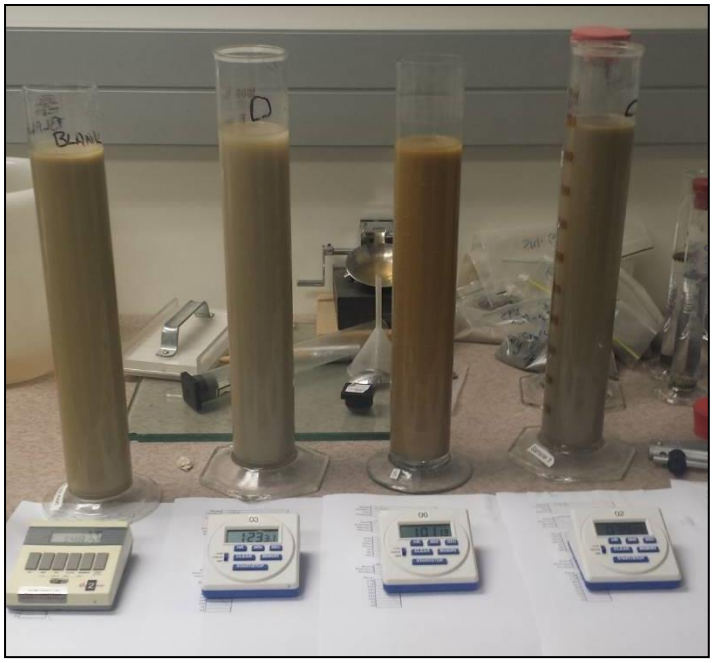

Figure 2-2. Tram Road samples during the hydrometer test

Calculations:

Unlike the data obtained from the dry sieving process, the data from the hydrometer test needed to be converted to grain size. The following calculations, as presented in NZS 4402 (Standards Association of New Zealand, 1986), were undertaken to achieve this:

a) The dry mass of the sediment sample was calculated from:

$$M = M_w - \frac{M_w . w}{100} \quad (1)$$

Where,

M_w = Wet mass of the soil [M]

w = Water content of the soil as a percentage [Dimensionless]

b) The equivalent particle diameter was calculated from the following formula:

$$D = k\sqrt{H_R/t} \quad (2)$$

Where,

D = Equivalent particle diameter [L]

k = Constant, depending on solid density of the particles and the temperature of the suspension [Dimensionless]

r = Hydrometer reading [ML^{-3}]

R'_h = Hydrometer reading in the form $1000(r - 1)$ [ML^{-3}]

H_R = Effective depth corresponding to R'_h [L]

t = Elapsed time [T]

The effective depth is the distance from the surface of the suspension to the point where the density is being measured and varies depending on the type of hydrometer used. In this instance the 151H model hydrometer was used. For this hydrometer the effective depth was calculated as follows:

$$H_R = 16.295 - 0.2645R'_h \quad (3)$$

c) The percentage of particles finer by weight than the corresponding equivalent particle diameters was calculated from the formula:

$$P = \frac{100\rho_s}{M(\rho_s - 1)}(R'_h + x) \quad (4)$$

Where,

P = Particles finer, expressed as a percentage [Dimensionless]

M = Total dry mass of soil [M]

ρ_s = Solid density of soil particles [ML^{-3}]

x = Composite correction, ($\rho_c - 1$) [ML^{-3}]

2.2.4 Analysis

Following completion of the calculations, a data set for each sample was established consisting of the grain diameter and the corresponding percentage of the sample finer by weight. The data were then plotted on a semi-logarithmic graph with grain diameter on the x-axis. These particle size distribution curves contain information crucial to many empirical models. Particle size analysis software GRADISTAT (Blott & Pye, 2000) was used to gain sample descriptions and parameters. This software automatically calculates statistical parameters through the graphical method described by Folk & Ward (1957) and provides sample names and textural descriptions after Folk (1954).

In consideration of the literature, the models chosen for analysis were those developed by Hazen (1892), Slichter (1905), Kozeny-Carman (1927, 1937), and Beyer (1964). All of these empirical models are based on a general formula. This formula has been summarised by Vukovic and Soro (1992) as follows:

$$K = \frac{g}{v} \cdot C \cdot f_{(n)} \cdot d_e^2 \qquad (5)$$

Where,

g = Acceleration due to gravity [LT^{-2}]

ν = Kinematic viscosity of water [L^2T^{-1}]

C = Sorting coefficient [dimensionless]

$f_{(n)}$ = Porosity function [-]

d_e = Effective grain diameter [L]

The effective grain diameter, in the form d_{10}, was read off the particle size distribution graph. This is the grain diameter where 10% of the sample is finer. Additionally, the effective grain diameter was used to estimate sorting using the following equation that describes the coefficient of uniformity, C_μ:

$$C_\mu = \frac{d_{60}}{d_{10}} \quad (6)$$

Where,

d_{10} = Effective grain diameter: grain size where 10% of the sample is finer by weight [L]

d_{60} = Grain size where 60% of the sample is finer by weight [L]

Many empirical models also require an estimate of porosity (n), which is dimensionless. This was acquired using the following empirical relationship between porosity and the coefficient of uniformity (Kasenow & Röhrich, 2001):

$$n = 0.255(1 + 0.83^{C_\mu}) \quad (7)$$

The four empirical models used in this project are based on the general form presented in equation 5, although the values of C, $f_{(n)}$, and d_e differ between models (Odong, 2007).

It should be noted that various authors present these equations differently. The form used in this occasion is presented after Vukovic & Soro (1992).

2.2.4.1 Hazen

The Hazen model (1892) was one of the first empirical models developed to estimate hydraulic conductivity (Kasenow & Röhrich, 2001). It is based on a simple formula that assumes a uniformly graded sample. The equation is as follows:

$$K = \frac{g}{v}\ 6\ \times 10^{-4}(1 + 10(n - 0.26))\ d_{10}^{2} \tag{8}$$

Although this method is most applicable for uniformly graded sand, it can also be applied to a range of grain sizes from fine sand to gravel (Odong, 2007). As a rule, C_{μ} must not exceed five, with a d_{10} range between 0.1 and 3 mm i.e. fine sand – fine gravel range (Kasenow and Röhrich, 2001).

2.2.4.4 Slichter

The Slichter model (1905) was developed incorporating both porosity and effective grain diameter. It is the only valid method for use with gravel samples according to its domain of applicability. The model is based on the following formula:

$$K = \frac{g}{v}\ 1\ \times 10^{-2} n^{3.287}\ d_{10}^{2} \tag{9}$$

This model was used in this study due to the majority of samples being sandy gravel, which fits within the domain of applicability.

2.2.4.2 Kozeny-Carman

The Kozeny-Carman model was first developed by Kozeny (1927) and later modified by Carman (1937). Equation 10 is a summarised version of the formula, although the relationship accounts for the specific surface area of the particles in addition to porosity and effective grain diameter. Carrier III (2003), Pucko & Verbovsek (2015) and Zhang (2017) recommend the use of the Kozeny-Carman formula ahead of the Hazen formula.

$$K = \frac{g}{v}\ 8.3\ \times 10^{-3}\left(\frac{n^3}{(1-n)^2}\right)\ d_{10}^2 \tag{10}$$

The popularity of this model is also attributed to its wide range of applicability. However, Carrier III (2003) mentions that the formula loses accuracy for clayey soils, as well as coarse samples where d_{10} exceeds 3 mm.

2.2.4.3 Beyer

The Beyer model (1964) was developed to estimate hydraulic conductivity for poorly sorted, heterogeneous (C_μ < 20) particle size distributions (Odong, 2007; Zhang, 2017). However, porosity is not incorporated into the formula and therefore takes on a value of one. The formula is as follows:

$$K = \frac{g}{v}\ 6\ \times 10^{-4}\left(log\frac{500}{C_\mu}\right)\ d_{10}^2 \tag{11}$$

2.3 Results

The results of the laboratory experiments are presented in sections 2.3.1 and 2.3.2. Two particle size distribution plots have been created to compare the Tram Road and Adderley Terrace samples separately. From these plots, simplified bar graphs were created displaying the percentage of gravel, sand, silt and clay for each sample. Additionally, values important for application to the empirical models have been obtained from the particle size distribution curves and are presented in these sections. Section 2.3.3 contains the hydraulic conductivity estimates obtained from the empirical models.

2.3.1 Particle size distribution of aquifer sediments Tram Road wells screen

The particle size distribution curves of the Tram Road wells are presented in Figure 2-3. The illustration shows that all samples are very poorly sorted i.e. there is large variance in the range of particle sizes. All samples include sediment ranging from gravel down to clay. However, differing proportions of grain sizes has resulted in varying curve shapes. To better illustrate this, a bar graph was created from the curves that simplifies the data by grouping the grain sizes into four categories (Figure 2-4). It is evident that all samples are predominantly gravel that generally decrease in abundancy with depth. NB5 which screens the Bromley Formation is distinctive as it contains the least amount of gravel of the Tram Road samples, accompanied by the highest silt and clay content. In contrast, water table well NB3 contains over 80% gravel and the lowest content of fine material.

The values of effective grain diameter, median grain diameter, and the coefficient of uniformity have been extracted from the particle size distribution curves and are presented in Table 2-2. The effective grain diameter and the median grain size are highly variable for the different samples. The effective grain diameter is low for all samples; however, it is significantly larger for NB3 at 270 µm. All of the samples also have very high coefficient of uniformity values, so they do not fit within the domain of applicability of some empirical models.

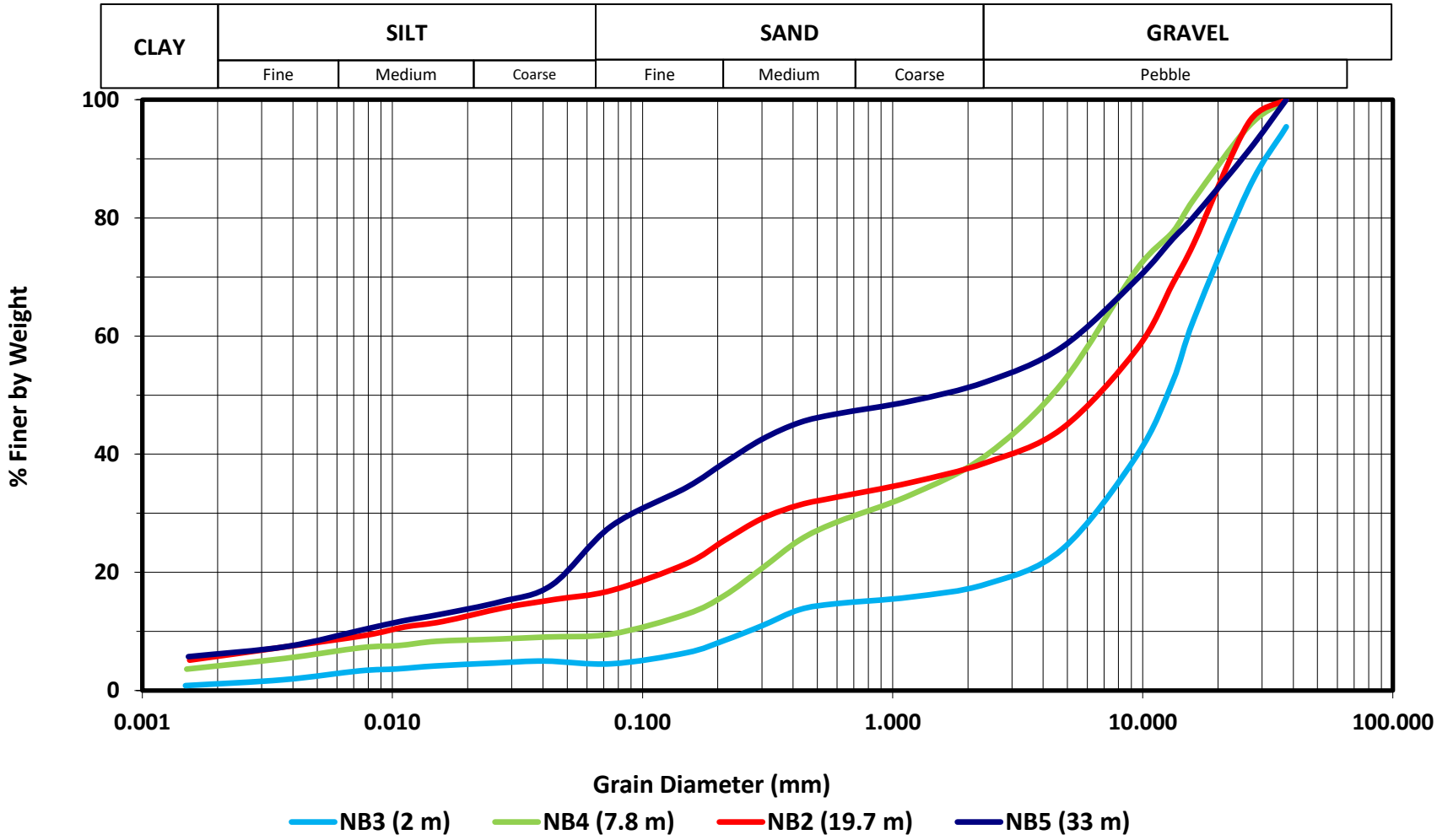

Figure 2-3. Particle size distribution curves for aquifer sediments Tram Road wells screen (showing depth to top of well screen)

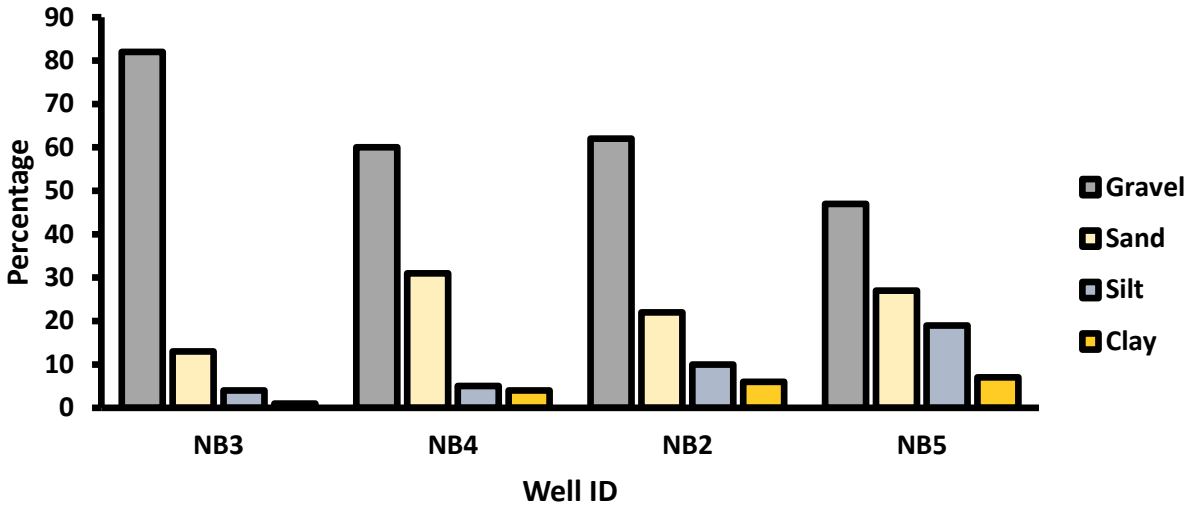

Figure 2-4. Simplified particle size distribution of aquifer sediments Tram Road wells screen presented in order of increasing depth

Table 2-2. Sample descriptions and parameters (Folk, 1954; Folk & Ward, 1957) and values obtained from particle size distribution curves for aquifer sediments Tram Road wells screen

	NB3	NB4	NB2	NB5
Screen depth (m bgl)	2 - 3	7.8 – 8.3	19.7 - 20.2	33 – 33.5
Sediment name (Folk, 1954)	Coarse gravel	Fine silty sandy fine gravel	Coarse silty sandy coarse gravel	Very coarse silty sandy coarse gravel
Textural group (Folk, 1954)	Gravel	Muddy sandy gravel	Muddy sandy gravel	Muddy sandy gravel
Sorting (Folk & Ward, 1957)	Very poorly sorted	Very poorly sorted	Very poorly sorted	Very poorly sorted
Mean particle size (Folk & Ward, 1957)	Fine gravel	Very fine gravel	Very fine gravel	Very coarse sand
Effective grain diameter, d_{10} (µm)	270	83	9.3	7.0
Median grain diameter, d_{50} (mm)	13	4.3	6.6	1.6
Coefficient of uniformity, C_{μ}	59	76	1081	771

2.3.2 Particle size distribution of aquifer sediments Adderley Terrace wells screen

Most of the sediments sampled from various depths at the Adderley Terrace site show similar particle size distribution trends to those from the Tram Road site. All samples are poorly to very poorly sorted (Table 2-3), containing grains ranging from gravel down to clay, and follow a similar pattern (Figure 2-5). The exception is AT2 as the particle size distribution curve displays a steep slope in the medium sand range. This represents the presence of a large proportion of medium sand in the sample. Figure 2-6 also illustrates this. AT2 contains 85% sand, in contrast to the other samples which all contain less than 35% sand. All other wells follow the trend of the Tram Road wells, where gravel is the most abundant particle size, followed by sand with minor silt and clay. However, in contrast, gravel generally becomes more abundant with depth at Adderley Terrace.

Overall, the effective grain diameter of the samples from Adderley Terrace is larger than the Tram Road samples. Additionally, although still high, the coefficient of uniformity values for these samples is much lower than those from Tram Road. This means that the empirical models are more applicable to the Adderley Terrace samples based on the coefficient of uniformity requirements. AT2 is the most uniform sample and is the only sample that matches the uniformity requirement for the Beyer method.

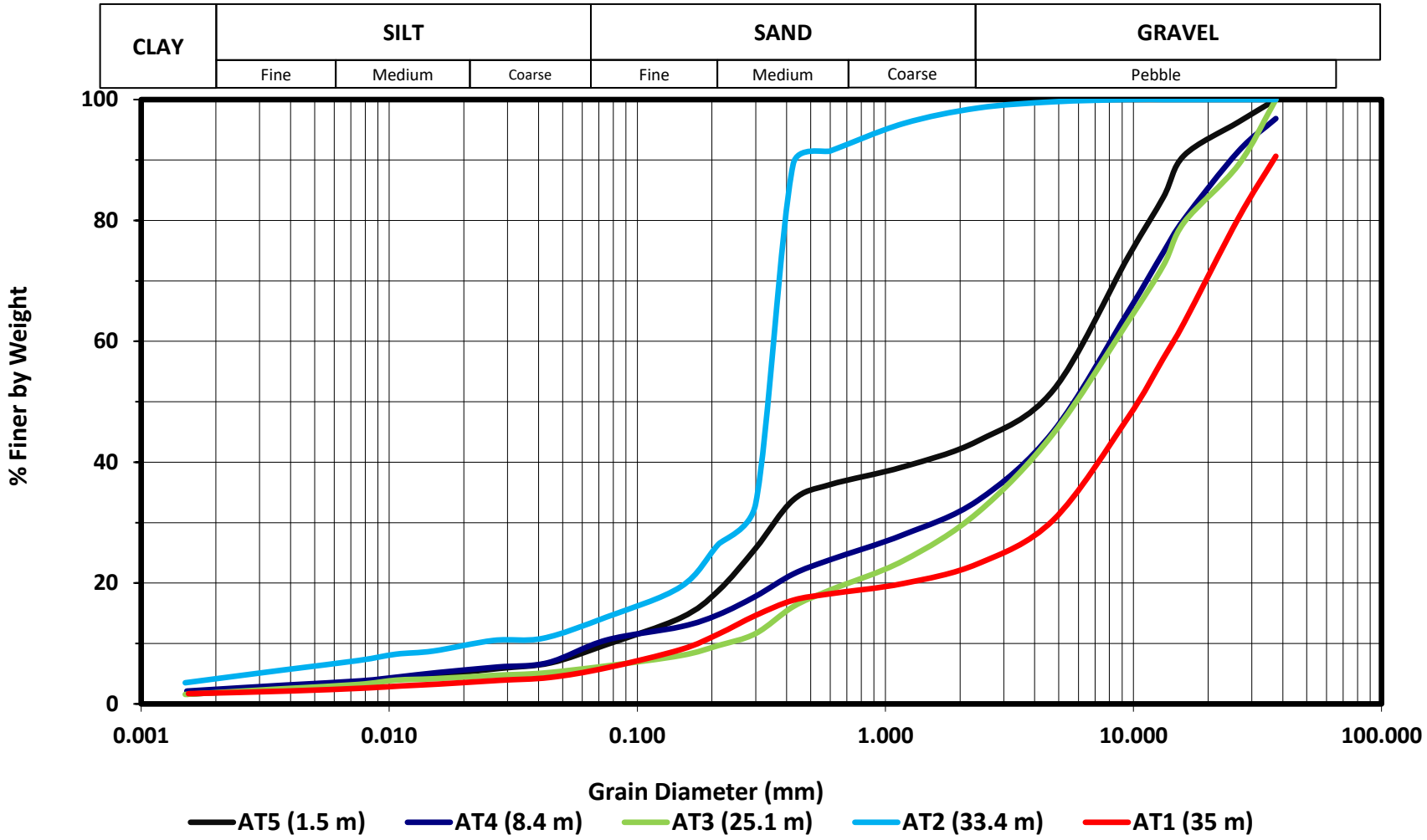

Figure 2-5. Particle size distribution curves for aquifer sediments Adderley Terrace wells screen (showing depth to top of well screen)

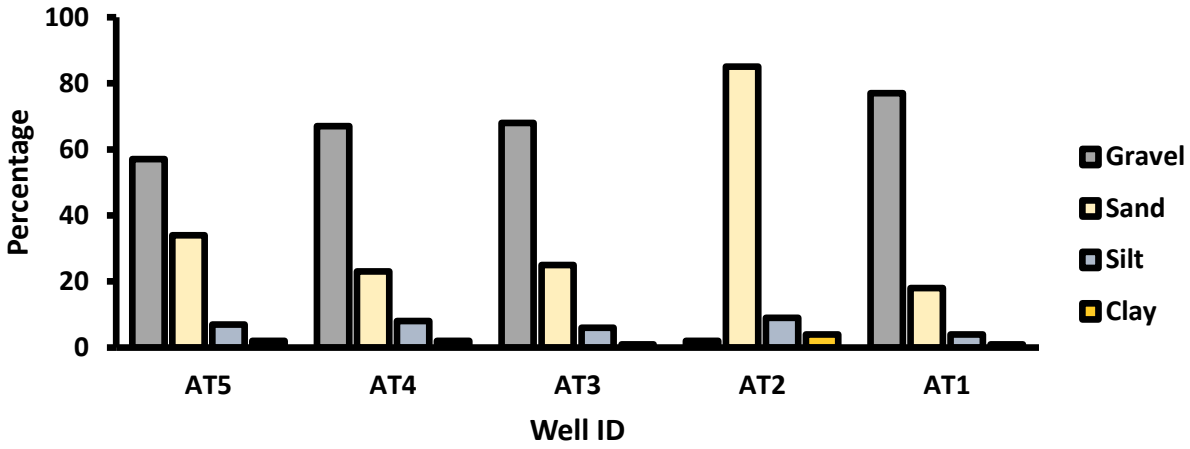

Figure 2-6. Simplified particle size distribution of aquifer sediments Adderley Terrace wells screen presented in order of increasing depth

Table 2-3. Sample descriptions and parameters (Folk, 1954; Folk & Ward, 1957) and values obtained from particle size distribution curves for aquifer sediments Adderley Terrace wells screen

	AT5	AT4	AT3	AT2	AT1
Screen depth (m bgl)	1.5 – 2.5	8.4 – 8.9	25.1 – 25.6	33.4 – 33.9	35 – 35.5
Sediment name (Folk, (1954)	Very coarse silty sandy medium gravel	Very coarse silty sandy medium gravel	Very coarse silty sandy medium gravel	Slightly very fine gravelly very coarse silty medium sand	Very coarse silty sandy coarse gravel
Textural group (Folk, (1954)	Muddy sandy gravel	Muddy sandy gravel	Muddy sandy gravel	Slightly gravelly muddy sand	Muddy sandy gravel
Sorting (Folk & Ward, 1957)	Very poorly sorted	Very poorly sorted	Very poorly sorted	Poorly sorted	Very poorly sorted
Mean particle size (Folk & Ward, 1957)	Very fine gravel	Very fine gravel	Very fine gravel	Medium sand	Fine gravel
Effective grain diameter, d_{10} (µm)	75	67	230	22	180
Median grain diameter, d_{50} (mm)	4.2	5.8	5.9	0.27	10.1
Coefficient of uniformity, C_μ	83	121	37	16	58

2.3.3 Hydraulic conductivity

The hydraulic conductivity estimates gained from empirical modelling are displayed in Table 2-4:

Table 2-4. Hydraulic conductivity values (m/d) determined using empirical models

Well ID	Depth (m bgl)	Hydro-stratigraphic unit	Hazen	Slichter	Kozeny-Carman	Beyer
NB3	2 - 3	Springston Formation	320	63	140	310
NB4	7.8 – 8.3	Contact: Springston Formation / Riccarton Gravel	30	6.0	13	26
NB2	19.7 – 20.2	Riccarton Gravel	0.38	0.075	0.17	n/a
NB5	33 – 33.5	Base of Bromley Formation / top of Linwood Gravel	0.22	0.042	0.94	n/a
AT5	1.5 – 2.5	Christchurch Formation	27	5.3	12	23
AT4	8.4 – 8.9	Top of Riccarton Gravel	20	3.9	8.6	13
AT3	25.1 – 25.6	Riccarton Gravel	230	46.0	100	280
AT2	33.4 – 33.9	Base of Bromley Formation / top of Linwood Gravel	2.4	0.49	1.1	3.4
AT1	35 – 35.5	Linwood Gravel	140	28	62	120

It is evident that the Hazen method produces the highest values of hydraulic conductivity. The Beyer method produced similar, although slightly lower values. Two of these values were negative which isn't physically meaningful. Thus, they were ignored. In contrast, the Slichter method consistently produced the lowest values by far. The hydraulic conductivity estimates gained using the Kozeny-Carman equation are under half of those obtained from applying the Hazen model.

Chapter 3. SLUG TESTS

3.1 Introduction

Hydraulic pumping tests, where a well is pumped to measure the water level response, enable parameter estimation over large volumes of aquifer. However, they are an expensive and time-consuming means of measuring hydraulic conductivity (Fetter, 2000). Slug tests offer a low cost, simple, relatively fast alternative method that have been widely used by hydrogeologists for decades (Ross & McElwee, 2007). The slug test simply measures the rate at which the hydraulic head in the well recovers following an instantaneous change in water level (Butler, 1997; Fetter, 2000; Freeze & Cherry, 1979). Conventional slug test methods include adding or removing a volume of water to the well or using a solid slug to displace the water. Pneumatic slug testing is a more recent technique that utilises compressed air equipment to artificially lower the water level. This method is superior to conventional methods, producing more accurate results (Lewis, 2013). Analytical models are applied to slug test data to obtain an estimate of the hydraulic conductivity. Various analytical models have been developed to simulate different boundary conditions i.e. confined or unconfined aquifers; fully or partially penetrating wells; different well installation design and different head response patterns. The water in the well can either respond in a smooth, approximately exponential manner (overdamped response), or the water may oscillate about the static water level before stabilising (underdamped response) (Fetter, 2000). This literature review will evaluate both the use of slug tests for estimating hydraulic conductivity, and the application of various analytical models. The wells used in this study are partially penetrating, and are screened within unconfined and confined hydro-stratigraphic units, or across the water table. Only those analytical methods applicable to these conditions will be evaluated in this literature review.

3.1.1 Review of the analysis of slug tests in confined aquifers

The most common analytical models associated with the measurement of confined aquifers are those of Cooper et al. (1967) and Hvorslev (1951). The Cooper method was originally developed for fully penetrating wells, and later modified to simulate partially penetrating wells (Butler, 1997). The only difference with the partial penetration variant is that the effective screen length is used instead of the formation thickness. For correct use of these models, the slug test data must display an overdamped response (Fetter, 2000). A limitation of these models is that they adopt a more simplified version of the groundwater flow. It is assumed that there is an absence of vertical flow in response to disturbance of the slug (Butler, 1997). Hyder et al. (1994) attempted to quantify the error resulting from this assumption. They concluded that the hydraulic conductivity estimates obtained from this method are overestimated unless the aquifer storage parameter or aspect ratio (aquifer thickness / well radius) is large. The Hvorslev method has also been developed for use in wells partially penetrating a confined aquifer, however there are also assumptions and issues of practical importance to be considered. A very important consideration, due to the potential error, is that of fitting a straight line to the head response data. A concave upward curve often occurs when the normalised logarithm of the response data is plotted against time. Therefore, error may occur depending on the method used for fitting a straight line to this data. Butler (1996) recommends fitting the trendline to the normalised recovered head range of 0.15-0.25 to obtain the best hydraulic conductivity estimate. Fitting the trendline to just the data at the start of the test or the entire test will affect the slope, and yield different hydraulic conductivity estimates.

3.1.2 Review of the analysis of slug tests in unconfined aquifers

A common application of slug tests is in contaminated site investigations (Butler, 1997). Analysis of these tests are commonly undertaken using the method of Hvorslev (1951), or the method of Bouwer and Rice (1976). These two methods are similar, except for the fact that the latter takes into account the effective well radius (Kasenow and Röhrich, 2001). The Bouwer and Rice model assumes that the water table position remains stable during the test, and that elastic storage mechanism effects can be ignored (Butler 1997). The effects of the elastic storage mechanism are responsible for the concave upward curve displayed when the logarithm of normalised head is plotted against time (Butler, 1997). Thus, the model theoretically should display a straight line fit for this data plot. Butler (1996) recommends fitting the trendline to normalised head values in the range 0.2 to 0.3 for the most reliable hydraulic conductivity estimate. Slug tests undertaken on wells screened across the water table, particularly those surrounded by a filter pack, can exhibit what has been termed the double straight-line effect (Bouwer, 1989). This is a result of the filter pack quickly draining at the start of the slug test, before the water in the aquifer enters the well. This slug test response is evident when the plot of head versus time displays a steep straight line at the beginning of the test followed by a shallower straight line. Bouwer (1989) recommends that in analysis of slug tests displaying the double straight-line effect, the Bouwer and Rice (1976) method be applied to the second straight line as it is representative of the aquifer response to the displacement in the well.

3.1.3 Limitations and considerations of slug tests for determining hydraulic conductivity

The accuracy of slug tests for estimating hydraulic conductivity is often questioned, due to discrepancy in hydraulic conductivity estimates gained from slug tests and pump tests (Butler, 1997). It has been concluded that high margins of error can occur from the use of analytical models (Kasenow & Röhrich, 2001). According to Butler (1997), this error is

a result of two factors. The first being a process called the skin effect. During the installation of the well, the rotation of the drill equipment can smear a layer of fine-grained material on the borehole wall (Fetter, 2000; Cheong et al., 2008). This can significantly affect the hydraulic conductivity values obtained from the test. Well development is a key process for preventing the skin effect. This is usually achieved by pumping water from the well to flush out fine material forming the borehole skin (Fetter, 2000). However, excessive well development may equally result in removal of the pre-existing fine-grained material around the borehole, thus raising the hydraulic conductivity values. The second factor that Butler (1997) considers to cause high error margins, is the range of assumptions and simplifications used in the analytical models. Common assumptions amongst the models include homogeneous and isotropic conditions (Freeze & Cherry, 1976). In reality, aquifers are heterogeneous and anisotropic. Potential errors can be mitigated through careful well construction and development, as well as attention to detail in the design, performance and analysis phases of the slug test (Butler, 1997). Consideration should be taken in the interpretation of the hydraulic conductivity values derived from slug tests. As these tests only affect a small portion of the aquifer, the hydraulic conductivity values only represent the sediments in the immediate vicinity of the well. The results of slug tests are therefore more suitable for small scale studies, such as contaminant transport (Butler, 1997).

3.1.4 Barometric pressure

Static water levels in aquifers are susceptible to the effects of barometric pressure. An increase in barometric pressure is transferred directly onto the water in the well resulting in a decrease in water level. Conversely, a decrease in barometric pressure results in an increase in water level in the well. Barometric pressure effects are more pronounced in confined aquifers. In these conditions, a change in barometric pressure generally results in an instantaneous water level response (Spane, 1999). For unconfined aquifers, changes in barometric pressure are transferred equally to the aquifer and the water in the well, so the effects are often negligible (Kasenow & Röhrich, 2001). Measured slug test

water level recovery data can be corrected for the effects of barometric pressure to avoid error. Correction methods are described in section 3.2.2.1.

3.1.5 Numerical modelling

Numerical modelling is another form of mathematical modelling. It is often used as an alternative to analytical modelling for problems that require less simplifying assumptions, and enables better mathematical representation of physical boundary conditions (Anderson & Woessner, 1992). Unlike analytical models, numerical models can incorporate complex geometry, multiple aquifers, recharge sources, boundary conditions and anisotropic conditions. The most popular method of numerical groundwater modelling is the finite-difference method due to its algebraic simplicity (Batu, 2006). This method is used to solve the partial differential equations that govern groundwater flow. A finite-difference model consists of a series of grid cells to which hydrogeological properties are assigned. Each cell has a node either at its centre (block centred nodes) or at the intersection of the grid lines (mesh centred nodes). Analytical models should be considered supplementary to numerical models (Batu, 2006), and assist in the process of inverse modelling. This form of modelling is used to estimate a hydrogeological parameter by applying an initial estimate of the parameter, and calibrating it until the output data from the model matches the field data. Therefore, the results from the analytical model can be used as the initial estimate of the parameter to be calibrated through numerical inversion.

3.2 Methods and materials

Physical slug tests were initially conducted on the Tram Road wells on the 21st and 22nd of July 2017. Repeat tests using a smaller diameter slug were made on the 13th of September 2017. The Adderley Terrace wells were tested on the 17th of September 2017. Subsequent data analysis was undertaken with the aid of Microsoft Excel. The literature review helped inform the choice of analytical models used in this study. Both the Hvorslev method and the Bouwer and Rice method were used to account for the unconfined and confined conditions. Finally, a numerical approach was applied to infer hydraulic conductivity from the slug test data using numerical modelling software Modflow (Harbaugh, 2005). The methodology and materials used for both the slug tests and the analysis are described below.

3.2.1 Field data collection

Pneumatic slug test equipment was not available, so solid slug apparatus were used.
The materials used to perform the slug test included:

- A 1 m long concrete pipe with a PVC casing, attached to rope. Two slugs of different diameters were trialled (32.0 mm, 43.2 mm)
- Water level dipper
- Pressure transducer (Solinst level logger)
- Barometric pressure logger (Solinst barologger)
- Stop watch
- Step ladder
- PVC standpipes for artesian flowing wells

It is important to have background barometric pressure and water level data prior to, during, and after the slug tests. These data are required to correct water level measurements for the effects of barometric pressure. In this case the barometric pressure logger was placed at the site a couple of months before slug tests had begun and set to log at 15 min intervals. This ensured that there was a high chance of recording a period of several consecutives day where no precipitation occurred.

Setting up the slug test:

Firstly, each well was dipped using the water level dipper to determine the depth to the water level before the test. It is important to note where the measurement is taken from. In this case it was the top of the well casing.

The barometric pressure logger was set to record at 15 min intervals over the duration of the testing period. The pressure transducer was then set to log data at intervals depending on the expected response rate of the well. For wells screened in fast responding aquifer material, the logger was set to log eight times per second, which is the fastest possible frequency for the equipment. For the two wells screened in the Bromley Formation, the loggers were set to record at 1 s intervals.

All wells screening the Linwood Gravel and the Bromley Formation were under free-flowing artesian conditions. PVC extension pipes were attached to these wells above the height of the hydraulic head, so that a static water level could be measured in the open well. A step ladder was often required to conduct tests on wells with these standpipes.

The pressure transducer was suspended by a cable within the well, deep enough that it would not interfere with the slug during the test. A length of rope for the slug was measured out, ensuring that the slug was fully submerged below the water.

Performing the slug test:

The slug was lowered and removed from the well quickly to create an instantaneous displacement. However, caution was taken to avoid splashing or other disturbances resulting from introducing or removing the slug too vigorously. It was difficult to avoid measurement error when performing the slug test. For example, it was very common for the pressure transducer cable to get snagged when pulling out the slug. The results cannot be used when the pressure transducer becomes displaced during the period of the test. For most wells, the slug test was repeated 10 times to ensure there were at least a few good tests to gain an average from. Fewer tests were conducted on the slower responding wells due to time constraints. Although, the likelihood of measurement error decreased when performing slug tests on lower conductivity formations because it was not necessary to displace the water rapidly.

The test was performed for a length of time that allowed the water level to fully recover. To determine this, a practice slug test was conducted and the recovery time recorded. The water level dipper was used to check when full recovery had occurred. The majority of the wells took 1 min or less to conduct a single test, with the exception of AT2 and NB5 which screen the Bromley Formation. Tests conducted on AT2 were run for 10 mins, whereas tests on NB5 were run overnight to allow the head to fully recover.

Both falling head and rising head slug tests were performed. Falling head tests were conducted by inserting the slug. Conversely, rising head tests were conducted by removing the slug.

Following full completion of the tests on the well, the results were transferred from the pressure transducer to a laptop.

Finally, the water levels were measured again using the water level dipper as a control check.

3.2.2 Analytical models

Before the analytical models were applied to slug test data, the data were first corrected for the effects of barometric pressure, and then processed to generate the required graphs and inform analysis decisions. The steps taken are described in the following sections.

3.2.2.1 Barometric correction

Changes in barometric pressure can result in error when analysing slug test data. The error may be significant for slow responding tests, however barometric effects for fast responding tests (< 10 min) are likely negligible and can be ignored if the barometric pressure does not change significantly during the test. For this study, pressure changes of 1 cmH_2O or more were considered as significant. In this case, NB5 was identified as the only well requiring barometric pressure correction. This was expected as it was the slowest responding well and the slug test was required to run overnight.

Because the pressure transducer used for the slug tests was unvented, it was measuring the pressure head i.e. the sum of the water pressure and the atmospheric pressure. Therefore, the atmospheric pressure was subtracted from the pressure head to obtain the actual water level above the pressure transducer:

$$h_{obs} = P_h - P_b \tag{12}$$

Where,

h_{obs} = Water level in well above pressure transducer (gauge pressure) [L]

P_h = Pressure head (measured by unvented pressure transducer) [L]

P_b = Barometric pressure [L]

After the pressure transducer data was corrected to gauge pressure, the water level was then corrected for the effects of barometric pressure on the aquifer. Firstly, the ratio of the change in the water-level to a concurrent change in atmospheric pressure is required. This is the barometric efficiency, which is a dimensionless parameter based on the following relationship (Rasmussen & Crawford, 1997):

$$BE = -\frac{\Delta h_{obs}}{\Delta P_b} \tag{13}$$

The barometric efficiency was determined using long-term water level data. A period of six days where no precipitation occurred was extracted and compared to the corresponding barometric pressure data. The water level data were plotted against the barometric pressure data, and the slope of the graph determined (Figure 3-1). A barometric efficiency of 26% was determined for NB5 i.e. the well screening the bottom of the Bromley Formation and the top of the Linwood Gravel in confined conditions.

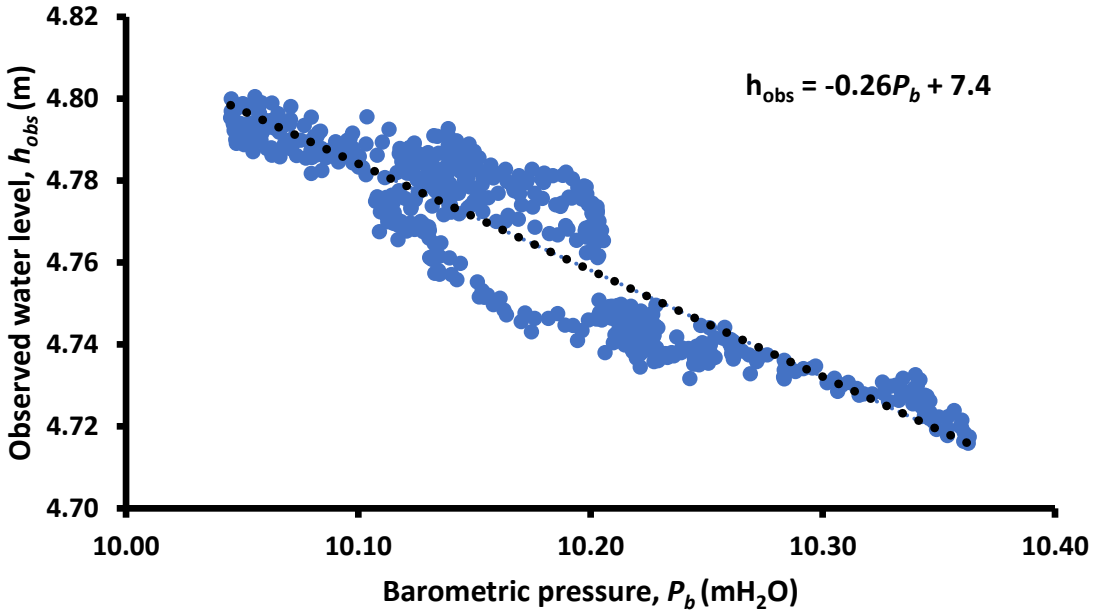

Figure 3-1. Barometric efficiency determined from slope of graph of h_{obs} vs P_b

Following determination of the barometric efficiency for the well, the water level for the slug test was corrected for the effects of barometric pressure using the following equation (Rasmussen & Crawford, 1997):

$$h_{corr} = h_{obs} + BE(P_b - C) \quad (14)$$

Where,

h_{corr} = Water level corrected for the effects of barometric pressure [L]

C = Constant (mean barometric pressure at sea level) [L]

Mean barometric pressure at sea level = 10.33 mH_2O (International Organization for Standardization, 1975)

The corrected data were then ready to be processed for hydraulic conductivity as per the methods described below.

3.2.2.2 Data processing

The data were processed prior to conducting the slug test analyses. Firstly, a graph of the head versus time was produced for an initial analysis of the results using Microsoft Excel. Evidently, the falling head tests produced much more noise in its response than the rising head tests (Figure 3-2). It is suspected that the noise in the data was a result of friction effects from the slug causing a pressure wave in the well. Naturally, the process of removing the slug from the well to conduct the rising head slug test did not result in a pressure wave effect. Because of this, only the rising head slug tests were analysed for determination of hydraulic conductivity.

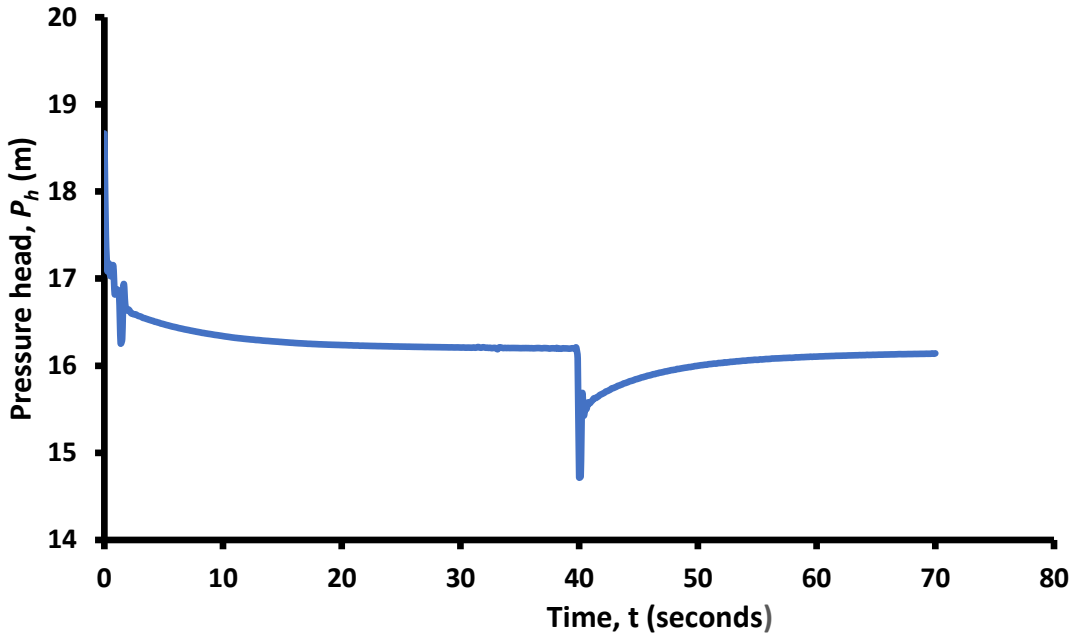

Figure 3-2. Example of falling head (left) and rising head (right) slug tests on NB1 using the thick diameter slug

To assist in the interpretation of these graphs the theoretical initial displacement was determined. Firstly, the volume of the slug was calculated using the following equation:

$$V_s = \pi r_s{}^2 h_s \quad (15)$$

Where,

V_s = Volume of the slug [L^3]

r_s = Radius of the slug [L]

h_s = Height of the slug [L]

Two slugs that differed only in diameter were trialled for these tests. Volumes were calculated as 1.48 L for the “thick slug” and 0.811 L for the “thin slug.”

The previous equation was then rearranged to solve for the theoretical initial displacement. However, the radius of the well casing was substituted for the radius of the slug, and the theoretical initial displacement was substituted for the height of the slug:

$$s_{th} = \frac{V_s}{\pi r^2} \quad (16)$$

Where,

s_{th} = Theoretical initial displacement [L]

r = Radius of the well casing [L]

The theoretical initial displacements for the thick and thin slugs were calculated as 0.75 m and 0.41 m respectively.

A comparison of slug test responses revealed that the thin slug generally produced more consistent results with initial displacements closer to that of the theoretical initial displacement. This is discussed further in section 5.2.2. Although slug tests were undertaken using both the thin slug and the thick slug, hydraulic conductivity estimates were obtained only from the thin slug tests.

The pre-test head was then determined by calculating an average of the head data immediately prior to commencement of the slug test. This is the static water level from which the water should return to after the slug displaces the water. In cases where the water level in the well changed significantly over the duration of the testing period, the pre-test head was re-calculated for each slug test to avoid error. The water level can change as a result of barometric or recharge effects.

The rising head slug test data were extracted from the raw data and placed into an excel spreadsheet. The slug test displacement was then calculated using the equation:

$$s(t) = h(t) - h(0) \quad (17)$$

Where,

$s(t)$ = Displacement at time t [L]

$h(t)$= Head at time t [L]

$h(0)$ = Pre-test head i.e. static water level [L]

The head data were then normalised. This was achieved using the equation:

$$s'(t) = \frac{s(t)}{s(0)} \tag{18}$$

Where,

$s'(t)$ = Normalised displacement [dimensionless]

$s(0)$ = Initial displacement [L]

The logarithm of the normalised data was then plotted against the time elapsed since the start of the test (Figure 3-3a). An issue sometimes arises when the maximum initial displacement is used as the start of the test. Figure 3-3a displays two distinct lines. The steep line occurs when the initial displacement is greater than the theoretical initial displacement, whereas the shallow line is representative of the response of the aquifer. Consequently, this steep line must be removed from the data before analysis begins to avoid large errors. A blanket rule was created and applied to all tests displaying this steep line. It was discovered that the steep line occurred for roughly the first second of every test. Therefore, the first second of each test was removed for wells that displayed this pattern. The result is shown in Figure 3-3b. A check was made to ensure the revised start of test had a similar initial displacement to the theoretical initial displacement.

Both the Hvorslev method and the Bouwer and Rice method utilise this graph to determine the hydraulic conductivity.

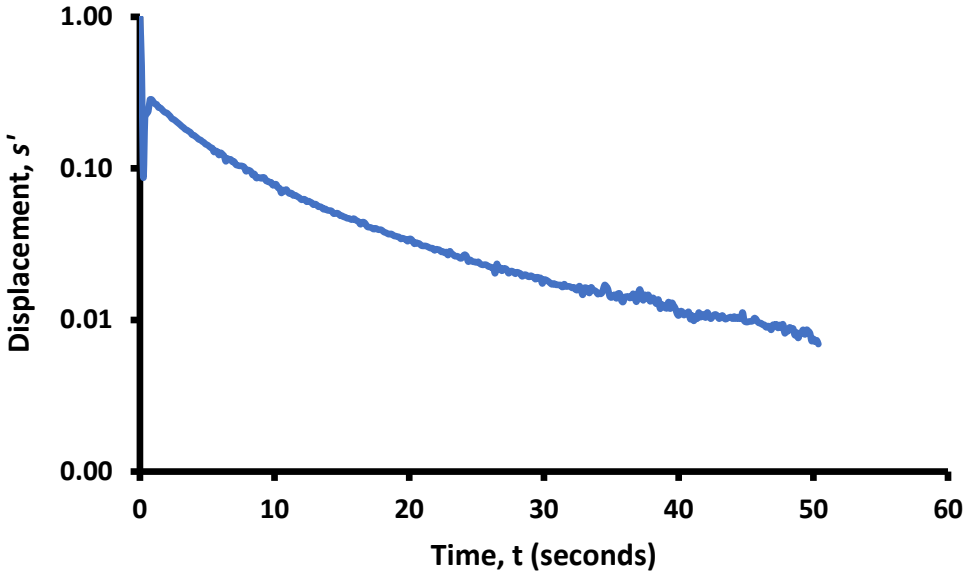

Figure 3-3a. Slug test recovery curve using the point of greatest displacement as start of test

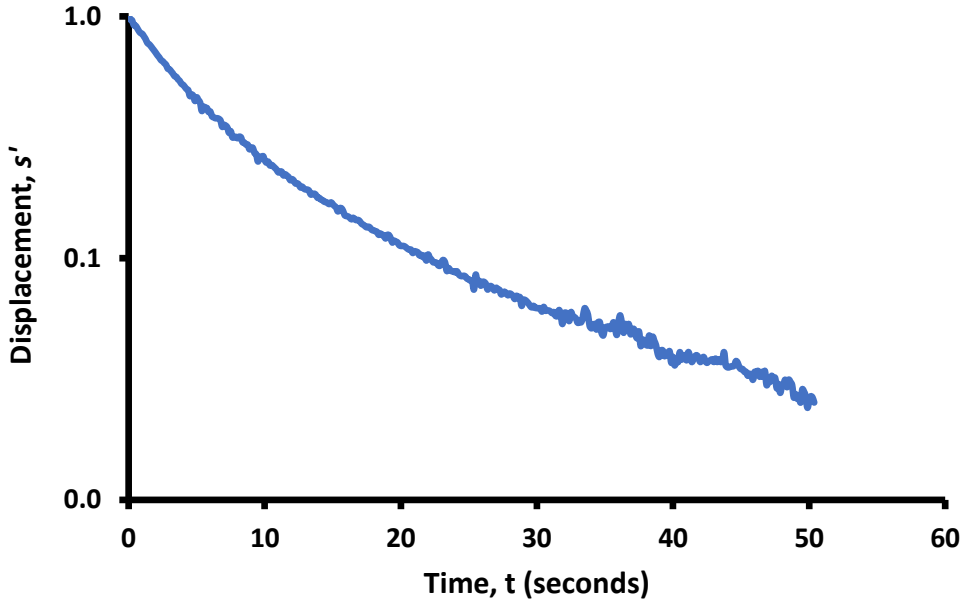

Figure 3-3b. Slug test recovery curve after removal of initial steep slope

3.2.2.3 Hvorslev method

The Hvorslev method was applied to slug test data in all wells. An estimate of the hydraulic conductivity is obtained from solving the following equation:

$$K = \frac{{r_c}^2 ln(\frac{R_e}{r_w})}{2LT_0} \quad (19)$$

Where,

r_c = Radius of the well casing [L]

R_e = Effective radius of slug test [L]

r_w = Effective radius of well screen [L]

L = Effective screen length [L]

$s'(0)^*$ = Revised initial displacement i.e. the y-intercept of the fitted trendline [L]

T_0 = Time it takes for water to rise or fall to 37% of $s'(0)^*$ [T]

The effective radius of the slug test is unknown, and in the case of partially penetrating wells the effective screen length should be used instead (Butler, 1997). Because a filter pack is present in the well design, the radius of the borehole was used as the effective radius of the well screen.

Equation 19 is the variant used for wells that partially penetrate an aquifer, as it uses the effective screen length instead of the aquifer thickness. The well construction dimensions are simply substituted into the equation. The T_0 parameter is more difficult to obtain and was gained first by fitting a straight line to the graph of normalised head versus time (Figure 3-4). As stated in the literature, the method of fitting a straight line to the data is important as the hydraulic conductivity estimate can be greatly affected. Butler (1996)

recommends using a trendline range of 0.15 < *s'* < 0.25 for the Hvorslev method. The application of this trendline range is illustrated in Figure 3-4.

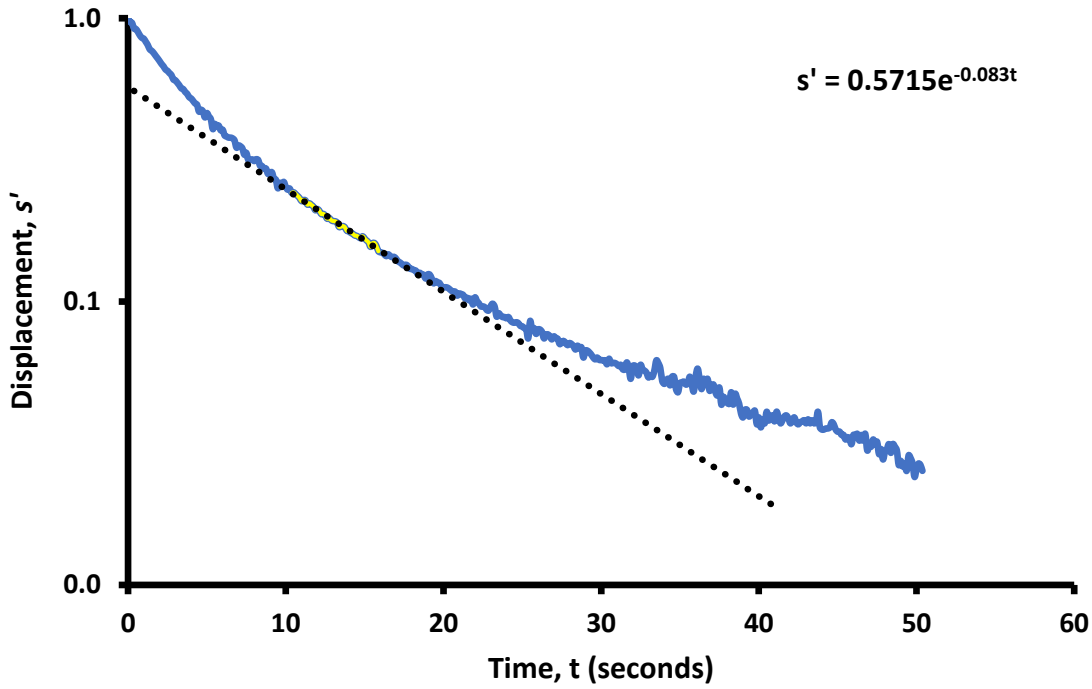

Figure 3-4. Example of a straight line fit to the slug test recovery data to obtain the slope equation. The trendline is fitted to the yellow portion of the data (0.15 < s' < 0.25).

The slope *s'* is used to obtain T_0 first by calculating 37% of the revised initial displacement, $s'(0)^*$. This value is then substituted into the equation of the slope as *s'*, and then solved to obtain t. The resulting value is T_0.

3.2.2.4 Bouwer and Rice method

An estimate of hydraulic conductivity is obtained from solving the following equation:

$$K = \frac{{r_c}^2 ln(\frac{R_e}{r_w^*})}{2LT_0} \quad (20)$$

Where,

r_w^* = $r_w(\frac{K_z}{K_r})^{\frac{1}{2}}$

K_z = Vertical component of hydraulic conductivity [L/T]

K_r = Horizontal component of hydraulic conductivity [L/T]

Isotropy was assumed such that r_w^* is equal to r_w. Equation 20 is very similar to equation 19, however the way that the effective radius (R_e) is estimated differs. For a partially penetrating well, R_e is estimated using a series of equations written in terms of $ln(\frac{R_e}{r_w^*})$ (Butler, 1997):

$$\ln(\frac{R_e}{r_w^*}) = [\frac{1.1}{\ln\left(\frac{d+L}{r_w^*}\right)} + \frac{A+B(\ln\left[\frac{B-(d+L)}{r_w^*}\right])}{L/r_w^*}]^{1/2} \quad (21)$$

Where,

d = distance from top of screen to the water table in an unconfined formation, or to an impermeable boundary in a confined formation [L]

A, B = empirical coefficients [dimensionless]

The empirical coefficients *A* and *B* were determined using the following equations (Butler, 1997):

$$A = 1.4720 + 3.537 \times 10^{-2}\left(\frac{L}{r_w^*}\right) - 8.148 \times 10^{-5}\left(\frac{L}{r_w^*}\right)^2 + 1.028 \times 10^{-7}\left(\frac{L}{r_w^*}\right)^3 - 6.484 \times 10^{-11}\left(\frac{L}{r_w^*}\right)^4 + 1.573 \times 10^{-14}\left(\frac{L}{r_w^*}\right)^5 \quad (22)$$

$$B = 0.2372 + 1.151 \times 10^{-3}\left(\frac{L}{r_w^*}\right) - 2.682 \times 10^{-6}\left(\frac{L}{r_w^*}\right)^2 - 3.491 \times 10^{-10}\left(\frac{L}{r_w^*}\right)^3 + 4.738 \times 10^{-13}\left(\frac{L}{r_w^*}\right)^4 \quad (23)$$

These expressions also form a plot that can be used as an alternative method of determining the empirical coefficients (Figure 3-5). Once the value of $ln(\frac{R_e}{r_w^*})$ had been determined, the hydraulic conductivity was calculated. T_0 was determined using the same procedure as described above for the Hvorslev method. However, the recommended trendline range of 0.2 < s' < 0.3 (Butler, 1997) was fitted instead.

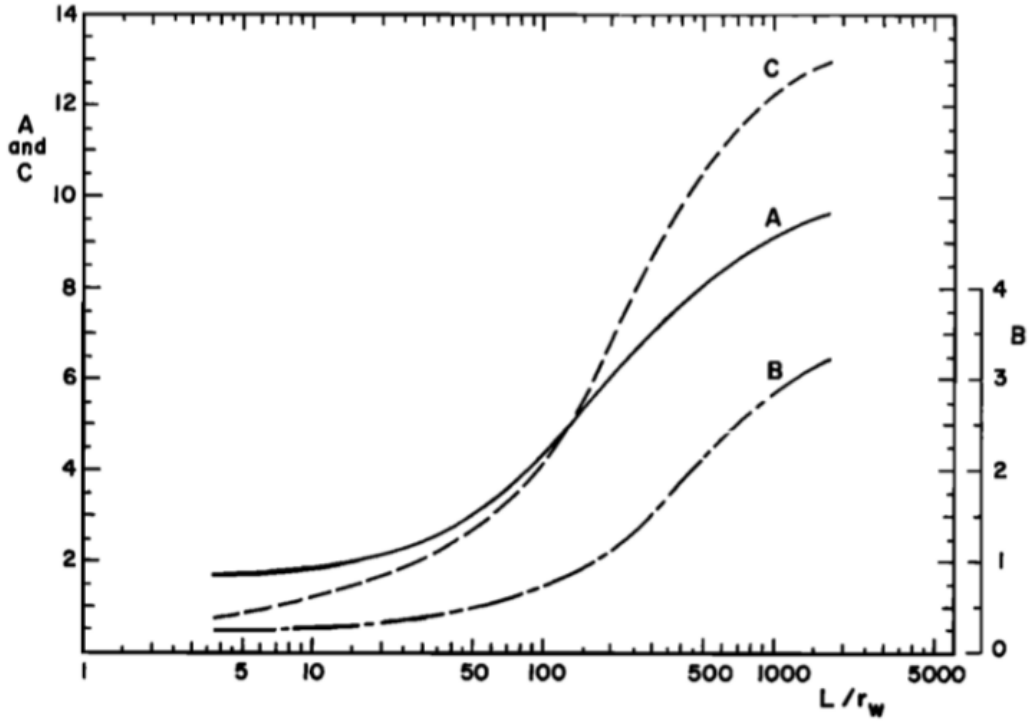

Figure 3-5. Graph for determining coefficients A and B for partially penetrating wells, and C for fully penetrating wells (Bouwer & Rice, 1976)

Slug tests were only conducted on one well (NB3) that was screened across the water table. The double straight-line effect, as described by Bouwer (1989), was evident for all tests conducted on this well. Because the first linear segment in the semi-log plot is representative of the filter pack drainage, only the second linear segment was analysed. Thus, the slope of *s'* was applied to the second linear segment only. This meant that the recommended head ranges of Butler (1997) were not applicable to this scenario. Instead, both analytical models were applied using one slope representative of the second linear segment of the semi-log plot.

All normalised slug test recovery plots with trendlines fitted are displayed in Appendix C.

3.2.2.5 Underdamped slug tests

It was evident from the slug test recovery curves that NB4, which screens the margin between the Christchurch Formation and the Riccarton Gravel, was displaying underdamped behaviour. Oscillations occurred between 1 and 8 s since the start of each test. Analytical modelling software AQTESOLV was used as an aid to gain a hydraulic conductivity estimate for this well. This software utilises existing analytical models and incorporates visual and automatic curve matching tools. NB4 slug test data were applied to the Springer and Gelhar solution (1991) for analysis of underdamped slug tests in unconfined aquifers. The automatic curve matching tool utilises a method of non-linear least squares to optimise the match between the slug test data and the analytical solution. Five slug tests from NB4 were analysed using this software, and the average taken.

3.2.3 Numerical models

MODFLOW is a widely accepted finite-difference three-dimensional groundwater flow model developed by the USGS (Harbaugh, 2005). Processing Modflow for Windows (PMWIN) (Chiang & Kinzelbach, 1998) was the graphical user interface used to build the slug test model for this study. One model was created for each of the nine wells that had undergone slug tests. Each model was set up identically with the exception of aquifer thickness, depth, aquifer type (i.e., unconfined or confined) storage and screen length. This was possible because all the wells have identical construction in terms of borehole and well casing diameter, and the use of a filter pack and bentonite seal. The inverse modelling method was applied using the hydraulic conductivity values obtained from the analytical models as an initial estimate. A graph of head in the well over time was produced using the model output data. This curve was calibrated with the slug test recovery curve by manually changing the hydraulic conductivity of the aquifer in PMWIN until the curves matched each other. The hydraulic conductivity value that produced the matching curve was taken as the final result. Numerical model output / slug test inverse curve matching plots are located in Appendix D.

Model domain:

A grid consisting of 112 rows and 112 columns was generated in Modflow. One quarter of the problem was simulated, such that the well was located in the corner of the grid. The well and the surrounding filter pack were simulated using 12.5 mm cells. The well was two cells wide, and the filter pack three cells wide. Each successive cell increased in size by 1.06, resulting in an outer boundary cell approximately 6 m wide. Overall, the model domain was 100 m in length and width. A constant-head boundary condition was assigned to the two outer boundaries because the head should not be affected by the slug test, and the boundaries adjacent to the well were defined as no-flow boundaries. It

was observed that the model extent was large enough that the water levels in the well were not significantly affected by the constant head boundary condition.

Hydro-stratigraphic unit parameters:

The aquifer material was simulated by assuming isotropy. All layers were initially assigned a hydraulic conductivity value determined from the analytical models. Porosity and specific yield of the aquifers are not known and were assumed equal. Johnson (1963) defines average values of specific yield for a range of materials, some of which are presented in Table 3-1. As the aquifers consist mostly of either sandy gravel or medium sand, 25% porosity and specific yield was used for all models. The hydro-stratigraphic units under confined conditions require a value of specific storage for the model. A range of specific storage values for different unconsolidated materials are presented by Domenico & Mifflin (1965) in Table 3-2. Because the aquifer material consists of sandy gravel with minor silt and clay, the upper value in the dense sandy gravel range of 1.0×10^{-4} m^{-1} was used. The Strongly Implicit Procedure (SIP) solver package was used to solve the finite-difference equations at each time step of the stress period, utilising its default settings.

Table 3-1. Specific yield values for various materials (adapted from Johnson, 1963)

Material	**Specific yield % (average)**
Fine sand	21
Medium sand	26
Coarse sand	27
Gravelly sand	25
Fine gravel	25

Table 3-2. Specific storage range for various materials (adapted from Domenico & Mifflin, 1965)

Material	**Specific storage, m^{-1}**
Plastic clay	$2.6 \times 10^{-3} \rightarrow 2.0 \times 10^{-2}$
Stiff clay	$1.3 \times 10^{-3} \rightarrow 2.6 \times 10^{-3}$
Medium hard clay	$9.2 \times 10^{-4} \rightarrow 1.3 \times 10^{-3}$
Loose sand	$4.9 \times 10^{-4} \rightarrow 1.0 \times 10^{-3}$
Dense sand	$1.3 \times 10^{-4} \rightarrow 2.0 \times 10^{-4}$
Dense sandy gravel	$4.9 \times 10^{-5} \rightarrow 1.0 \times 10^{-4}$

Well construction:

The vertical positioning of the well screen within the aquifer was defined using a single layer. Specific storage and porosity values of 1 were applied for all well cells to simulate the water column. To differentiate the filter pack from the rest of the aquifer, a different value of hydraulic conductivity was used. This was derived from applying the 2 mm particle size of the filter pack to the Hazen empirical formula. The Hazen formula was considered the most reliable empirical model to use in this instance because the domain of applicability is specifically for uniform sediments.

3.3 Results

3.3.1 Slug tests

NB3 (Springston Formation):

NB3 is screened across the water table in the Springston Formation. Due to a low water level in the well, it was not possible to fully submerge the slug to conduct the slug test. Instead, the slug was partially submerged and pulled out once the water level had stabilised. A very low initial displacement occurred as a result. Figure 3-6 displays two distinct lines. As identified in the literature review, when performing a slug test on wells screening the water table an initial steep line may occur due to water moving through the highly conductive filter pack. The analyses should be undertaken on the second slope which is representative of the aquifer. This procedure was adopted for the analysis of the slug tests on NB3.

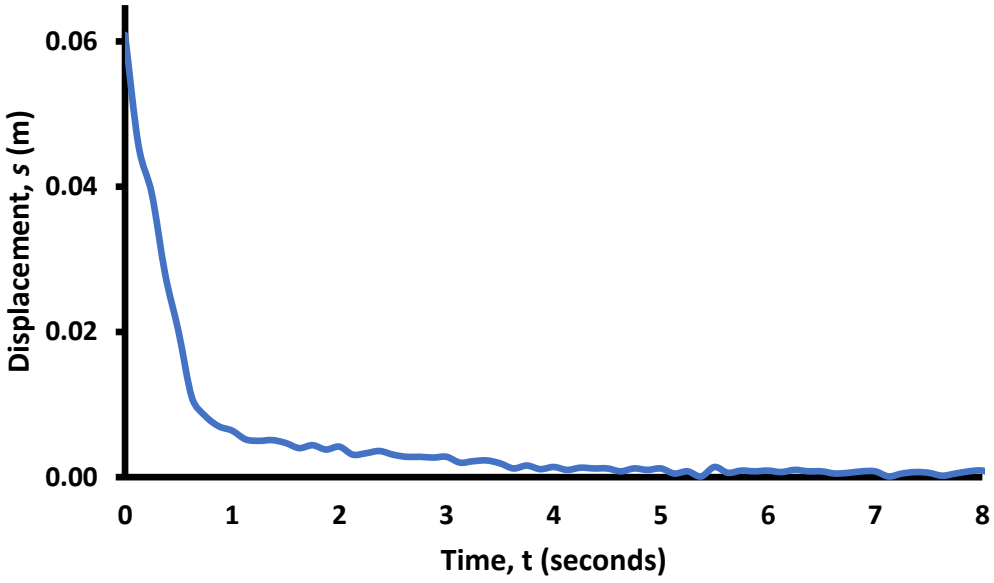

Figure 3-6. Example of rising head slug test recovery curve for NB3

NB4 (interface of Springston Formation and Riccarton Gravel):

The slug tests conducted on NB4 recovered quite quickly, however the response curve (Figure 3-7) displays an uneven oscillatory pattern. All tests on the well displayed the same response pattern. The oscillations occur between 1 and 8 s where there is a trough followed by a peak.

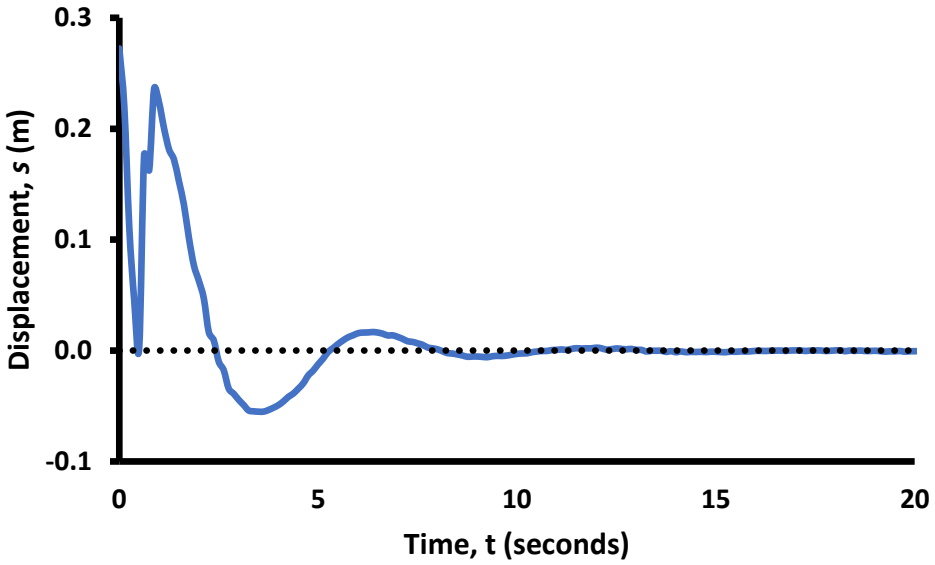

Figure 3-7. Example of rising head slug test recovery curve for NB4

NB2 (Riccarton Gravel):

NB2 screens the unconfined Riccarton Gravel so the head in the well was below ground level. This allowed for better control over the slug. The initial displacement for all tests on this well varied between 0.3 and 0.4 m, which is slightly under the theoretical initial displacement of 0.41 m. The slug test recovery curve displays a bumpy response, although with a clear trend (Figure 3-8). It is evident that the water level rose slightly past the pre-test head before returning to back to the static water level. This slug test response is termed critically damped. A critically damped system is in between the extremes of underdamped (oscillatory) and overdamped behaviour, signifying that there is some influence of momentum in the water column coming from the aquifer. The test reached static water level in about 6 s.

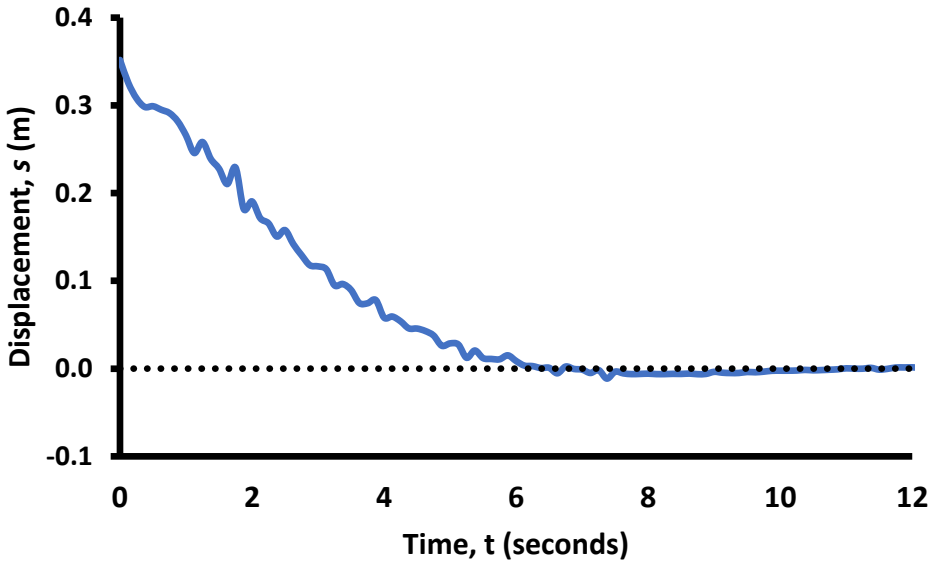

Figure 3-8. Example of rising head slug test recovery curve for NB2

NB5 (bottom of Bromley Formation):

NB5 is the only well at the Tram Road site screened in the Bromley Formation. Like NB1, this hydro-stratigraphic unit is also under artesian pressure and required a PVC standpipe to stabilise the head. The slug was withdrawn in the afternoon and the pressure transducer left in the well overnight to ensure the water level had enough time to recover. The water recovered in a smooth exponential manner, taking about 3 h to reach static level (Figure 3-9). Note that this figure and the overall analysis has been corrected for the effects of barometric pressure as a change in barometric pressure of more than 1 cm H_2O was recorded over the duration of test.

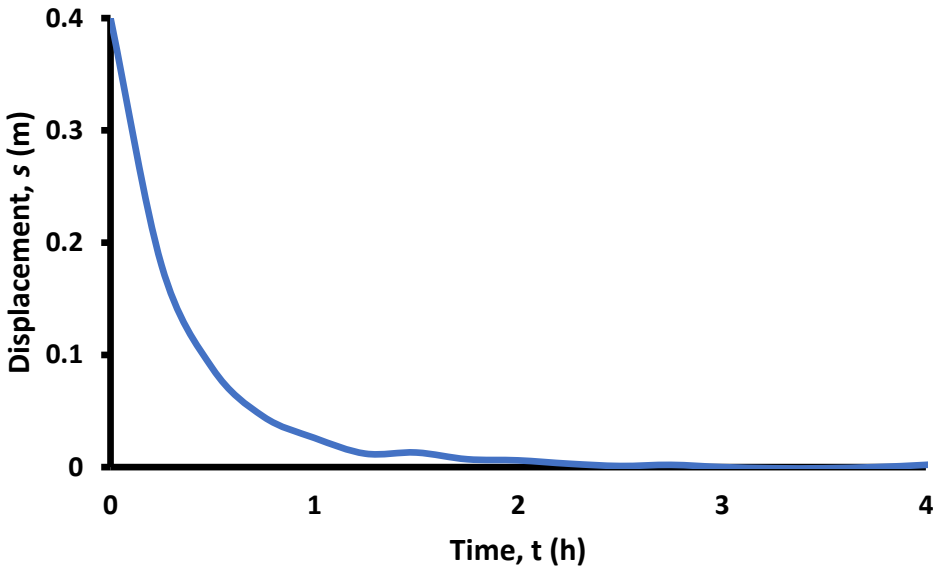

Figure 3-9. Example of rising head slug test recovery curve for NB5 (corrected for the effects of barometric pressure)

NB1 (top of Linwood Gravel):

It should be noted that this well required a PVC standpipe and a step ladder to conduct the test making handling the slug difficult. The slug test recovery curve displays a large initial displacement and oscillatory pattern within the first second of the slug test (Figure 3-10). A smooth recovery curve follows this, taking about 40 s to fully recover.

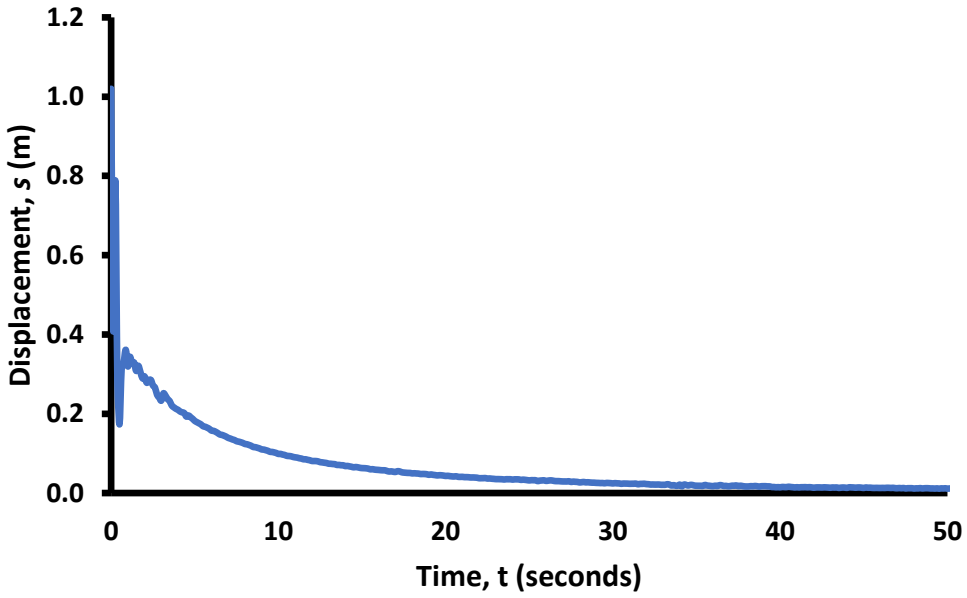

Figure 3-10. Example of rising head slug test recovery curve for NB1

AT4 (boundary of Christchurch Formation and Riccarton Gravel):

Slug tests performed on AT4 displayed a smooth response. Similarly to the NB2 slug test response, Figure 3-11 displays critically damped behaviour. However, this is more pronounced for AT4 signifying that this well has a greater influence of momentum in the water column coming from the aquifer. The initial displacement is also relatively low at just 0.25 m. Full recovery was reached in about 8 s.

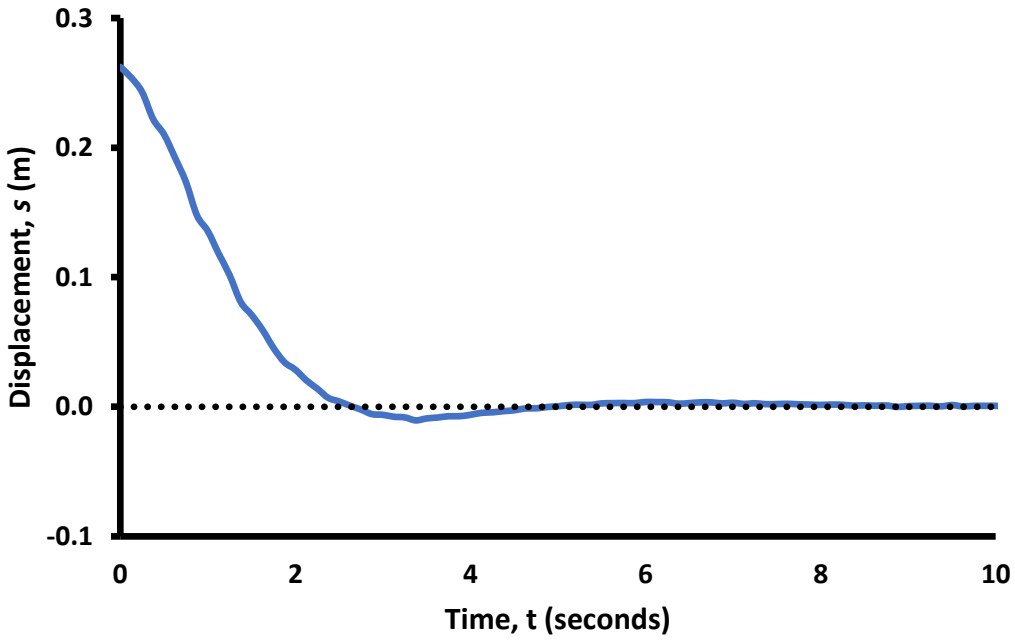

Figure 3-11. Example of rising head slug test recovery curve for AT4

AT3 (Riccarton Gravel aquifer):

The slug tests conducted on AT3 produced smooth exponential recovery curves (Figure 3-12). Compared to the other wells screened in the Riccarton Gravel aquifer, this well took the longest to fully recover (~ 90 s). This contrasts to the wells corollary NB2, at the Tram Road site further inland, which recovered in just 6 s.

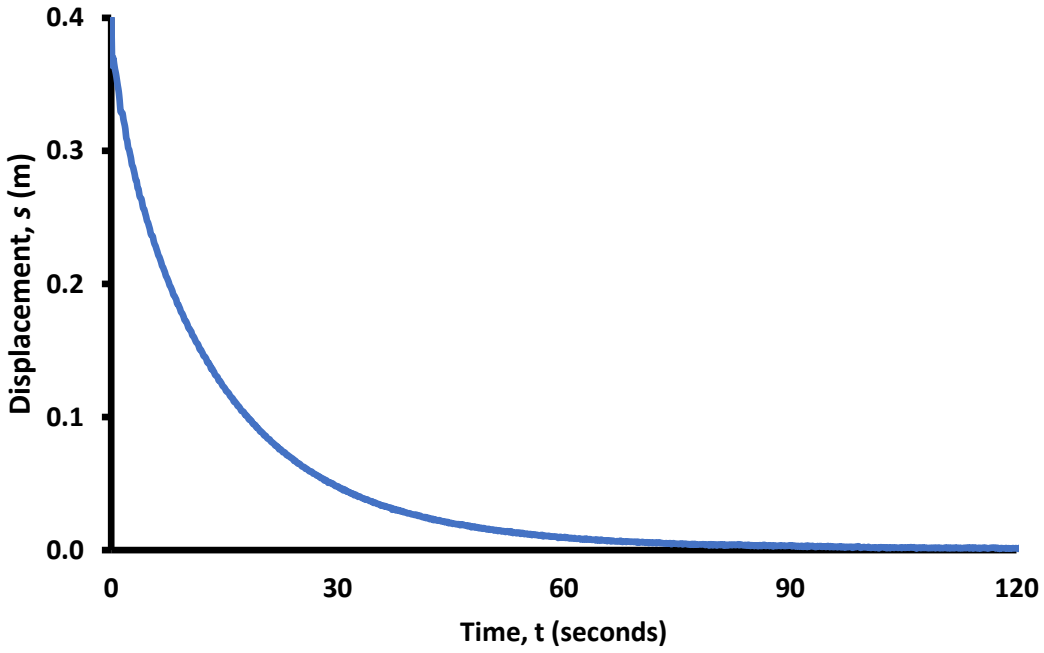

Figure 3-12. Example of rising head slug test recovery curve for AT3

AT2 (bottom of Bromley Formation aquitard):

AT2 also required a PVC standpipe, although the head was low compared to the artesian wells at the Tram Road site. This was the slowest responding well at the Adderley Terrace site, corresponding to NB5. However, AT2 reached full recovery in less than 3 min (Figure 3-13), compared to 3 h for NB5. The initial displacement of just under 0.4 m is similar to the majority of the slug tests conducted on the other wells.

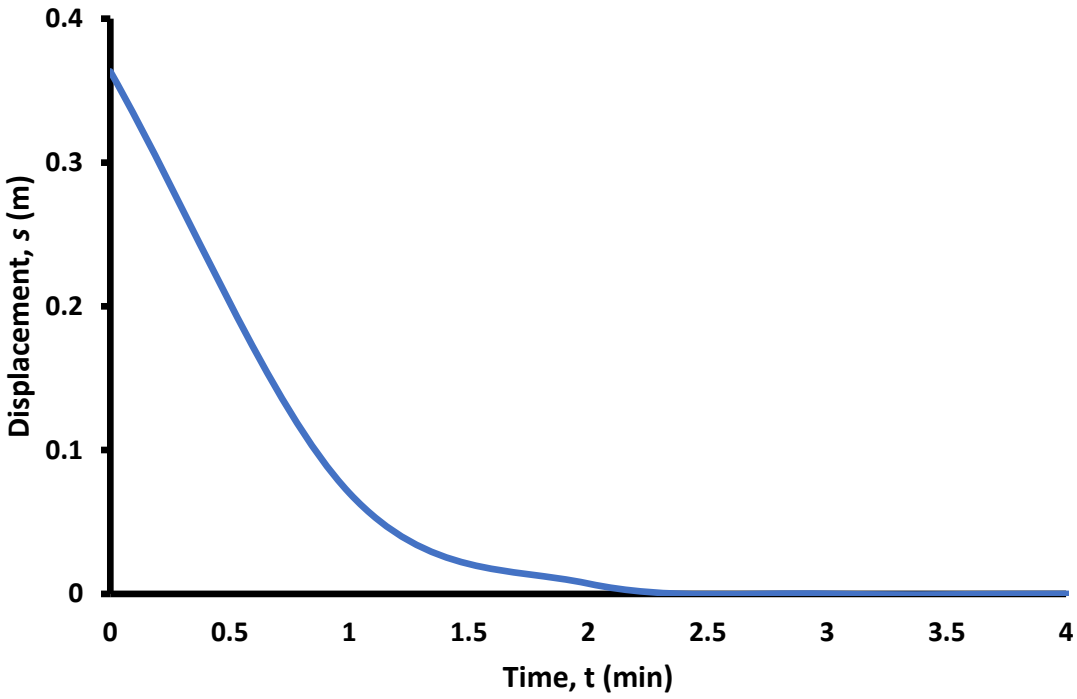

Figure 3-13. Example of rising head slug test recovery curve for AT2

AT1 (top of Linwood Gravel aquifer):

AT1 corresponds to NB1 in terms of screen depth, however the head in the well was much lower for AT1. A PVC standpipe was used, although no step ladder was required meaning the slug was easy to handle. Figure 3-14 illustrates a smooth exponential recovery. The water level recovered fully in about 17 s, which was much faster than NB1. The initial displacement was also close to the theoretical displacement.

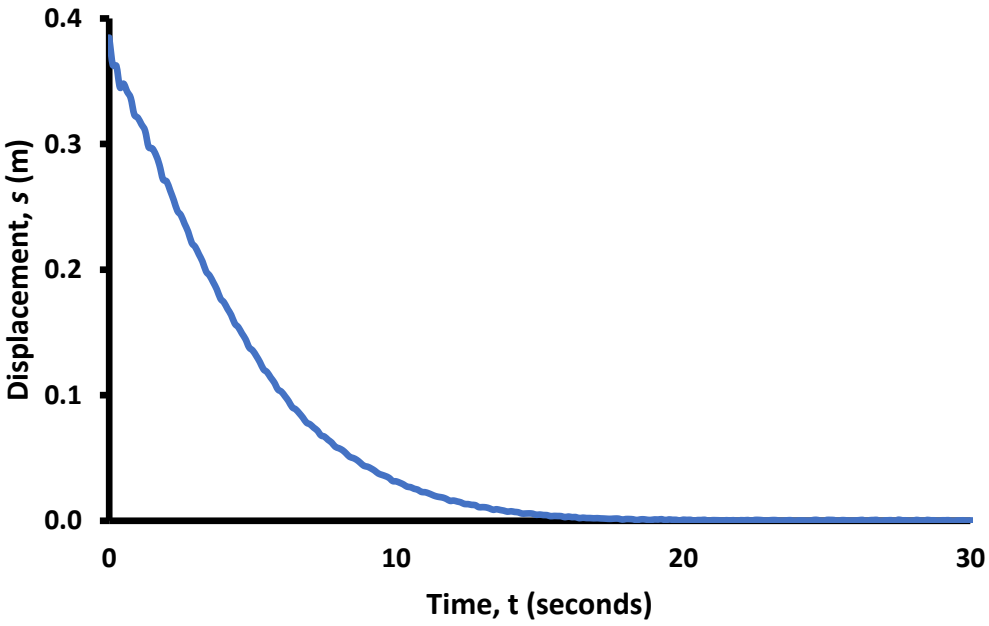

Figure 3-14. Example of rising head slug test recovery curve for AT1

3.3.2 Hydraulic conductivity

The following table summarises the hydraulic conductivity values obtained using the Hvorslev and Bouwer and Rice analytical models. It is evident from Table 3-3 that both analytical modelling methods used generally produced similar values. However, the Bouwer and Rice method consistently produced lower results. A vertical profile of hydraulic conductivity through the Tram Road and Adderley Terrace sites is illustrated in Figure 3-15.

Table 3-3. Hydraulic conductivity values (m/d) obtained from analytical and numerical modelling of slug tests

Well ID	Depth (m bgl)	Hydro-stratigraphic Unit	Springer & Gelhar	Hvorslev	Bouwer & Rice	Numerical model
NB3	2 - 3	Springston Formation	n/a	43	29	53
NB4	7.8 – 9.3	Contact: Springston Formation / Riccarton Gravel	54	n/a	n/a	n/a
NB2	19.6 - 20.1	Riccarton Gravel	n/a	89	65	57
NB5	33 - 33.5	Bromley Formation	n/a	0.092	0.088	0.10
NB1	38.5 - 39	Linwood Gravel	n/a	9.8	7.9	18
AT4	8.4 - 8.9	Top of Riccarton Gravel	n/a	210	190	130
AT3	25.1 - 25.6	Riccarton Gravel	n/a	7.4	7.2	12
AT2	33.5 - 34	Base of Bromley Formation / top of Linwood Gravel	n/a	3.5	3.1	3.4
AT1	39.9 – 40.4	Linwood Gravel	n/a	34	25	25

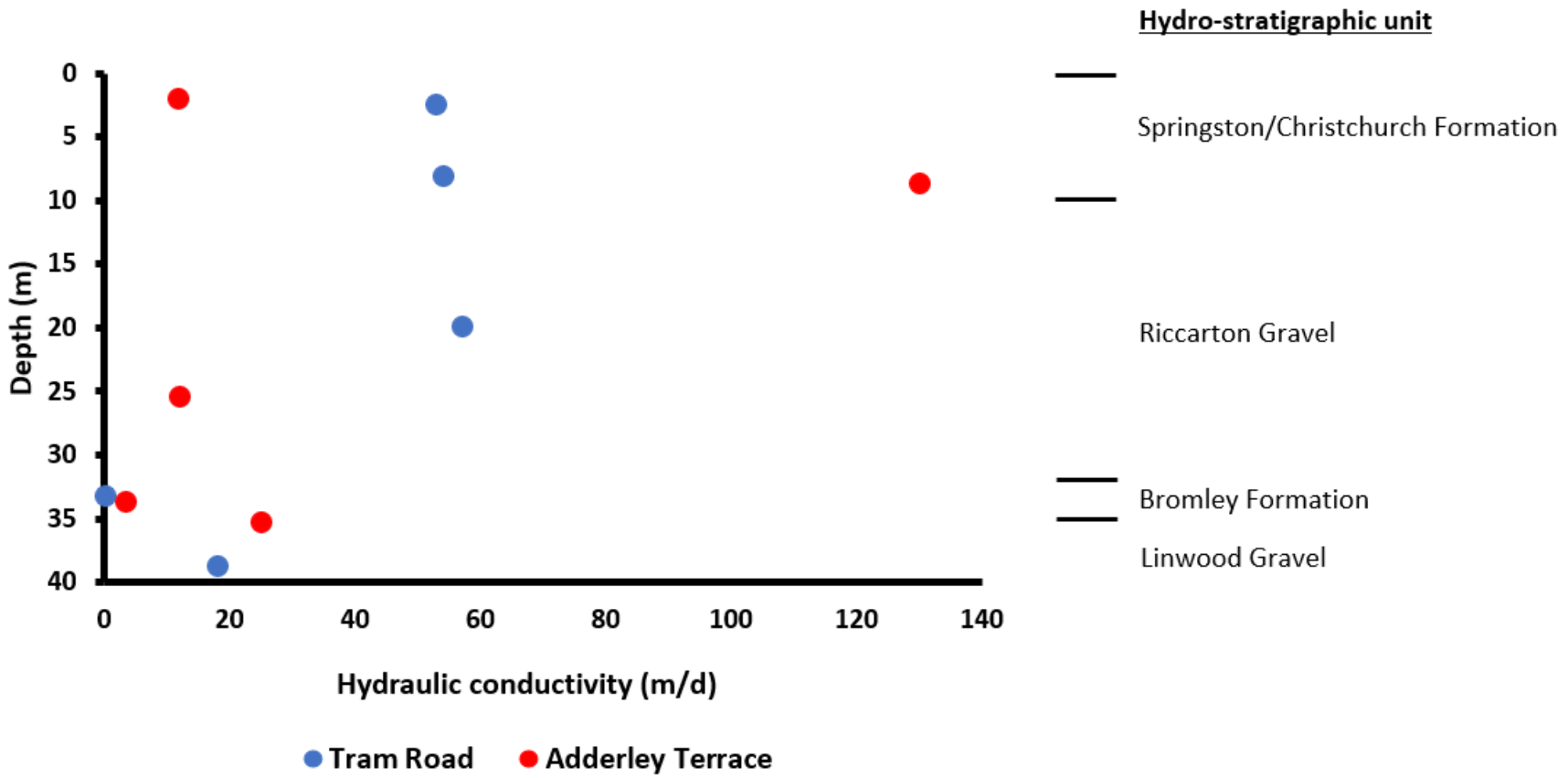

Figure 3-15. Vertical profile of hydraulic conductivity through hydro-stratigraphic units at Tram Road and Adderley Terrace sites, obtained from numerical modelling results. Due to unavailability of numerical modelling results for NB4 and AT5, analytical or empirical modelling results were used instead.

Chapter 4. DISCUSSION

In this section, the methods and results will be discussed in relation to the aims of this study i.e. the characterisation of an extension to the Christchurch City aquifer, and critical evaluation of methods for determining hydraulic conductivity of aquifer sediments. In doing this, comparisons will be made between the results obtained from each method, as well as between the two sites for assessment of spatial variability. Table 4-1 includes hydraulic conductivity estimates gained from all methods and allows direct comparison between results. Ultimately, the reliability and significance of these results in the context of the study aim is dependent on the methods applied to acquire them. This will be discussed below.

4.1 Particle size distribution analysis

Particle size distribution analysis is widely perceived to be a very simplified approach, yielding unreliable results. The range of limitations must be considered when interpreting the significance of the results. One important limitation is the sample size. The bulk sediment samples used for the analysis were very small (1.5 – 3.0 kg), and therefore do not incorporate heterogeneity within the hydro-stratigraphic unit. There is a high possibility that the sediment samples were taken from a section of relatively low permeability, or alternatively, a high permeability area such as a buried gravel channel conduit. Further error was produced through destruction of sediment structure, and from application of the various empirical models which produced variable results.

Table 4-1. Hydraulic conductivity values (m/d) gained from empirical, analytical, and numerical model assessments

			Particle size distribution				**Slug tests**		
Well ID	Hydro-stratigraphic Unit	Depth (m bgl)	Hazen	Slichter	Kozeny Carman	Beyer	Hvorslev	Bouwer & Rice	Numerical model
NB3	Springston Formation	2 - 3	320	63	140	310	43	29	53
NB4	Contact: Springston Formation / Riccarton Gravel	7.8 – 8.3	30	6.0	13	26	n/a	n/a	n/a
NB2	Riccarton Gravel	19.7 - 20.2	0.38	0.075	0.17	n/a	89	65	57
NB5	Base of Bromley Formation / top of Linwood Gravel	33 - 33.5	0.22	0.042	0.94	n/a	0.92	0.88	0.10
NB1	Linwood Gravel	38.5 - 39	n/a	n/a	n/a	n/a	9.8	7.9	18
AT5	Christchurch Formation	1-5 – 2.5	27	5.3	12	23	n/a	n/a	n/a
AT4	Top of Riccarton Gravel	8.4 - 8.9	20	3.9	8.6	13	210	190	130
AT3	Riccarton Gravel	25.1 - 25.6	230	46	100	280	7.4	7.2	12
AT2	Base of Bromley Formation / top of Linwood Gravel	33.4 - 33.9	2.4	0.49	1.1	3.4	3.5	3.1	3.4
AT1	Linwood Gravel	35 - 35.5	140	28	62	120	34	25	25

4.1.1 Significance of particle size distribution to aim of thesis

Firstly, it is crucial to emphasise that all of the samples used in the particle size distribution analysis were extracted from one borehole from each site i.e. NB5 and AT2 which screen the bottom of the Bromley Formation. Given that the wells in the cluster are separated by several metres, direct comparisons between particle size distribution results and slug test results can only confidently be made for wells NB5 and AT2. All other samples have been subjected to potentially large amounts of error because the samples have not been directly extracted from the borehole that is being tested.

Regardless of the large margins of error associated with this method, these results are still useful for the purpose of the study. The results show how hydraulic conductivity varies vertically throughout the aquifer system. Additionally, the results show how hydraulic conductivity varies horizontally between the two sites, showing the extent of heterogeneity in the hydro-stratigraphic units. Overall, an initial estimate of hydraulic conductivity is gained through these tests, that is both cheap and easy to achieve. Firstly, the results give confirmation that the aquifer system is highly heterogeneous based on horizontal variability between locations. Secondly, the results confirm that the system is highly conductive e.g. both the Springston Formation and Riccarton Gravel aquifers have hydraulic conductivity estimates exceeding 50 m/d.

4.1.2 Comparison of corresponding wells

With the data available, there are three pairs of wells that correspond to each other that are screened at similar depths. Figure 4-1 displays particle size distribution curves comparing NB5 and AT2, both of which screen the Bromley Formation. Both of these samples include higher proportions of sand and silt compared to the other wells. However, both the range of grain sizes and their proportions are very different. Whilst NB5 is a well graded sample, where all grain sizes from clay to gravel are represented, AT2 is poorly graded and consists predominantly of medium sand. This is further evidence to support

the interpretation of a highly heterogeneous aquifer system. The Bromley Formation was formed under a marine/estuarine depositional system. The bore logs illustrate a lot of geological variation in this hydro-stratigraphic unit, with beds of silt, clay, peat and sand. This stratigraphy is associated with an aggrading/retrograding coastal unit. The presence of a significant amount of gravel in well NB5 could be a result of a river flood deposit. It is more likely, however, that the well is screening the very top of the Linwood Gravel. This highlights the difficulties in defining hydro-stratigraphic unit boundaries for the aquifer system. Although there are often markers within a formation to help distinguish it e.g. peat bed in Bromley Formation, the margins are often not obvious and defining them is subjective.

From the empirical modelling, AT2 returned hydraulic conductivity estimates ranging from 0.49 to 3.4 m/d. Analysis of NB5 returned lower estimates of < 0.22 m/d as expected due to the high proportion of fine grains in the sample. The large range of values calculated from the different empirical models is reflective of the uncertainty resulting from particle size distribution analysis.

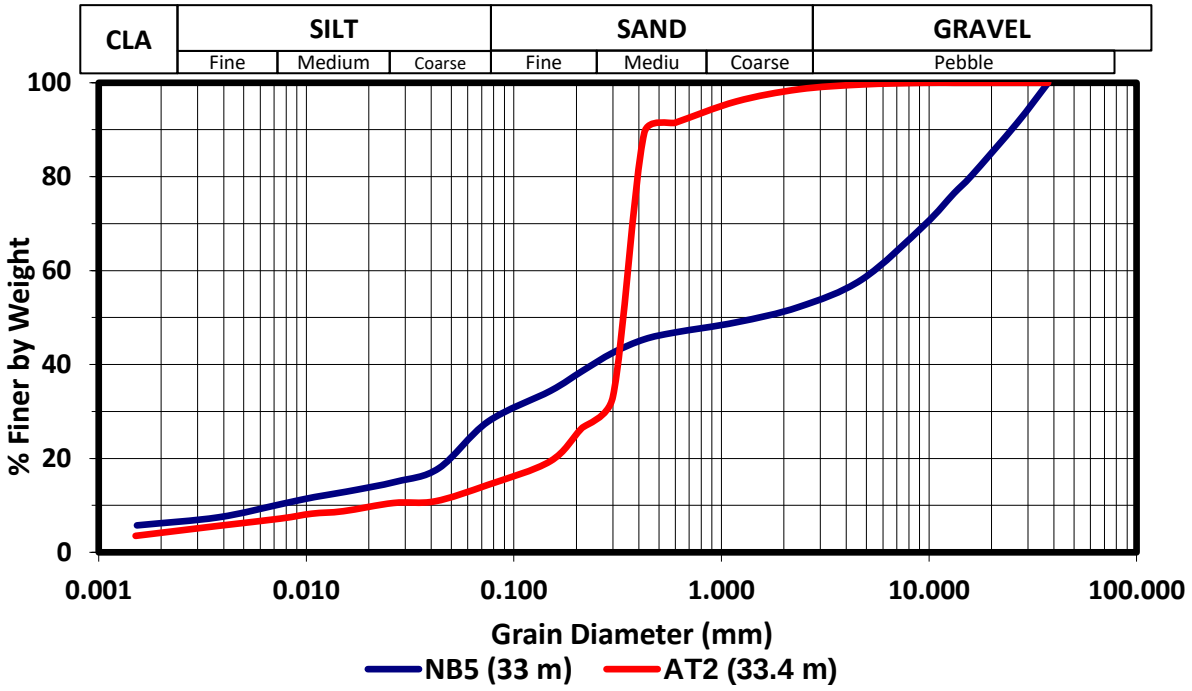

Figure 4-1. Particle size distribution comparison between NB5 and AT2 (showing depth to top of well screen)

Wells NB4 and AT4 both screen the margin between the two shallowest hydro-stratigraphic units at approximately 8-9 m depth. As the top hydro-stratigraphic unit is different between sites (Springston Formation/Christchurch Formation) it can be expected that the hydraulic conductivities may differ, especially given that the Christchurch Formation is a confining aquitard. The particle size distribution curves comparing these wells is displayed in Figure 4-2. They are in fact quite similar curves both in terms of shape and proportions of particles sizes. Well AT4 has a slighter higher proportion of coarse grains. This is reflected in the hydraulic conductivity estimates, where NB4 ranges from 6.0 to 30 m/d and AT4 having lower, although similar values of 3.9 to 20 m/d. The expectation was that the AT4 particle size distribution would yield a significantly lower hydraulic conductivity value due to the presence of the Christchurch Formation. The similarities in results could be a result of three possibilities:

1. The majority of the bulk sediment sample was extracted from the Riccarton Gravel aquifer and excludes representative material from the Christchurch Formation.
2. The bulk sediment sample was taken from a highly conductive portion of the Christchurch Formation. This is conceivable due to the findings of Talbot et al. (1986) i.e. gravel channels resulting from river flood events have been identified within the Christchurch Formation and are likely to be found within deeper confining units.
3. Much of what is perceived to be the Christchurch Formation at Adderley Terrace is alluvial gravel deposited by the Kaiapoi River, which was included in the sample. This is highly plausible given that the well cluster is situated on the bank of the river.

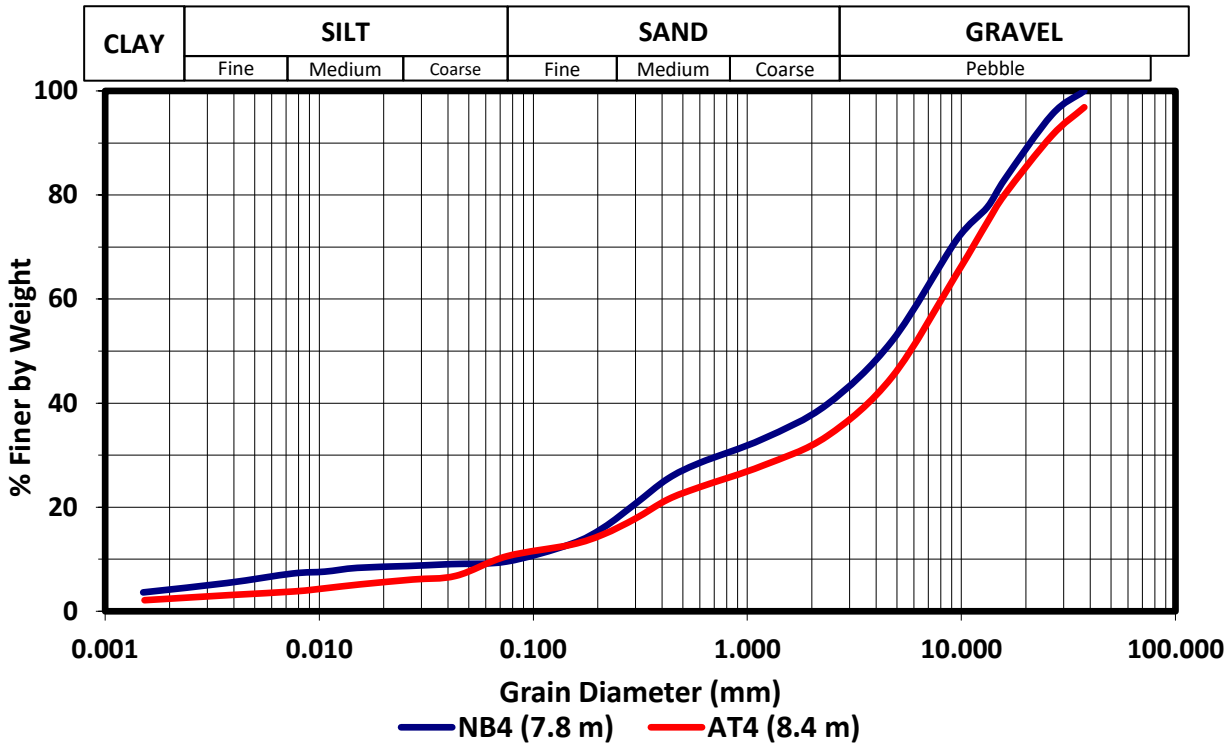

Figure 4-2. Particle size distribution comparison between NB4 and AT4 (showing depth to top of well screen)

Particle size distributions of NB3 which screens the water table in the Springston Formation aquifer, and AT5 which screens the water table in the Christchurch Formation are compared in Figure 4-3. NB3 has over 80% gravel, 15% sand and a minor silt and clay content. AT5 has a similar silt and clay content, although there is a much higher proportion of sand and lower proportion of gravel. This is characteristic of the differing depositional environments of this hydro-stratigraphic unit. Tram Road (including NB3) is located on the periphery of the mapped coastal confined area, on the unconfined Plains aquifer side that incorporates the Springston Formation. The results represent this change with NB3 returning a highly conductive range of 63 – 320 m/d reflecting the permeable alluvial gravel deposit. AT5 returned lower hydraulic conductivity estimates ranging between 5.3 and 27 m/d which is more reflective of the marine/estuarine depositional setting. However, this is still quite conductive which is partially due to the gravel presence within the sample. There is a high likelihood that this gravel incursion was deposited from a river flood event as per the findings of Talbot et al. (1986). AT5 is

screened well within the Christchurch Formation in very young sediments so there is no chance that the well is screening part of the Riccarton Gravel aquifer below.

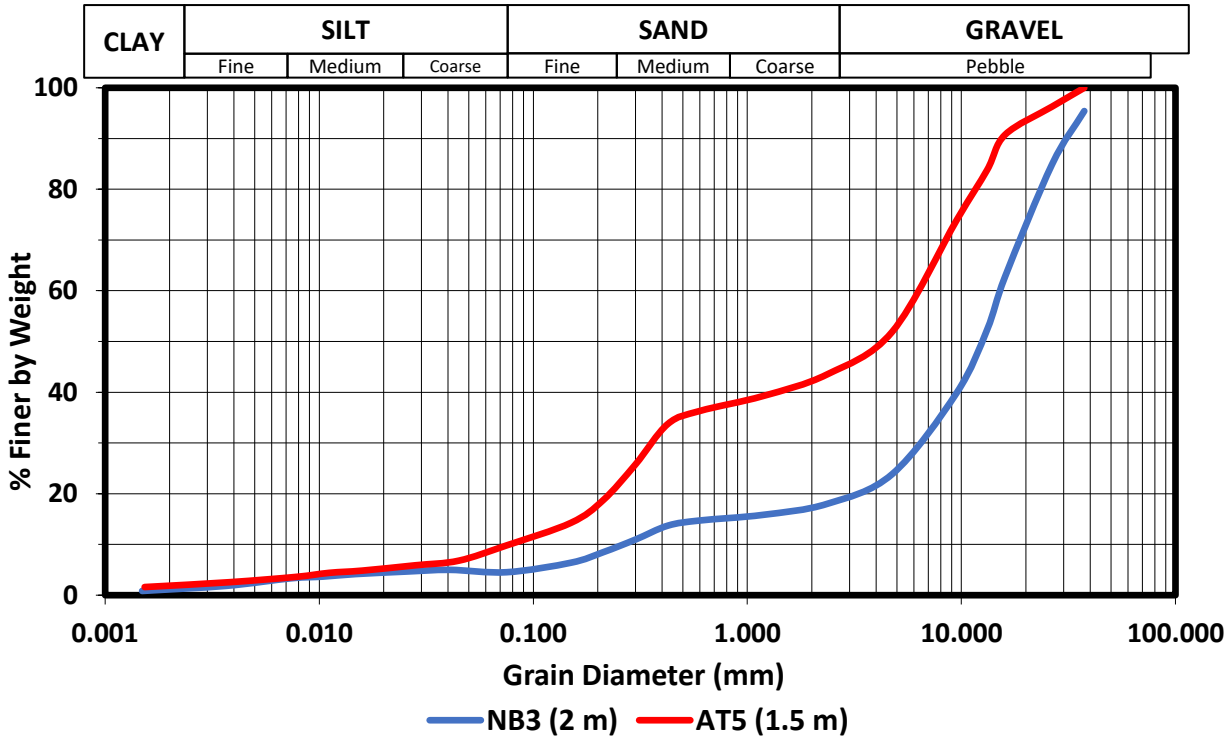

Figure 4-3. Particle size distribution comparison between NB3 and AT5 (showing depth to top of well screen)

4.1.3 Reliability of empirical models

The literature review identified that the Kozeny-Carman method was recommended by many authors (Carrier III, 2003; Pucko & Verbovšek, 2015; Zhang, 2017) for use with a wide range of materials. Therefore, it is suggested that empirical models that produce vastly different values are unreliable. Both the Hazen method and the Beyer method produced very high hydraulic conductivity estimates. However, the Beyer method does not produce valid estimates for highly heterogeneous material where $C_\mu > 500$. This was the case for two of the samples. Thus, the Beyer method results can be discarded as unreliable. The Hazen method, however, is widely used for well graded sand, provided it

has a uniformity coefficient less than five. AT2, which screens a sandy section of the Bromley Formation, was the most uniform sample. However, the uniformity coefficient was 16, far exceeding the domain of applicability for the Hazen method. The Slichter method produced the lowest values of all methods. The values are in general less than 50% of the values obtained using the Kozeny-Carman method, which returned the next lowest values. Contention between Pucko & Verbovškev (2015) and Odong (2007) on the accuracy of the Slichter method, combined with the degree of difference in the values compared to other methods offers low confidence in these results. For wells NB3 and AT3, the Slichter method did provide the closest results compared to the slug test analyses. However, comparisons of this type are inconclusive because the samples were not taken from the well being measured. Therefore, it is suggested that the Kozeny-Carman results provide the best estimation of hydraulic conductivity of the empirical models used in this study.

4.2 Slug test analysis

Slug test analyses provide more reliable results than those obtained from particle size distribution analysis. This is because the data are derived from an in-situ field testing method, thus the actual aquifer system is being tested with the structure intact. Additionally, a larger volume of aquifer is being tested compared to the particle size distribution method. During slug testing there are several ways in which human error can be induced. In this study, it was difficult to consistently obtain smooth slug test recovery curves. Manually inserting a concrete slug seemed to create noise in the data, as well as an initial displacement that was in some cases much greater than the theoretical displacement. More commonly, the initial displacement was less than the theoretical displacement. These difficulties were exacerbated due to the highly conductive nature of the aquifer system. Many of the wells exhibited different response patterns, including oscillations, and inconsistent sharp peaks. This made analysis much more difficult. The analytical models are still very simplified and do not represent the complex reality of the aquifer setting. However, they can provide a rough estimate that is more reliable than

particle size distribution analysis. Numerical modelling, which is associated with less assumptions and simplifications regarding boundary conditions than analytical modelling, was expected to provide the most reliable and accurate hydraulic conductivity estimates. This will also be discussed.

4.2.1 Significance of slug test analysis to aim of thesis

As with the particle size distribution results, the slug test results are not representative of the aquifer system on a regional scale because of the small volume of aquifer tested. Due to the heterogeneity of the aquifer system, there is a high likelihood that the well is screening an area of relatively low permeability or alternatively an area of high permeability such as a gravel flood deposit. Therefore, there is low confidence that the slug test hydraulic conductivity results represent the aquifer system regionally. Like the results from the particle size distribution analysis, they help construct a hydraulic profile of the shallow hydro-stratigraphic units at the groundwater discharge zone of the Ashley-Waimakariri Plains. Although neither the horizontal or vertical hydraulic conductivity is measured independently, the results still provide a useful means of understanding potential local movement of groundwater, which may aid future transport studies in the area. Hydraulic conductivity and hydraulic gradient govern groundwater flow. Thus, the high values of hydraulic conductivity signify potential for flow. Whether groundwater is flowing then depends on the hydraulic gradient, which can be measured.

4.2.2 Slug test error

There were various difficulties associated with the use of a concrete slug to undertake this testing. Firstly, it was necessary to conduct several tests (usually 10) for each well due to the likelihood of a failed test. The most common reason for a failed test was the pressure transducer snagging on the slug test rope. It is a requirement that the pressure transducer remains still throughout the test to correctly measure head in the well. This occurred often because the pressure transducer cable and the slug test rope were both hanging freely in the well and would sometimes intertwine.

The main issue that was discovered from examining slug test results was the initial displacement values from using the thick slug, the results of which were not analysed in this work. From looking at the head response plots it was evident that the falling head slug test was producing an inconsistent, non-repeatable response. The max displacements of the falling head slug tests were often very high compared to the rising head slug tests. Figure 4-4a is a comparison of rising head and falling head slug tests using the thick slug compared to the theoretical displacement of 0.75 m. The displacements caused by introducing the slug are in some cases over five times the theoretical displacement for the thick slug. It is hypothesised that this is due to a ‘piston effect’ where the slug creates a pressure wave after being inserted in the well. This mechanism may have also been responsible for other inconsistent response patterns that were common within the first second of the slug test. The thinner slug was used in conjunction with the rising head slug test to combat this issue. Although the result is still a higher displacement than expected (Figure 4-4b), it is both much more consistent and closer to the expected displacement of 0.41 m. However, the slug out displacement of the thinner slug was much greater than 0.41 m for NB1. This was the only well that exhibited such high slug out displacements. This was likely the result of human error as the slug tester was required to stand on a step ladder and reach above the PVC pipe to handle the slug for this well. In addition, it was observed to be a windy day when this test was done, resulting in further difficulty.

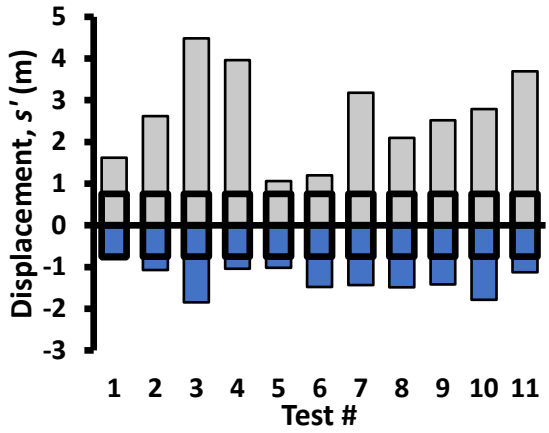

Figure 4-4a. Maximum slug displacement for slug tests on NB1 using thick slug

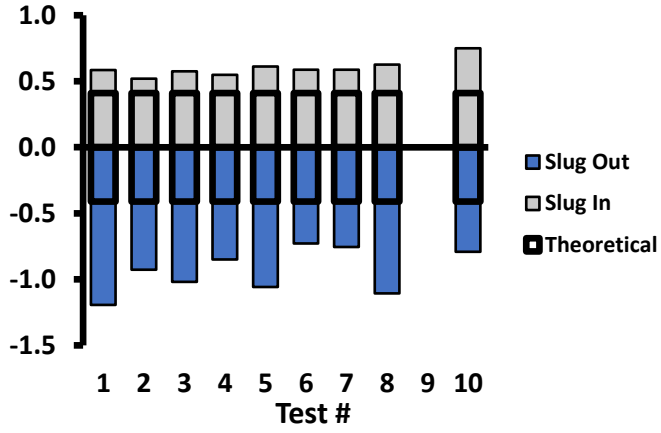

Figure 4-4b. Maximum slug displacement for slug tests on NB1 using thin slug

Although the use of the thin slug was effective in generating more consistent slug tests with reduced noise in the data, it also resulted in less displacement in the well. In effect, a smaller volume of the aquifer was being tested. It is more beneficial, and the results are more meaningful when the sample being tested is greater.

Overall the use of a solid slug was at times problematic and produced error that could have been avoided with the use a different method. The use of pneumatic slug test equipment would allow control over the initial displacement and would remove noise in the data associated with the solid slug. This process is faster to conduct and can provide more reliable results due to the reduced error. Additionally, the aquifer setting made the use of a solid slug more difficult. Highly conductive aquifers require an instantaneous displacement of water, and the slug test response data suggests that introducing or removing the slug quickly introduces unwanted noise in the data. More control was taken whilst conducting slug tests on the Bromley Formation, as the slug could be lowered and removed slowly knowing that no significant response from the aquifer would occur during that time. It is therefore suggested that the solid slug method is more appropriate for low conductivity sediments.

4.2.3 Analytical modelling results

It is well known that analytical models are based on a highly simplified version of reality. These models use a one-dimensional approach, and therefore do not incorporate spatial variability. Major limitations for the use of analytical models in this hydrogeological setting are the assumptions of homogeneity, isotropy, and the inability to correct for physical well design. Although the hydraulic conductivity estimates cannot be interpreted as exact values, they still provide a relative comparison of hydraulic conductivity throughout the shallow hydro-stratigraphic units of the extension to the Christchurch City aquifer system. Thus, the analytical results helped to achieve the aim of the thesis.

Well NB3 which screens the water table in the Springston Formation aquifer was not subjected to the same displacement as the other wells due to the low water level in the well. Slug tests and subsequent analysis were attempted regardless to gauge an approximate value of hydraulic conductivity for the aquifer. However, as only part of the slug was submerged the theoretical displacement was only 18 cm. This means an even smaller volume of aquifer was affected compared to the other wells. Therefore, the hydraulic conductivity estimate for NB3 should be interpreted to have a larger margin of error.

As noted previously, slug test recovery curves from NB2 and AT4 display critical damping behaviour as evident from the water level recovering past the static water level. This influences the slope of the trendline fitted to the semi-log plot of the slug test response (*s'*) because the shape of the curve becomes downward concave as opposed to upward concave. Even a small change in the slope of *s'* has a significant impact on the overall hydraulic conductivity estimate. The critical damping displayed by AT4 was much more pronounced than that displayed by NB2. The analytical results for these two wells are comparatively higher than the numerical results. This is much more apparent for AT4 as the numerical result is approximately 40% lower than the analytical results. This large difference in results is an isolated case for these wells as the numerical results for the other wells are comparatively higher than the analytical results. Therefore, it is suggested

that these analytical models overestimate hydraulic conductivity when applied to critically damped slug test data.

4.2.4 Numerical modelling results

Whereas the analytical models used in this study incorporate the borehole and well casing radius, they do not incorporate the more complex well components such as the filter pack and bentonite seal. The filter pack is a very influential well component on the water level recovery of a slug test. Therefore, significant error can occur when it is not accounted for. In addition, the smaller the initial displacement used to conduct the slug test, the greater the influence the filter pack has on the result. This is because the filter pack takes up a greater proportion of the aquifer being tested. In this study, the filter pack was simulated in the numerical model. This means that in principle, the numerical model is a more accurate representation of the actual system being tested compared to the analytical models. There is, however, opportunity to further increase the complexity of the numerical model by incorporating the bentonite seal that occurs both above the filter pack, and below it in the bottom of the borehole. It is not expected that these well components would have near as much influence on the results as the filter pack. Overall, the numerical results can be interpreted as the most reliable estimates of hydraulic conductivity gained in this study.

The act of matching the numerical modelling slug test recovery data to the actual slug test data was at times difficult. This was because the real-world slug test recovery incorporates external factors such as storage mechanisms and different extents of damping. While the numerical model does account for storage, an estimate was required for this study. As a result, in some cases, the water level recovery curves between the numerical model and the slug test were different shapes and difficult to match. This was particularly true for the wells displaying critical damping. It was observed that the influence of the momentum coming from the aquifer occurred late in the slug test. Therefore, in cases where the curves were different shapes, they were matched to the start of the slug test curve.

Chapter 5. CONCLUSIONS AND RECOMMENDATIONS

The aim of the thesis was two-fold. The principal aim was to obtain a vertical hydrogeological profile of the shallow hydro-stratigraphic units of the Christchurch City aquifer. An additional aim was to explore the different methods of determining hydraulic conductivity from particle size distribution analysis and single well tests. Hydraulic conductivity values were acquired at various depths within the top 40 m of the aquifer system at the site in Kaiapoi, and at the Tram Road site in Clarkville. The hydraulic conductivity varies considerably within and between individual hydro-stratigraphic units, as well as across the two sites. This provides sufficient evidence that the Christchurch City aquifer is a highly heterogeneous system. The hydraulic conductivity results confirmed that it is a highly conductive system as well. Difficulties arising from the use of a solid slug apparatus were deemed to be exacerbated by the conductivity of the system. It is recommended that the pneumatic slug test method should be trialled in future slug tests conducted on or in similar aquifer settings to the Christchurch City aquifer. This may reduce noise in the data, and other errors associated with the use of a solid slug.

Regardless of the large errors associated with determining hydraulic conductivity from particle size distribution analysis, it is still a useful tool for making relative comparisons of hydraulic conductivity within a vertical profile. The range of empirical models trialled in this study resulted in highly variable results. The Kozeny-Carman model provided the most reasonable results. Although, much of the confidence in this method was based on the findings of the literature. It was difficult to compare results directly because the samples were all extracted from two sediment cores, as opposed to the wells being tested. It is recommended that further testing is done comparing numerical and empirical modelling results of sediment samples extracted directly from the borehole being tested to confirm the method of Kozeny-Carman as the superior empirical model.

Analytical modelling of slug tests provided much more reliable results. From comparison of these results with the numerical modelling results, it is inconclusive whether the Hvorslev or Bouwer and Rice method is more reliable. These models are designed for

analysis of overdamped slug test responses. Two of the wells displayed critically damped responses, which is suggested to have resulted in significant error. These behaviours can be subtle and should not be overlooked. It is recommended that alternative methods are explored for analysis of critically damped slug tests.

Of all the methods used in this study, the hydraulic conductivity estimates gained from numerical modelling are considered the most reliable. However, there is still potential for improvements in the model through simulation of the bentonite seal above and below the filter pack. Also, the discretisation of vertical layers in the model could have been more complex, such that the well screen consisted of several layers instead of one. In the future, this could be tested to determine if any errors are occurring from over-simplification of vertical discretisation of the model. Additionally, measured values of porosity, specific yield, and specific storage would further enhance the complexity of the model and lead to more reliable results.

Finally, based on the limitations of small scale single well tests, it is recommended that pump tests are conducted on the multi-tier wells at both sites. This will allow direct comparison between small-scale slug tests and large-scale pump tests to evaluate the effects of incorporating heterogeneity. Additionally, these results would be more applicable to regional scale groundwater flow studies in the Christchurch City aquifer system. However, due to lack of observation wells, this study would be limited to evaluating hydraulic conductivity in the Riccarton Gravel aquifer.

REFERENCES

Anderson, M. P., & Woessner, W. W. (1992). Applied groundwater modeling: Simulation of flow and advective transport. San Diego: Academic Press.

Batu, V. (2006). Applied flow and solute transport modeling in aquifers: Fundamental principles and analytical and numerical methods. Boca Raton, Florida: Taylor & Francis.

Beyer, W. (1964). Zur Bestimmung der Wasserdurchlässigkeit von Kiesen und Sanden aus der Kornverteilungskurve [On the determination of hydraulic conductivity of gravels and sands from grain size distribution]. Wasserwirtschaft-Wassertechnik, 14(6), 165-168.

Brown, L. J., & Weeber J. H., (1992). Geology of the Christchurch urban area. Lower Hutt, 104: Institute of Geological and Nuclear Sciences.

Brown, L. J., & Weeber, J. H., (2002). Groundwaters of the Canterbury region. Christchurch, New Zealand: Environment Canterbury.

Browne, G. H., & Naish, T. R. (2003). Facies development and sequence architecture of a late quaternary fluvial-marine transition, Canterbury Plains and shelf, New Zealand: Implications for forced regressive deposits. Sedimentary Geology, 158(1), 57-86. doi:10.1016/S0037-0738(02)00258-0

Blott, S., & Pye, K. (2000). GRADISTAT Version 4.0. A grain size distribution and statistics package for the analysis of unconsolidated sediments by sieving or laser granulometer. Surface Processes and Modern Environments Research Group, Department of Geology, Royal Holloway, University of London, Surrey.

Bouwer, H., & Rice, R. C. (1976). A slug test for determining hydraulic conductivity of unconfined aquifers with completely or partially penetrating wells. Water Resources Research, 12(3), 423. doi:10.1029/WR012i003p00423

Bouwer, H. (1989). The Bouwer and Rice slug test—an update. Groundwater, 27(3), 304-309.

Butler, J. J. (1996). Slug tests in site characterization: Some practical considerations. Environmental Geosciences, 3(3), 154-163.

Butler, J. J. (1997). The design, performance, and analysis of slug tests. Boca Raton, Florida: Lewis.

Carman, P. C. (1937). Fluid flow through granular beds. Transactions-Institution of Chemical Engineers, 15, 150-166.

Carrier III, W. D. (2003). Goodbye, Hazen; hello, Kozeny-Carman. Journal of Geotechnical and Geoenvironmental Engineering, 129(11), 1054-1056.

Cheong, J., Hamm, S., Kim, H., Ko, E., Yang, K., & Lee, J. (2008). Estimating hydraulic conductivity using grain-size analyses, aquifer tests, and numerical modelling in a riverside alluvial system in South Korea. Hydrogeology Journal, 16(6), 1129-1143. doi:10.1007/s10040-008-0303-4

Chiang, W. H., & Kinzelbach, W. (1998). Processing Modflow. A simulation program for modelling groundwater flow and pollution. User manual.

Cohen, K. M., Finney, S. C., Gibbard, P. L., Fan, J. X. (2013). International chronostratigraphic chart. Retrieved from http://www.stratigraphy.org/icschart/chronostratchart2013-01.pdf

Cooper, H., Bredehoeft, J., & Papadopulos, I. (1967). Response of a finite-diameter well to an instantaneous charge of water. Water Resources Research, 3(1), 263-263. doi:10.1029/WR003i001p00263

Dark, A., K.C., B., & Kashima, A. (2017). National Irrigated Land Spatial Dataset: Summary of methodology, assumptions and results. Ministry for the Environment, C17042-1: Aqualinc Research Limited.

Dodson, M., Aitchison-Earl, P., & Scott, L. (2012). Ashley-Waimakariri groundwater resources investigation. Christchurch: Environment Canterbury.

Domenico, P. A., & Mifflin, M. D. (1965). Water from low-permeability sediments and land subsidence. Water Resources Research, 1(4), 563-576.

Environment Canterbury. (2016). BW24/0342 details. Retrieved from https://www.ecan.govt.nz/data/well-search/welldetails/QlcyNC8wMzQy/QlcyNC8wMzQy

Environment Canterbury. (2016). BW24/0337 details. Retrieved from https://www.ecan.govt.nz/data/well-search/welldetails/QlcyNC8wMzM3/QlcyNC8wMzM3

Eggleston, J., & Rojstaczer, S. (2001). The value of grain-size hydraulic conductivity estimates: Comparison with high resolution in-situ field hydraulic conductivity. Geophysical Research Letters, 28(22), 4255-4258. doi:10.1029/2000GL012772

Fetter, C. W. (2000). Applied hydrogeology. Upper Saddle River, New Jersey: Prentice Hall.

Folk, R. L. (1954). The distinction between grain size and mineral composition in sedimentary-rock nomenclature. The Journal of Geology, 62(4), 344-359.

Folk, R. L., & Ward, W. C. (1957). Brazos River bar: A study in the significance of grain size parameters. Journal of Sedimentary Research, 27(1).

Freeze, R. A., & Cherry, J. A. (1979). Groundwater. Englewood Cliffs, New Jersey: Prentice-Hall.

Hanson, M. (2016). Annual groundwater quality survey 2016. Christchurch: Environment Canterbury.

Harbaugh, A.W. (2005). MODFLOW-2005, the United States Geological Survey modular ground-water model -- the ground-water flow process: United States Geological Survey.

Hazen, A. (1892). Some physical properties of sands and gravels: With special reference to their use in filtration. Annual Report, Massachusetts State Board of Health, Boston, 539-556.

Hooke, R. L. (1967). Processes on arid-region alluvial fans. The Journal of Geology, 75(4), 438-460. doi: 10.1086/627271

Hvorslev, M. J. (1951). Time lag and soil permeability in ground-water observations, Bulletin 36, Waterways Experiment Station, Corporation of Engineers, United States Army, Vicksburg, Mississipi, 1-50.

Hyder, Z., Butler, J. J., McElwee, C. D., & Liu, W. (1994). Slug tests in partially penetrating wells. Water Resources Research, 30(11), 2945-2957.

International organization for standardization (1975). Standard atmosphere, ISO, 2533,

Johnson, A. I. (1967). Specific yield: Compilation of specific yields for various materials. United States Geological Survey. Denver, Colorado.

Kasenow, M., & Röhrich, T. (2001). Applied ground-water hydrology and well hydraulics (2nd ed.). Highlands Ranch, Colorado: Water Resources Publications, LLC.

Kozeny, J. (1927). Ueber kapillare leitung des wassers im boden [About capillary management of the water in the soil]. Sitzungsber Akad. Wiss., Wien, 136(2a), 271-306.

Lewis, M. (2013). A comparative analysis of two slug test methods in Puget lowland glacio-fluvial sediments near Coupeville, Washington (Master's thesis). University of Washington, Washington, United States of America.

Ministry of Health. (2008). Drinking-water standards for New Zealand 2005 (Revised edition). Wellington, New Zealand: Ministry of Health.

Odong, J. (2007). Evaluation of empirical formulae for determination of hydraulic conductivity based on grain-size analysis. Journal of American Science, 3(3), 54-60.

Pucko, T., & Verbovšek, T. (2015). Comparison of hydraulic conductivities by grain-size analysis, pumping, and slug tests in quaternary gravels, NE slovenia. Open Geosciences, 7(1), 308-317. doi:10.1515/geo-2015-0032

Rasmussen, T. C., & Crawford, L. A. (1997). Identifying and removing barometric pressure effects in confined and unconfined aquifers. Ground Water, 35(3), 502-511.

Rosas, J., Lopez, O., Missimer, T., Coulibaly, K., Dehwah, A., Sesler, K., Lujan, L., Mantilla, D. (2014). Determination of hydraulic conductivity from grain-size distribution for different depositional environments. Groundwater, 52(3), 399-413. doi:10.1111/gwat.12078

Ross, H. C., & McElwee, C. D. (2007). Multi-level slug tests to measure 3-D hydraulic conductivity distributions. Natural Resources Research, 16(1), 67-79. doi:10.1007/s11053-007-9034-9

Sarath Prasanth, S. V., Magesh, N. S., Jitheshlal, K. V., Chandrasekar, N., & Gangadhar, K. (2012). Evaluation of groundwater quality and its suitability for drinking and agricultural use in the coastal stretch of Alappuzha district, Kerala, India. Applied Water Science, 2(3), 165. doi:10.1007/s13201-012-0042-5

Sauerbrei, I. I. (1932). On the problem and determination of the permeability coefficient. Proceedings B. E. Vedeneev All-Russia Research Institute of Hydraulic Engineering, No. 3-5.

Slichter, C. S. (1905). Field measurements of the rate of movement of underground waters. United States Geological Survey Water-Supply and Irrigation Paper, 140.

Spane Jr, F. A. (1999). Effects of barometric fluctuations on well water-level measurements and aquifer test data (No. PNNL-13078). Pacific Northwest National Laboratory, Richland, Washington, United States of America.

Springer, R. K., & Gelhar, L. W. (1991). Characterization of large-scale aquifer heterogeneity in glacial outwash by analysis of slug tests with oscillatory response, Cape Cod, Massachusetts. United States Geological Survey Water Resources Investigation Report, 91, 36-40.

Standards Association of New Zealand. (1986). Methods of testing soils for civil engineering purposes. Wellington, New Zealand: Standards Association of New Zealand.

Stewart, M. K. (2012). A 40-year record of carbon-14 and tritium in the Christchurch groundwater system, New Zealand: Dating of young samples with carbon-14. Journal of Hydrology, 430-431, 50-68. doi:10.1016/j.jhydrol.2012.01.046

Suggate, R. P. (1958). Late quaternary deposits of the Christchurch metropolitan area. New Zealand Journal of Geology and Geophysics, 1(1), 103-122. doi:10.1080/00288306.1958.10422799

Svensson, A. (2014). Estimation of hydraulic conductivity from grain size analyses (Master's thesis). Chalmers University of Technology, Gothenburg, Sweden.

Talbot, J. D., Weeber, J. H., Freeman, M. C., Mason, C. R., & Wilson, D. D. (1986). The Christchurch artesian aquifers. North Canterbury Catchment Board, 159.

Trevis, I. A. (2012). Assessing and tracking nitrate contamination from a point source and the effects on the groundwater systems in Mid Canterbury, New Zealand (Master's thesis). University of Canterbury, Christchurch, New Zealand.

USBR (1978). Drainage manual: A water resources technical publication. United States Bureau of Reclamation.

Vukovic, M., & Soro, A. (1992). Determination of hydraulic conductivity of porous media from grain-size distribution. Water Resources Publications.

Wilson, D. D. (1976). Hydrogeology of metropolitan Christchurch. Journal of Hydrology (New Zealand), 15(2), 101-120.

Zhang, S. (2017). Relationship between particle size distribution and porosity in dump leaching (Doctoral dissertation). University of British Columbia, Vancouver, Canada.

APPENDICES

Appendix A: Geological bore logs for Tram Road and Adderley Terrace

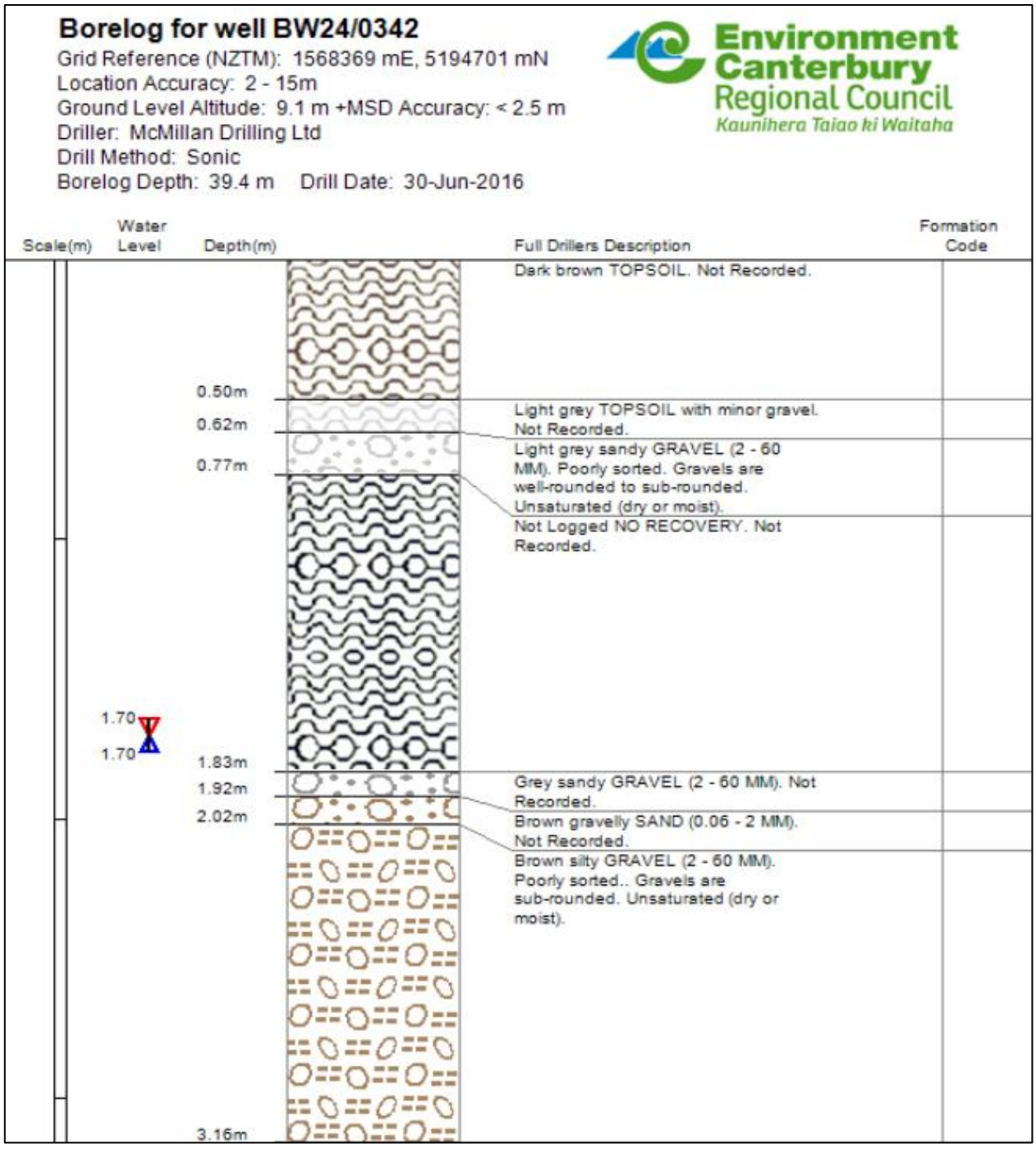

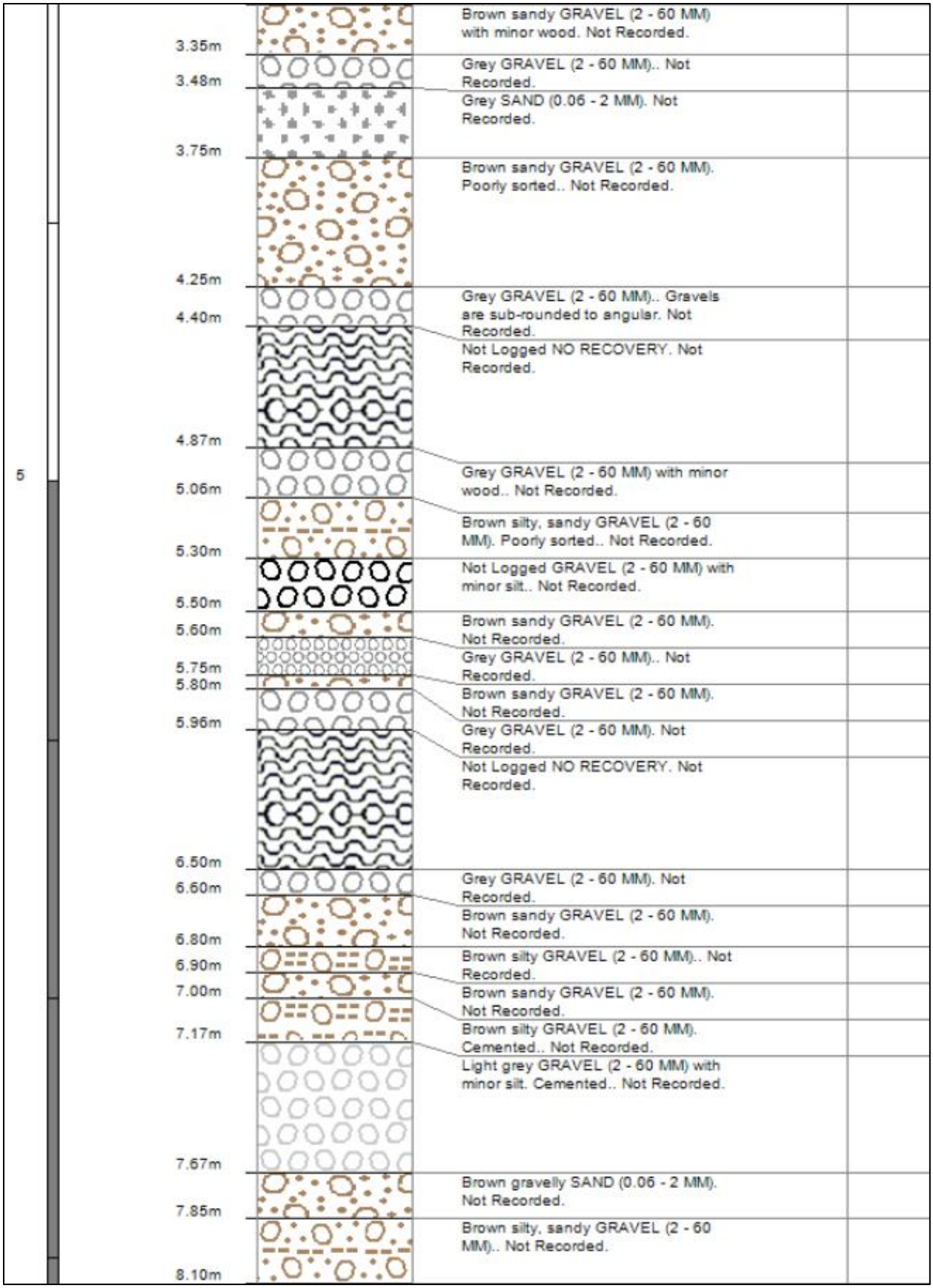
5
3.35m
Brown sandy GRAVEL (2 - 60 MM) with minor wood. Not Recorded.
3.48m
Grey GRAVEL (2 - 60 MM).. Not Recorded.
Grey SAND (0.06 - 2 MM). Not Recorded.
3.75m
Brown sandy GRAVEL (2 - 60 MM). Poorly sorted.. Not Recorded.
4.25m
Grey GRAVEL (2 - 60 MM).. Gravels are sub-rounded to angular. Not Recorded.
4.40m
Not Logged NO RECOVERY. Not Recorded.
4.87m
Grey GRAVEL (2 - 60 MM) with minor wood.. Not Recorded.
5.06m
Brown silty, sandy GRAVEL (2 - 60 MM). Poorly sorted.. Not Recorded.
5.30m
Not Logged GRAVEL (2 - 60 MM) with minor silt.. Not Recorded.
5.50m
Brown sandy GRAVEL (2 - 60 MM). Not Recorded.
5.60m
Grey GRAVEL (2 - 60 MM).. Not Recorded.
5.75m
5.80m
Brown sandy GRAVEL (2 - 60 MM). Not Recorded.
5.96m
Grey GRAVEL (2 - 60 MM). Not Recorded.
Not Logged NO RECOVERY. Not Recorded.
6.50m
Grey GRAVEL (2 - 60 MM). Not Recorded.
6.60m
Brown sandy GRAVEL (2 - 60 MM). Not Recorded.
6.80m
Brown silty GRAVEL (2 - 60 MM).. Not Recorded.
6.90m
Brown sandy GRAVEL (2 - 60 MM). Not Recorded.
7.00m
Brown silty GRAVEL (2 - 60 MM). Cemented.. Not Recorded.
7.17m
Light grey GRAVEL (2 - 60 MM) with minor silt. Cemented.. Not Recorded.
7.67m
Brown gravelly SAND (0.06 - 2 MM). Not Recorded.
7.85m
Brown silty, sandy GRAVEL (2 - 60 MM).. Not Recorded.
8.10m

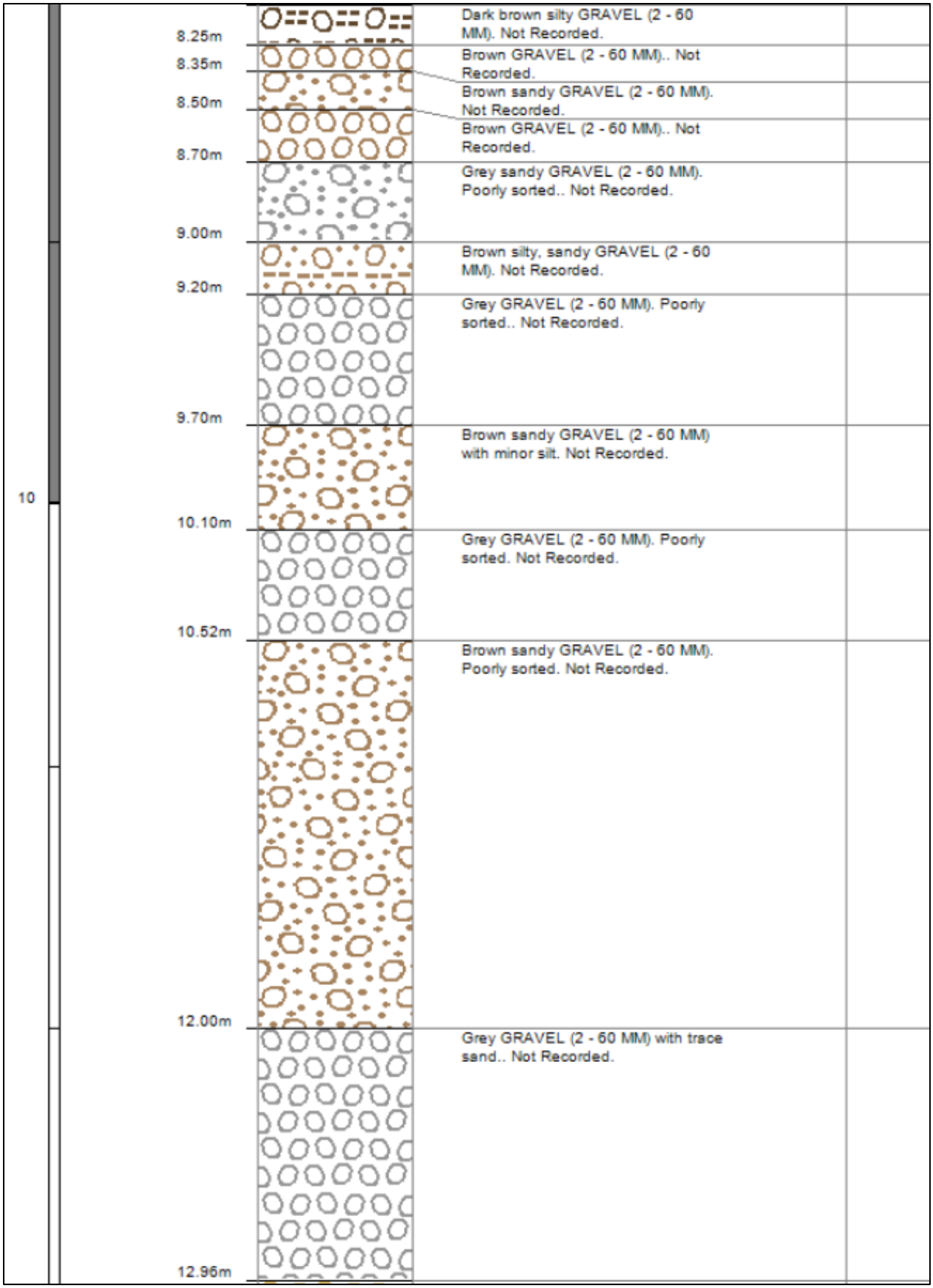
10
8.25m
Dark brown silty GRAVEL (2 - 60 MM). Not Recorded.
8.35m
Brown GRAVEL (2 - 60 MM).. Not Recorded.
8.50m
Brown sandy GRAVEL (2 - 60 MM). Not Recorded.
Brown GRAVEL (2 - 60 MM).. Not Recorded.
8.70m
Grey sandy GRAVEL (2 - 60 MM). Poorly sorted.. Not Recorded.
9.00m
Brown silty, sandy GRAVEL (2 - 60 MM). Not Recorded.
9.20m
Grey GRAVEL (2 - 60 MM). Poorly sorted.. Not Recorded.
9.70m
Brown sandy GRAVEL (2 - 60 MM) with minor silt. Not Recorded.
10.10m
Grey GRAVEL (2 - 60 MM). Poorly sorted. Not Recorded.
10.52m
Brown sandy GRAVEL (2 - 60 MM). Poorly sorted. Not Recorded.
12.00m
Grey GRAVEL (2 - 60 MM) with trace sand.. Not Recorded.
12.96m

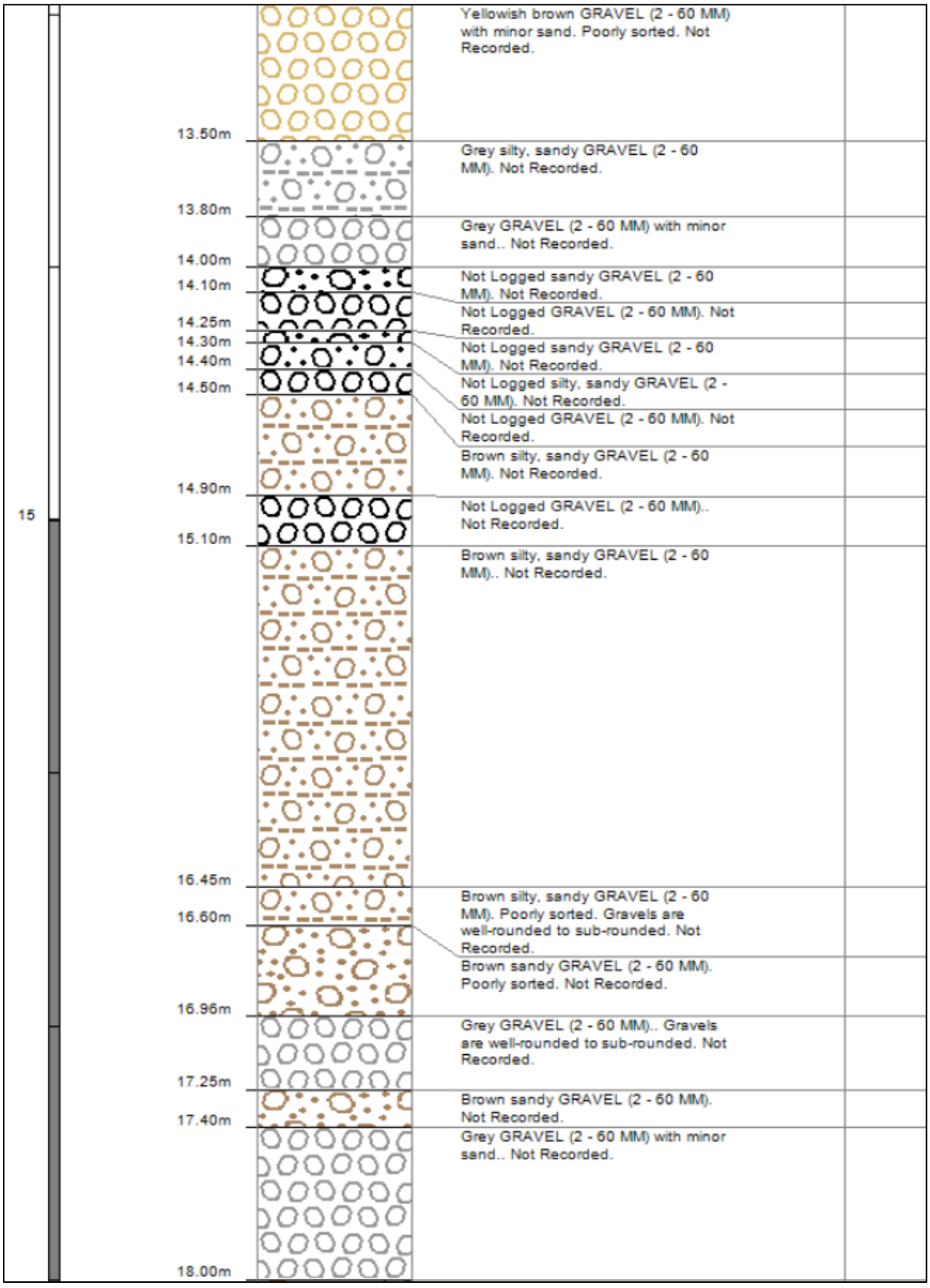
15
13.50m
13.80m
14.00m
14.10m
14.25m
14.30m
14.40m
14.50m
14.90m
15.10m
16.45m
16.60m
16.96m
17.25m
17.40m
18.00m
Yellowish brown GRAVEL (2 - 60 MM) with minor sand. Poorly sorted. Not Recorded.
Grey silty, sandy GRAVEL (2 - 60 MM). Not Recorded.
Grey GRAVEL (2 - 60 MM) with minor sand.. Not Recorded.
Not Logged sandy GRAVEL (2 - 60 MM). Not Recorded.
Not Logged GRAVEL (2 - 60 MM). Not Recorded.
Not Logged sandy GRAVEL (2 - 60 MM). Not Recorded.
Not Logged silty, sandy GRAVEL (2 - 60 MM). Not Recorded.
Not Logged GRAVEL (2 - 60 MM). Not Recorded.
Brown silty, sandy GRAVEL (2 - 60 MM). Not Recorded.
Not Logged GRAVEL (2 - 60 MM).. Not Recorded.
Brown silty, sandy GRAVEL (2 - 60 MM).. Not Recorded.
Brown silty, sandy GRAVEL (2 - 60 MM). Poorly sorted. Gravels are well-rounded to sub-rounded. Not Recorded.
Brown sandy GRAVEL (2 - 60 MM). Poorly sorted. Not Recorded.
Grey GRAVEL (2 - 60 MM).. Gravels are well-rounded to sub-rounded. Not Recorded.
Brown sandy GRAVEL (2 - 60 MM). Not Recorded.
Grey GRAVEL (2 - 60 MM) with minor sand.. Not Recorded.

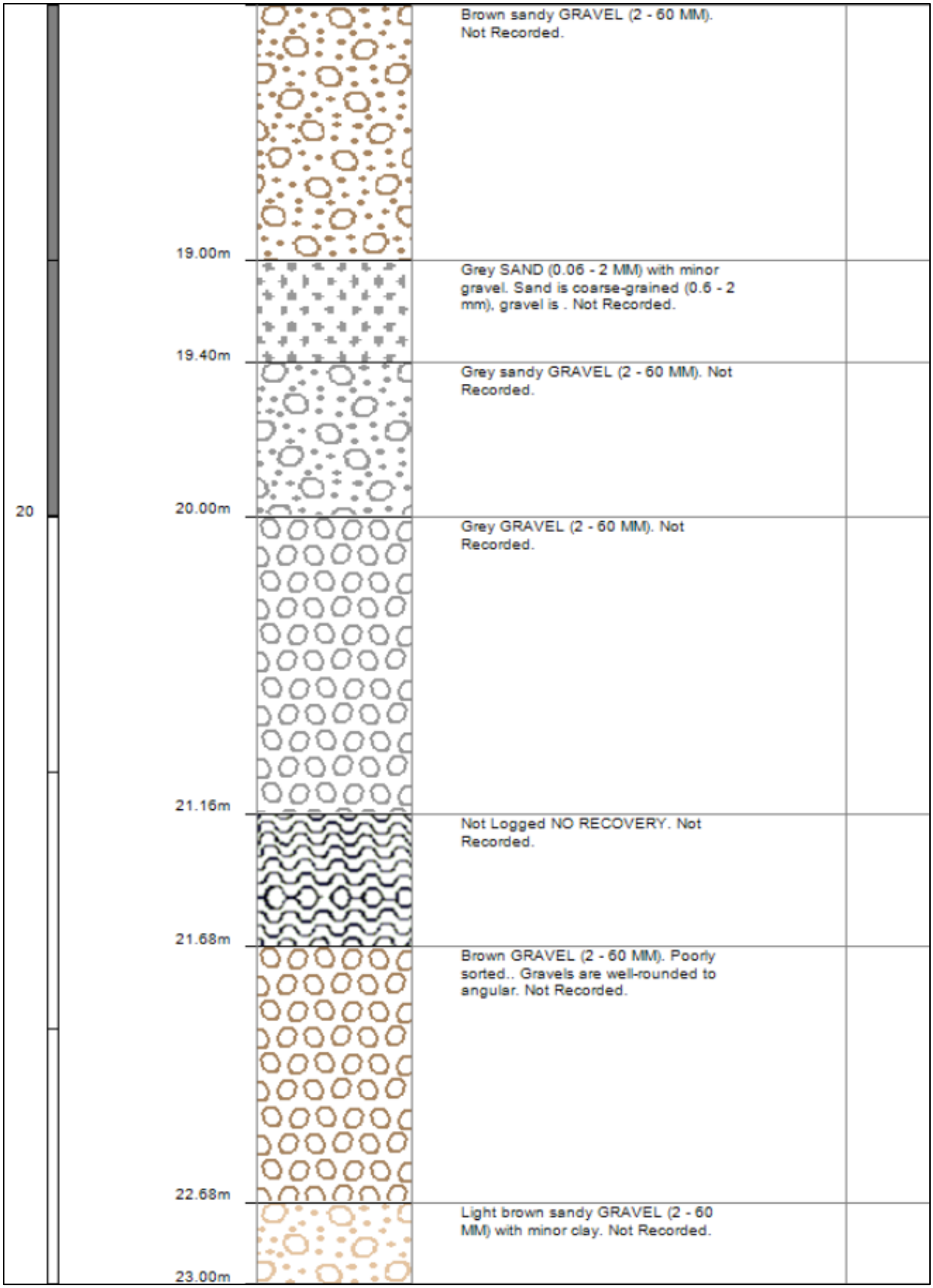
20
19.00m
Brown sandy GRAVEL (2 - 60 MM). Not Recorded.
19.40m
Grey SAND (0.06 - 2 MM) with minor gravel. Sand is coarse-grained (0.6 - 2 mm), gravel is . Not Recorded.
20.00m
Grey sandy GRAVEL (2 - 60 MM). Not Recorded.
21.16m
Grey GRAVEL (2 - 60 MM). Not Recorded.
21.68m
Not Logged NO RECOVERY. Not Recorded.
22.68m
Brown GRAVEL (2 - 60 MM). Poorly sorted.. Gravels are well-rounded to angular. Not Recorded.
23.00m
Light brown sandy GRAVEL (2 - 60 MM) with minor clay. Not Recorded.

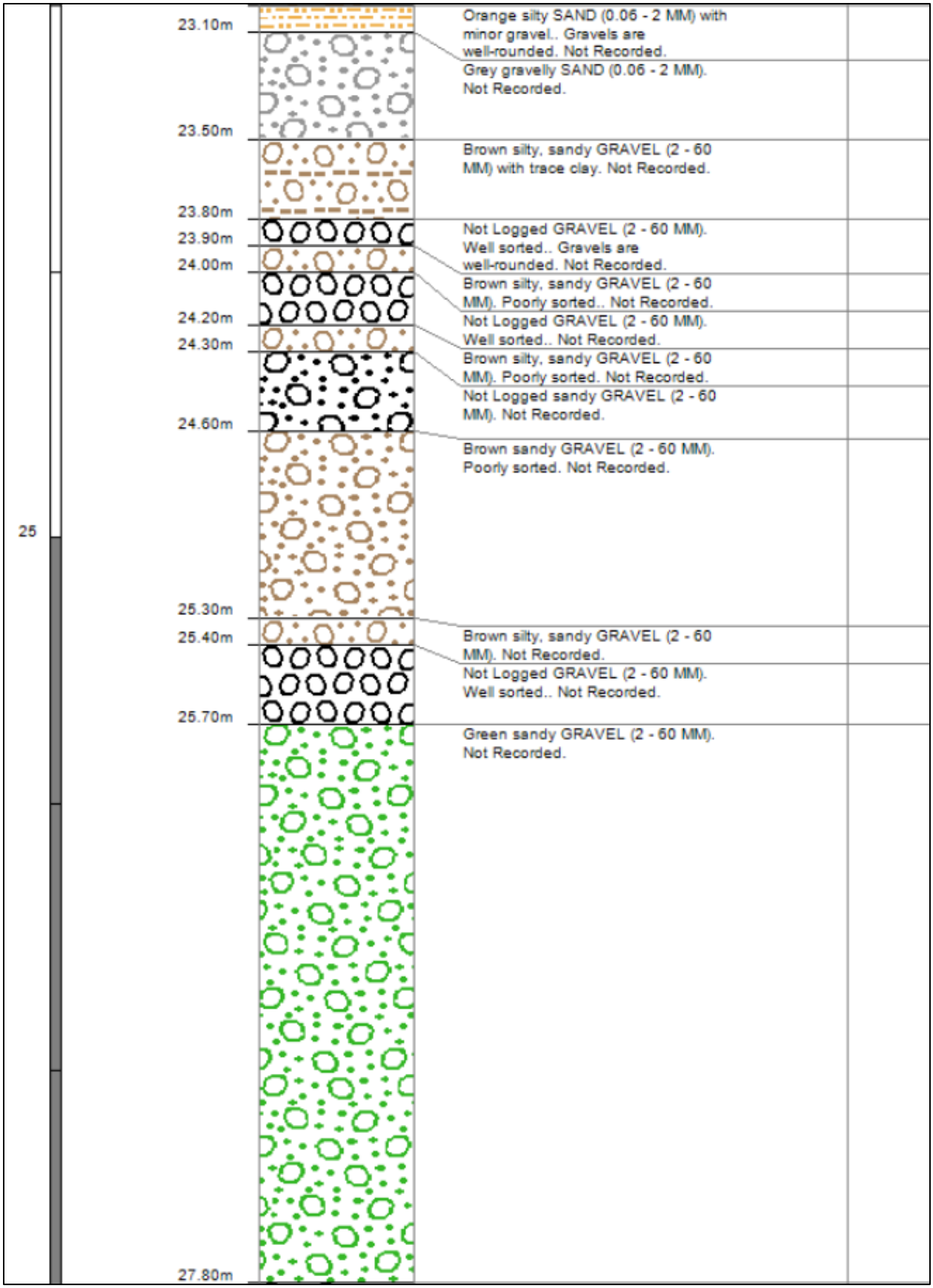
25
23.10m
23.50m
23.80m
23.90m
24.00m
24.20m
24.30m
24.60m
25.30m
25.40m
25.70m
27.80m
Orange silty SAND (0.06 - 2 MM) with minor gravel.. Gravels are well-rounded. Not Recorded.
Grey gravelly SAND (0.06 - 2 MM). Not Recorded.
Brown silty, sandy GRAVEL (2 - 60 MM) with trace clay. Not Recorded.
Not Logged GRAVEL (2 - 60 MM). Well sorted.. Gravels are well-rounded. Not Recorded.
Brown silty, sandy GRAVEL (2 - 60 MM). Poorly sorted.. Not Recorded.
Not Logged GRAVEL (2 - 60 MM). Well sorted.. Not Recorded.
Brown silty, sandy GRAVEL (2 - 60 MM). Poorly sorted. Not Recorded.
Not Logged sandy GRAVEL (2 - 60 MM). Not Recorded.
Brown sandy GRAVEL (2 - 60 MM). Poorly sorted. Not Recorded.
Brown silty, sandy GRAVEL (2 - 60 MM). Not Recorded.
Not Logged GRAVEL (2 - 60 MM). Well sorted.. Not Recorded.
Green sandy GRAVEL (2 - 60 MM). Not Recorded.

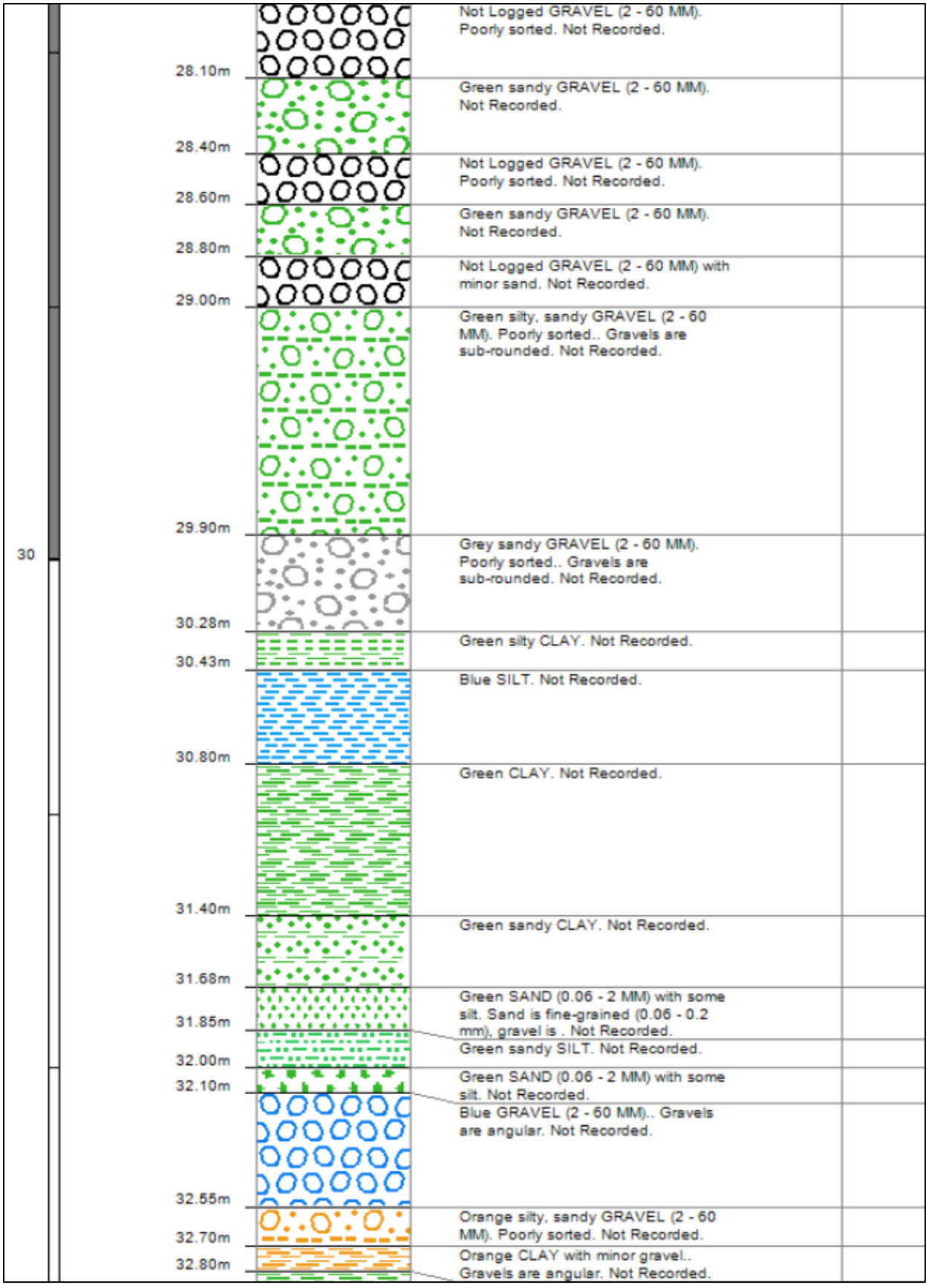
30
28.10m
Not Logged GRAVEL (2 - 60 MM). Poorly sorted. Not Recorded.
28.40m
Green sandy GRAVEL (2 - 60 MM). Not Recorded.
28.60m
Not Logged GRAVEL (2 - 60 MM). Poorly sorted. Not Recorded.
28.80m
Green sandy GRAVEL (2 - 60 MM). Not Recorded.
29.00m
Not Logged GRAVEL (2 - 60 MM) with minor sand. Not Recorded.
29.90m
Green silty, sandy GRAVEL (2 - 60 MM). Poorly sorted.. Gravels are sub-rounded. Not Recorded.
30.28m
Grey sandy GRAVEL (2 - 60 MM). Poorly sorted.. Gravels are sub-rounded. Not Recorded.
30.43m
Green silty CLAY. Not Recorded.
30.80m
Blue SILT. Not Recorded.
31.40m
Green CLAY. Not Recorded.
31.68m
Green sandy CLAY. Not Recorded.
31.85m
Green SAND (0.06 - 2 MM) with some silt. Sand is fine-grained (0.06 - 0.2 mm), gravel is . Not Recorded.
32.00m
Green sandy SILT. Not Recorded.
32.10m
Green SAND (0.06 - 2 MM) with some silt. Not Recorded.
32.55m
Blue GRAVEL (2 - 60 MM).. Gravels are angular. Not Recorded.
32.70m
Orange silty, sandy GRAVEL (2 - 60 MM). Poorly sorted. Not Recorded.
32.80m
Orange CLAY with minor gravel.. Gravels are angular. Not Recorded.

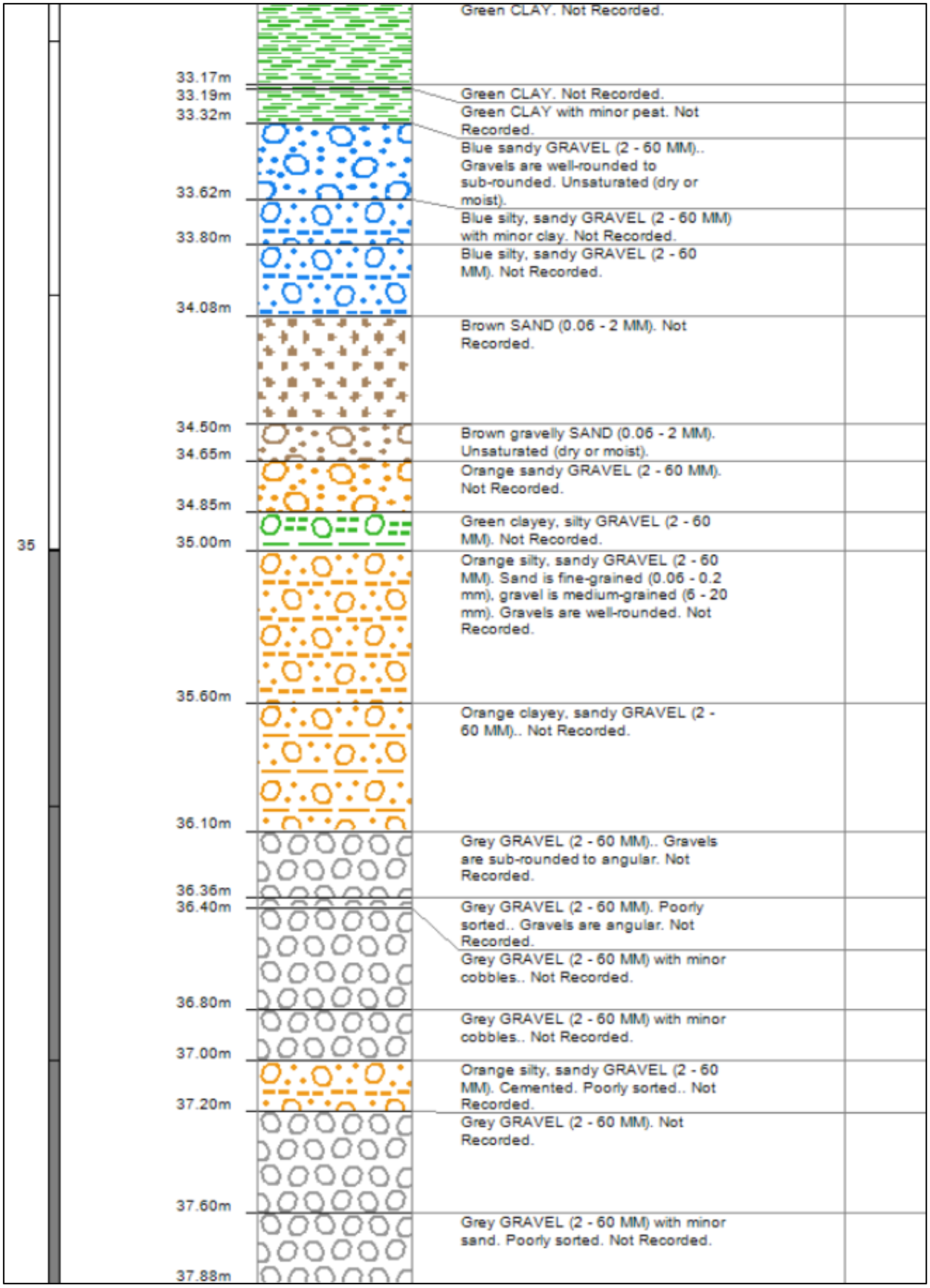
35
33.17m
33.19m
33.32m
33.62m
33.80m
34.08m
34.50m
34.65m
34.85m
35.00m
35.60m
36.10m
36.36m
36.40m
36.80m
37.00m
37.20m
37.60m
37.88m
Green CLAY. Not Recorded.
Green CLAY. Not Recorded.
Green CLAY with minor peat. Not Recorded.
Blue sandy GRAVEL (2 - 60 MM).. Gravels are well-rounded to sub-rounded. Unsaturated (dry or moist).
Blue silty, sandy GRAVEL (2 - 60 MM) with minor clay. Not Recorded.
Blue silty, sandy GRAVEL (2 - 60 MM). Not Recorded.
Brown SAND (0.06 - 2 MM). Not Recorded.
Brown gravelly SAND (0.06 - 2 MM). Unsaturated (dry or moist).
Orange sandy GRAVEL (2 - 60 MM). Not Recorded.
Green clayey, silty GRAVEL (2 - 60 MM). Not Recorded.
Orange silty, sandy GRAVEL (2 - 60 MM). Sand is fine-grained (0.06 - 0.2 mm), gravel is medium-grained (6 - 20 mm). Gravels are well-rounded. Not Recorded.
Orange clayey, sandy GRAVEL (2 - 60 MM).. Not Recorded.
Grey GRAVEL (2 - 60 MM).. Gravels are sub-rounded to angular. Not Recorded.
Grey GRAVEL (2 - 60 MM). Poorly sorted.. Gravels are angular. Not Recorded.
Grey GRAVEL (2 - 60 MM) with minor cobbles.. Not Recorded.
Grey GRAVEL (2 - 60 MM) with minor cobbles.. Not Recorded.
Orange silty, sandy GRAVEL (2 - 60 MM). Cemented. Poorly sorted.. Not Recorded.
Grey GRAVEL (2 - 60 MM). Not Recorded.
Grey GRAVEL (2 - 60 MM) with minor sand. Poorly sorted. Not Recorded.

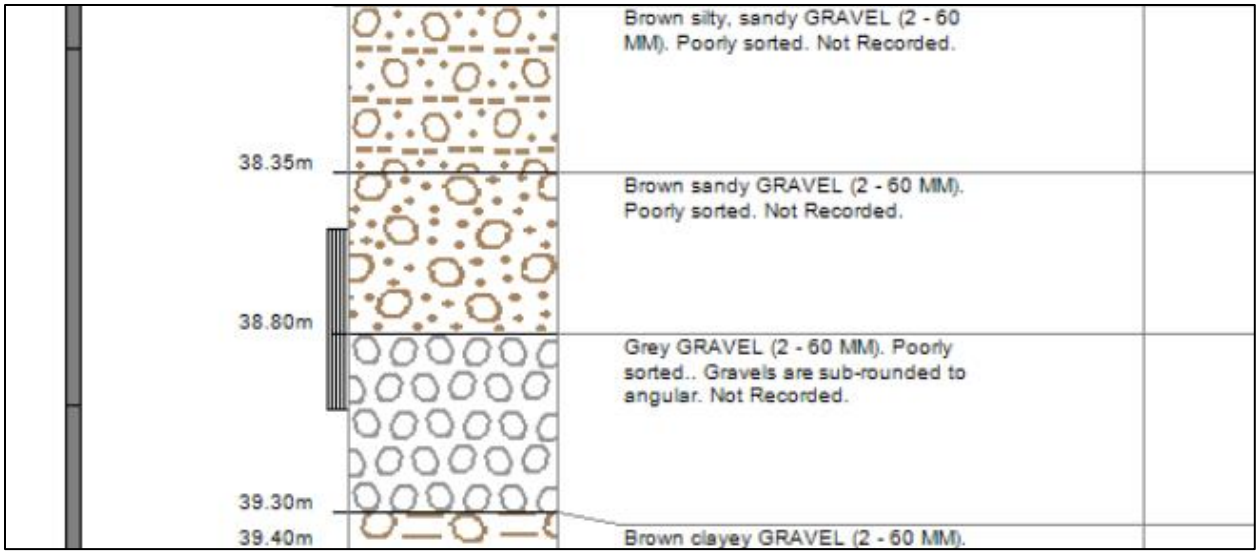

Figure A-1. Bore log for NB1 (Environment Canterbury, 2016)

Borelog for well BW24/0337

Grid Reference (NZTM): 1571037 mE, 5197366 mN
Location Accuracy: 2 - 15m
Ground Level Altitude: 2.7 m +MSD Accuracy: < 2.5 m
Driller: McMillan Drilling Ltd
Drill Method: Sonic
Borelog Depth: 44.0 m Drill Date: 14-Jul-2016

Environment Canterbury Regional Council
Kaunihera Taiao ki Waitaha

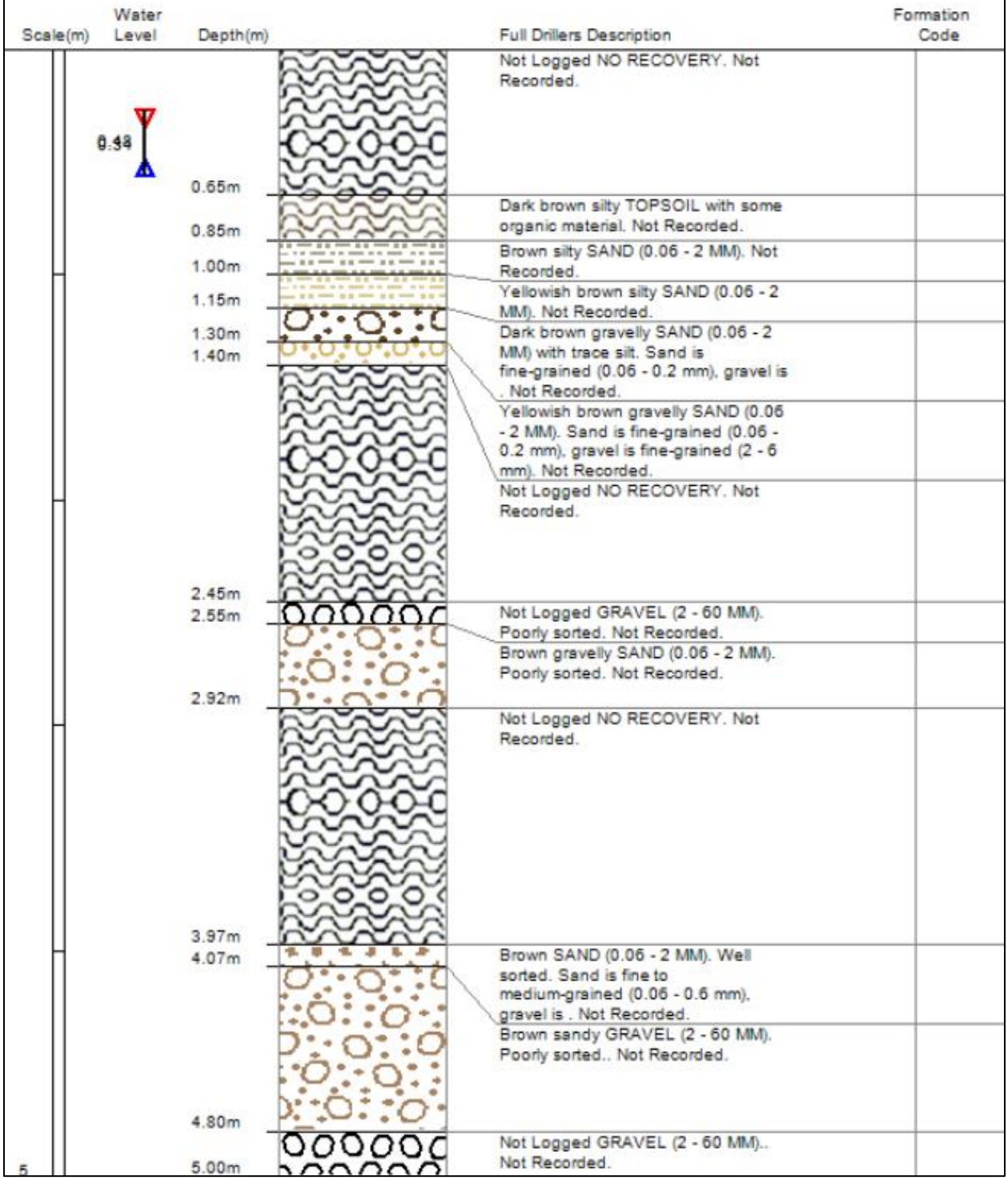

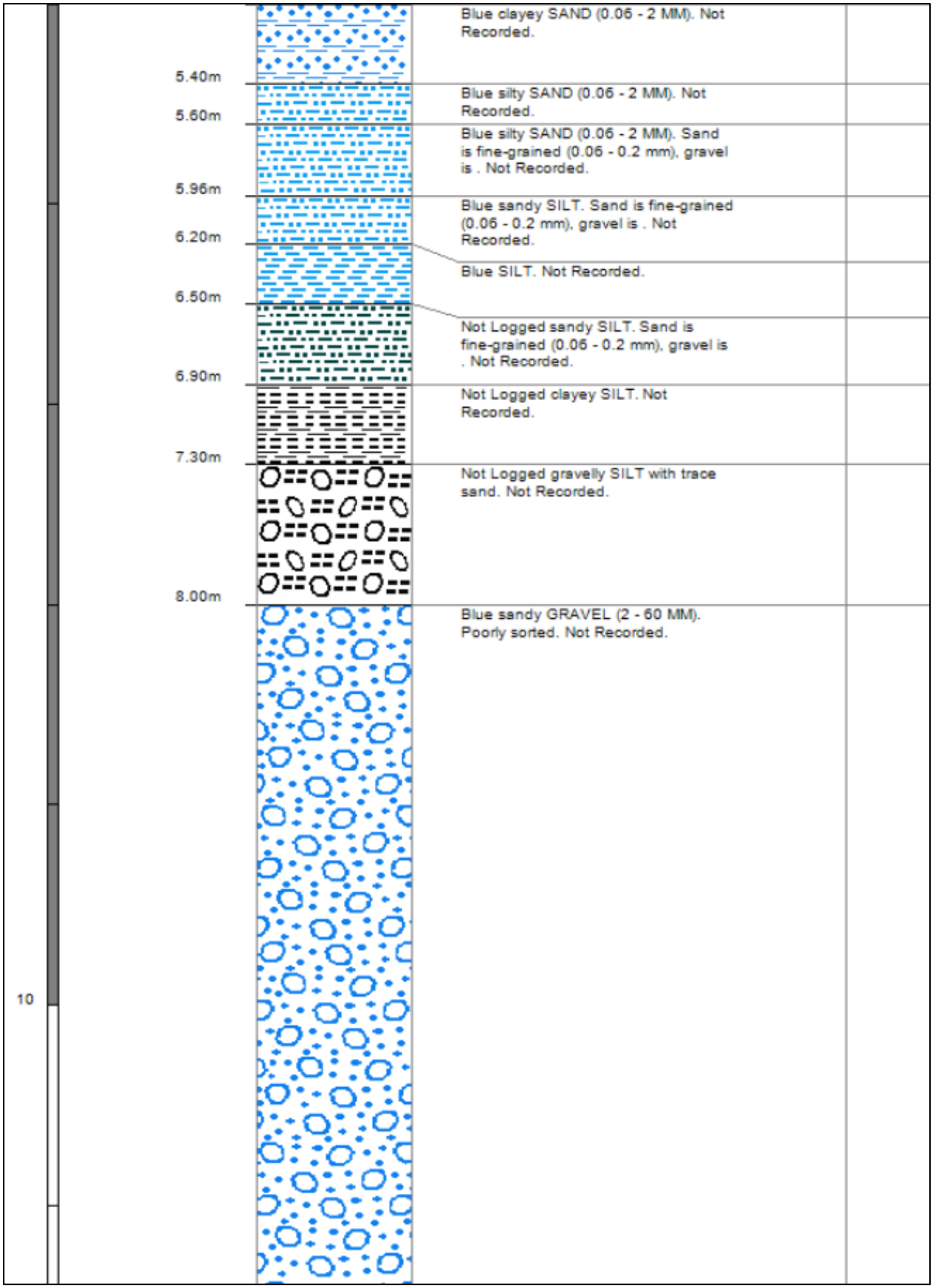
Blue clayey SAND (0.06 - 2 MM). Not Recorded.
5.40m
Blue silty SAND (0.06 - 2 MM). Not Recorded.
5.60m
Blue silty SAND (0.06 - 2 MM). Sand is fine-grained (0.06 - 0.2 mm), gravel is . Not Recorded.
5.96m
Blue sandy SILT. Sand is fine-grained (0.06 - 0.2 mm), gravel is . Not Recorded.
6.20m
Blue SILT. Not Recorded.
6.50m
Not Logged sandy SILT. Sand is fine-grained (0.06 - 0.2 mm), gravel is . Not Recorded.
6.90m
Not Logged clayey SILT. Not Recorded.
7.30m
Not Logged gravelly SILT with trace sand. Not Recorded.
8.00m
Blue sandy GRAVEL (2 - 60 MM). Poorly sorted. Not Recorded.
10

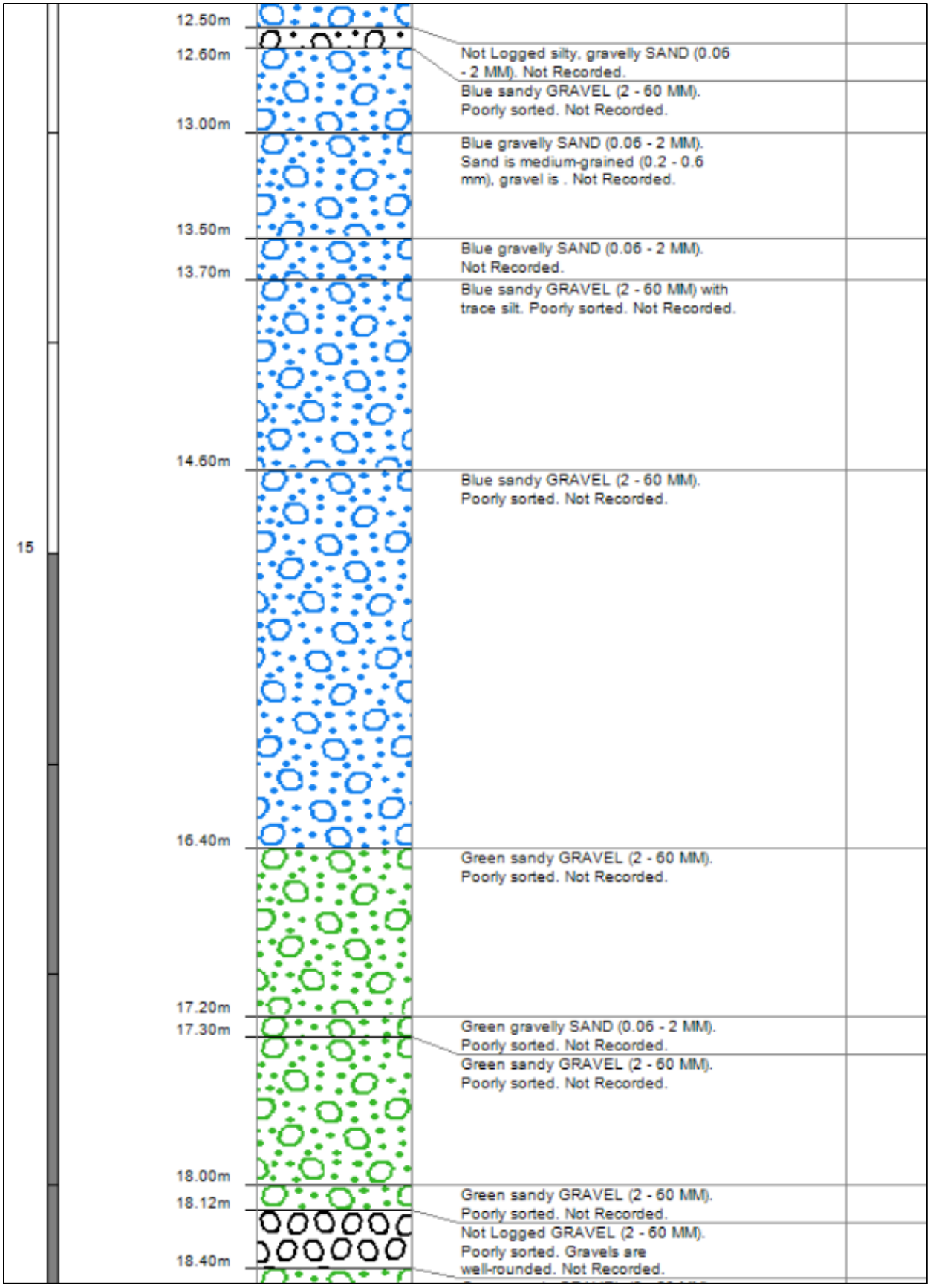
15
12.50m
12.60m
13.00m
13.50m
13.70m
14.60m
16.40m
17.20m
17.30m
18.00m
18.12m
18.40m
Not Logged silty, gravelly SAND (0.06 - 2 MM). Not Recorded.
Blue sandy GRAVEL (2 - 60 MM). Poorly sorted. Not Recorded.
Blue gravelly SAND (0.06 - 2 MM). Sand is medium-grained (0.2 - 0.6 mm), gravel is . Not Recorded.
Blue gravelly SAND (0.06 - 2 MM). Not Recorded.
Blue sandy GRAVEL (2 - 60 MM) with trace silt. Poorly sorted. Not Recorded.
Blue sandy GRAVEL (2 - 60 MM). Poorly sorted. Not Recorded.
Green sandy GRAVEL (2 - 60 MM). Poorly sorted. Not Recorded.
Green gravelly SAND (0.06 - 2 MM). Poorly sorted. Not Recorded.
Green sandy GRAVEL (2 - 60 MM). Poorly sorted. Not Recorded.
Green sandy GRAVEL (2 - 60 MM). Poorly sorted. Not Recorded.
Not Logged GRAVEL (2 - 60 MM). Poorly sorted. Gravels are well-rounded. Not Recorded.

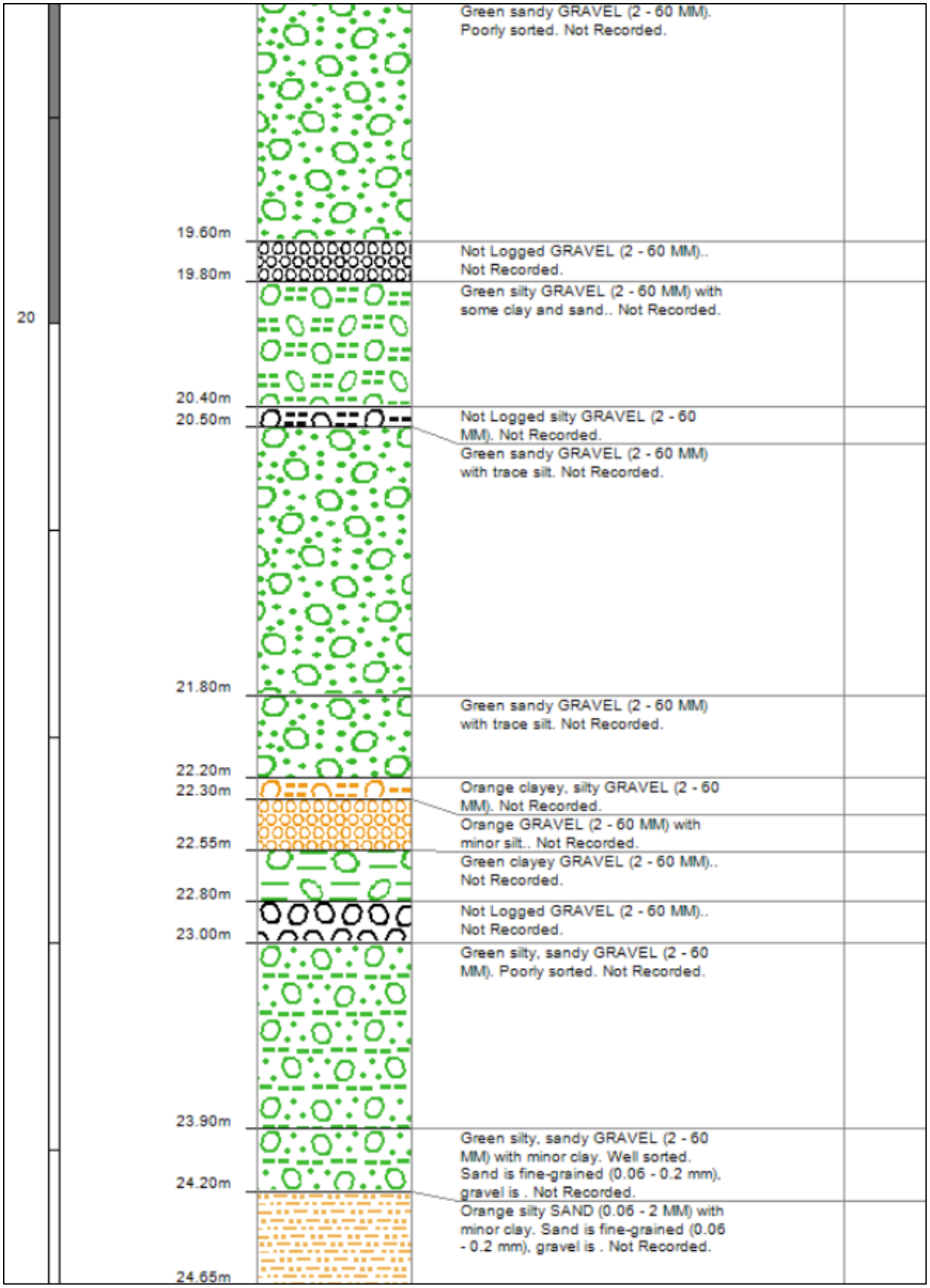
20
19.60m
19.80m
20.40m
20.50m
21.80m
22.20m
22.30m
22.55m
22.80m
23.00m
23.90m
24.20m
24.65m
Green sandy GRAVEL (2 - 60 MM). Poorly sorted. Not Recorded.
Not Logged GRAVEL (2 - 60 MM).. Not Recorded.
Green silty GRAVEL (2 - 60 MM) with some clay and sand.. Not Recorded.
Not Logged silty GRAVEL (2 - 60 MM). Not Recorded.
Green sandy GRAVEL (2 - 60 MM) with trace silt. Not Recorded.
Green sandy GRAVEL (2 - 60 MM) with trace silt. Not Recorded.
Orange clayey, silty GRAVEL (2 - 60 MM). Not Recorded.
Orange GRAVEL (2 - 60 MM) with minor silt.. Not Recorded.
Green clayey GRAVEL (2 - 60 MM).. Not Recorded.
Not Logged GRAVEL (2 - 60 MM).. Not Recorded.
Green silty, sandy GRAVEL (2 - 60 MM). Poorly sorted. Not Recorded.
Green silty, sandy GRAVEL (2 - 60 MM) with minor clay. Well sorted. Sand is fine-grained (0.06 - 0.2 mm), gravel is . Not Recorded.
Orange silty SAND (0.06 - 2 MM) with minor clay. Sand is fine-grained (0.06 - 0.2 mm), gravel is . Not Recorded.

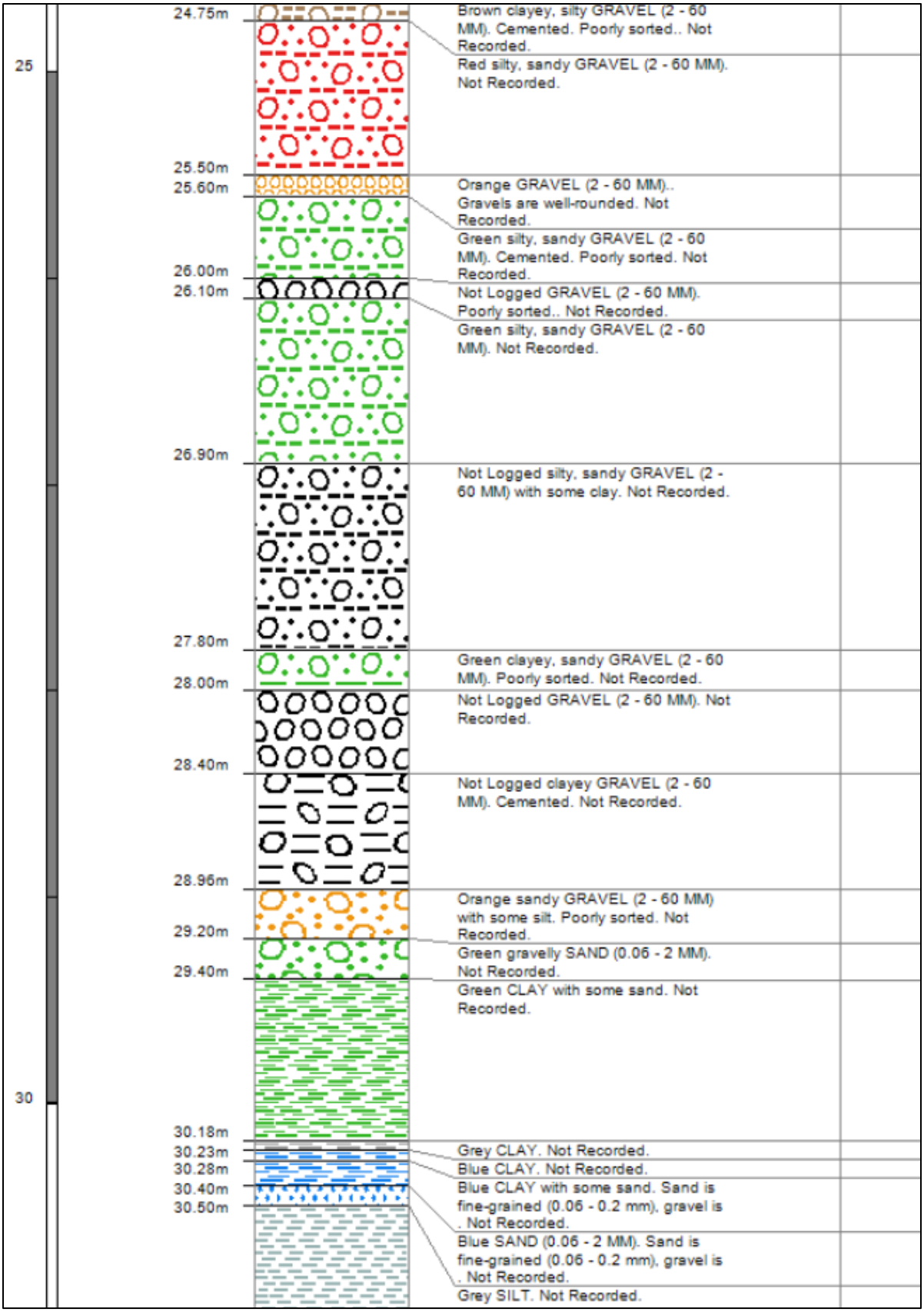
25
30
24.75m
Brown clayey, silty GRAVEL (2 - 60 MM). Cemented. Poorly sorted.. Not Recorded.
Red silty, sandy GRAVEL (2 - 60 MM). Not Recorded.
25.50m
25.60m
Orange GRAVEL (2 - 60 MM).. Gravels are well-rounded. Not Recorded.
Green silty, sandy GRAVEL (2 - 60 MM). Cemented. Poorly sorted. Not Recorded.
26.00m
26.10m
Not Logged GRAVEL (2 - 60 MM). Poorly sorted.. Not Recorded.
Green silty, sandy GRAVEL (2 - 60 MM). Not Recorded.
26.90m
Not Logged silty, sandy GRAVEL (2 - 60 MM) with some clay. Not Recorded.
27.80m
Green clayey, sandy GRAVEL (2 - 60 MM). Poorly sorted. Not Recorded.
28.00m
Not Logged GRAVEL (2 - 60 MM). Not Recorded.
28.40m
Not Logged clayey GRAVEL (2 - 60 MM). Cemented. Not Recorded.
28.96m
Orange sandy GRAVEL (2 - 60 MM) with some silt. Poorly sorted. Not Recorded.
29.20m
Green gravelly SAND (0.06 - 2 MM). Not Recorded.
29.40m
Green CLAY with some sand. Not Recorded.
30.18m
30.23m
Grey CLAY. Not Recorded.
30.28m
Blue CLAY. Not Recorded.
30.40m
Blue CLAY with some sand. Sand is fine-grained (0.06 - 0.2 mm), gravel is . Not Recorded.
30.50m
Blue SAND (0.06 - 2 MM). Sand is fine-grained (0.06 - 0.2 mm), gravel is . Not Recorded.
Grey SILT. Not Recorded.

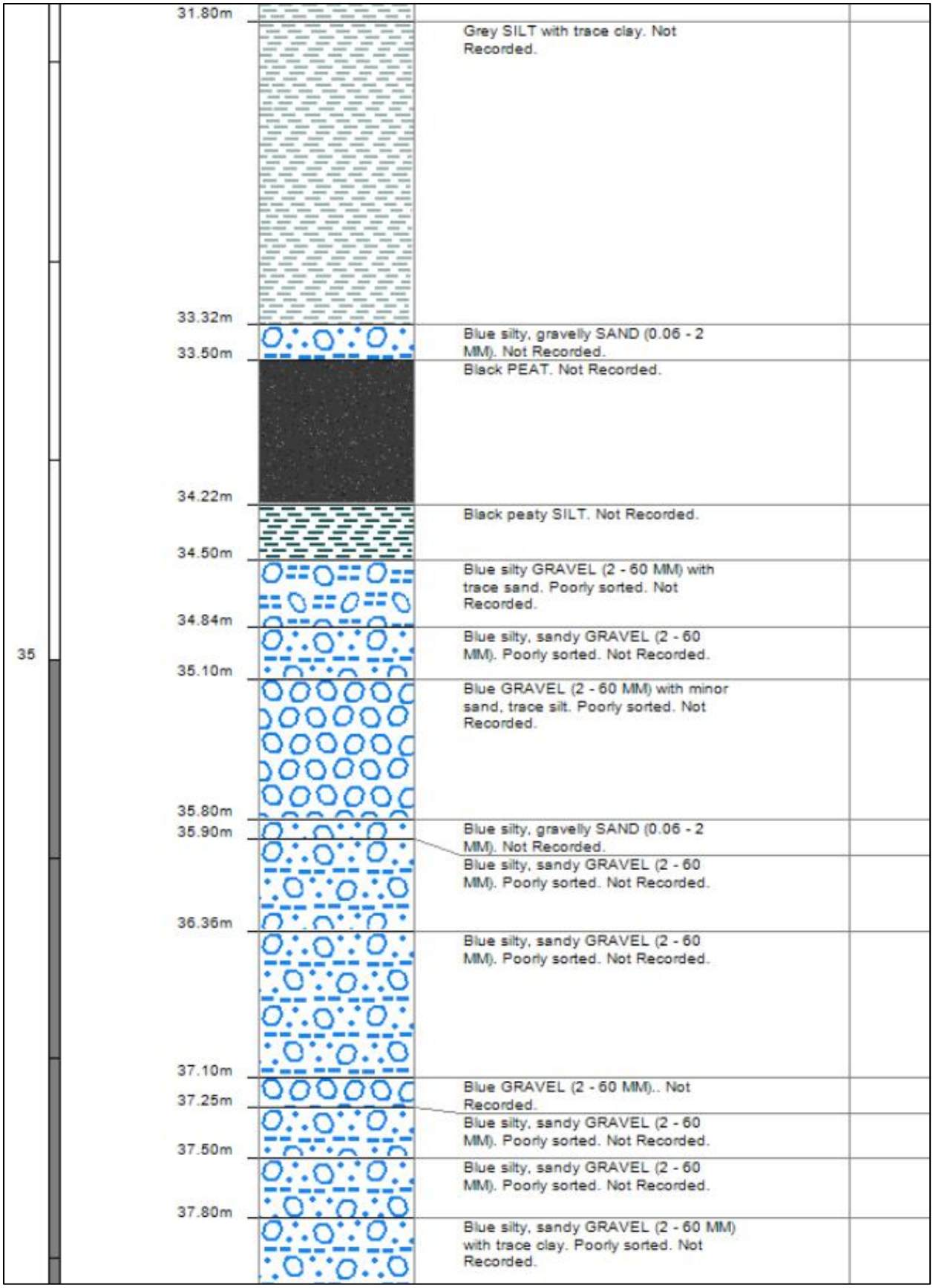
35
31.80m
Grey SILT with trace clay. Not Recorded.
33.32m
Blue silty, gravelly SAND (0.06 - 2 MM). Not Recorded.
33.50m
Black PEAT. Not Recorded.
34.22m
Black peaty SILT. Not Recorded.
34.50m
Blue silty GRAVEL (2 - 60 MM) with trace sand. Poorly sorted. Not Recorded.
34.84m
Blue silty, sandy GRAVEL (2 - 60 MM). Poorly sorted. Not Recorded.
35.10m
Blue GRAVEL (2 - 60 MM) with minor sand, trace silt. Poorly sorted. Not Recorded.
35.80m
35.90m
Blue silty, gravelly SAND (0.06 - 2 MM). Not Recorded.
Blue silty, sandy GRAVEL (2 - 60 MM). Poorly sorted. Not Recorded.
36.36m
Blue silty, sandy GRAVEL (2 - 60 MM). Poorly sorted. Not Recorded.
37.10m
37.25m
Blue GRAVEL (2 - 60 MM).. Not Recorded.
Blue silty, sandy GRAVEL (2 - 60 MM). Poorly sorted. Not Recorded.
37.50m
Blue silty, sandy GRAVEL (2 - 60 MM). Poorly sorted. Not Recorded.
37.80m
Blue silty, sandy GRAVEL (2 - 60 MM) with trace clay. Poorly sorted. Not Recorded.

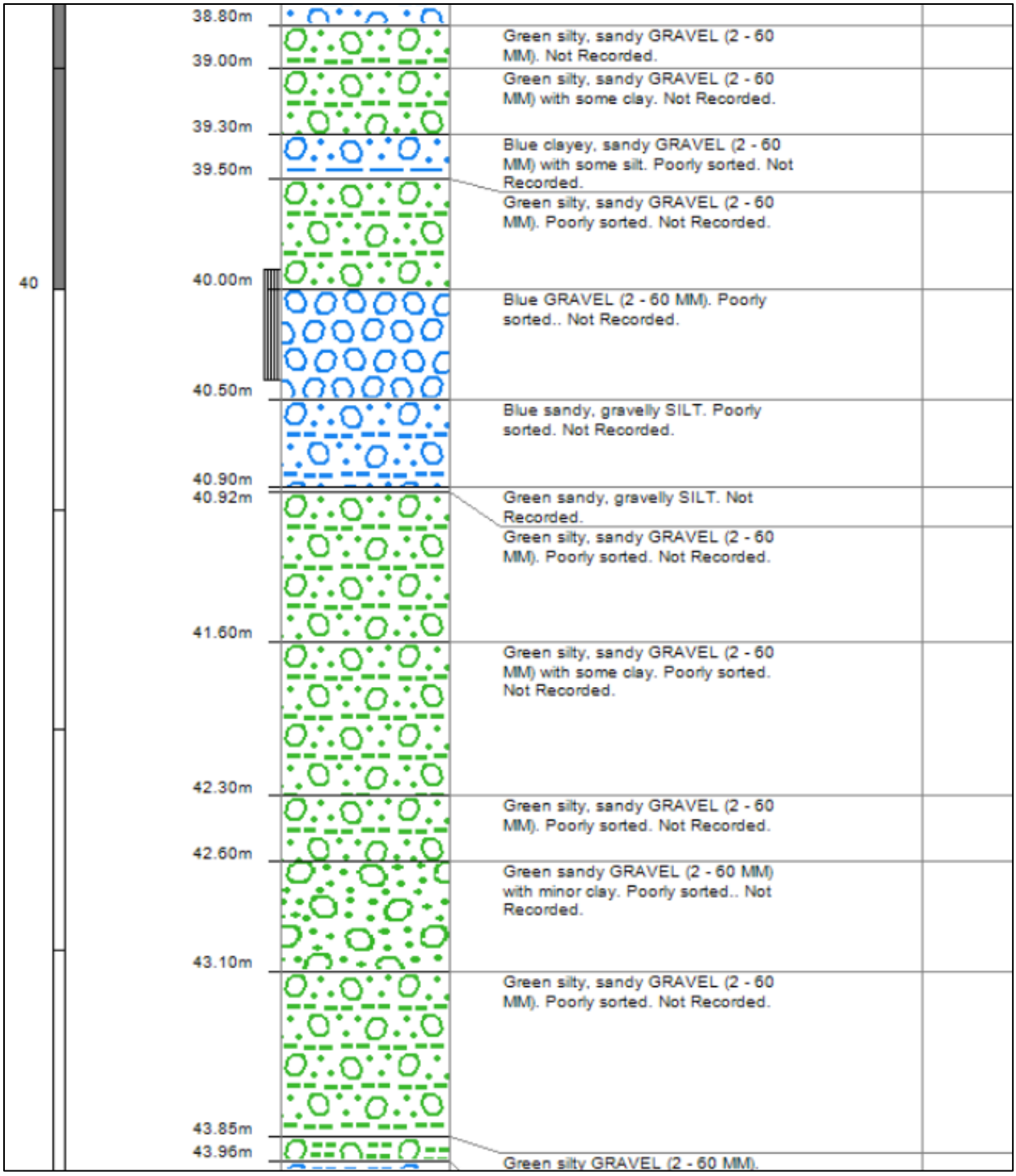

Figure A-2. Bore log for AT1 (Environment Canterbury, 2016)

Appendix B: Materials used for particle size distribution data collection

Table B-1. Particle size distribution analysis equipment

Wet sieving and dry sieving equipment	Hydrometer test equipment
Sediment sieves ranging from 64 mm to 63 µm	Graduated cylinders
Catch pan	Stop watches
Scales	Hydrometer – Type 151H
Large sink	Deionised water
Water	Squirt bottle
Drying oven, set to ~100 ˚C	Thermometer
Metal bowls	Rubber bung
Sieve brush	Sodium hexametaphosphate
	Magnetic mixer
	Funnel
	Beakers (250ml)
	Aluminium foil trays
	Drying oven, set to ~100 ˚C
	Temperature controlled room (20 ˚C)

Appendix C: Analytical model linear trendline fitting

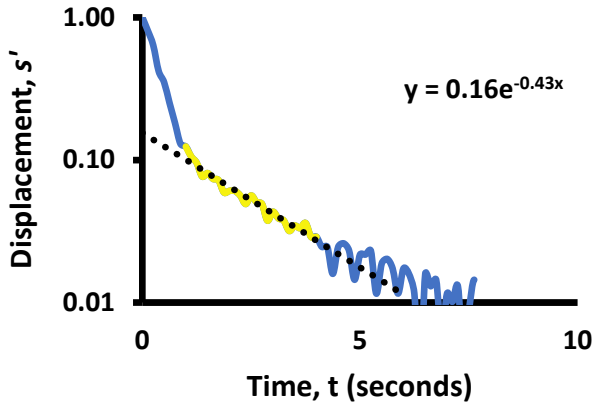

Figure C-1. NB3 trendline fitting (test 1)

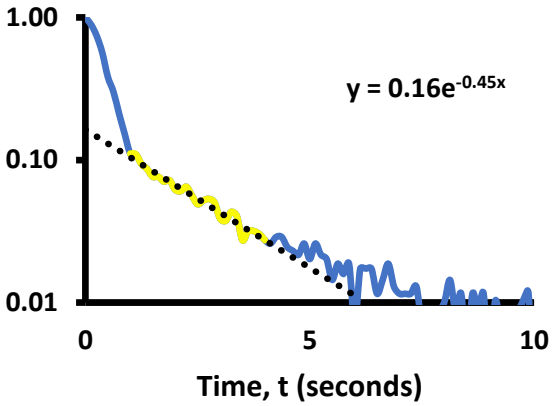

Figure C-2. NB3 trendline fitting (test 2)

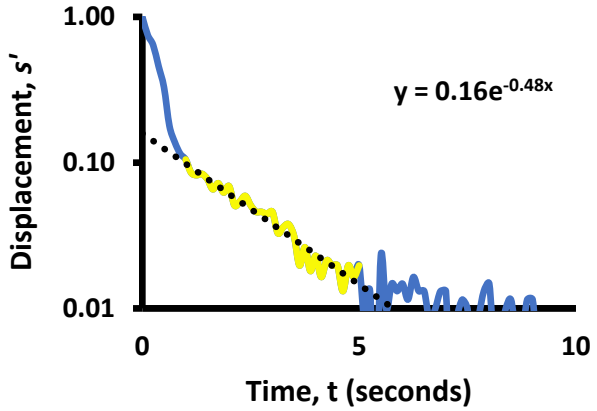

Figure C-3. NB3 trendline fitting (test 3)

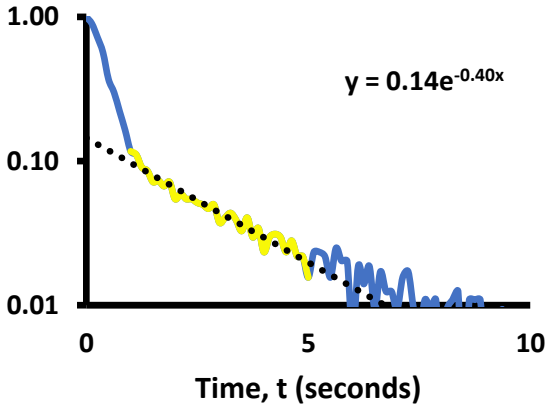

Figure C-4. NB3 trendline fitting (test 4)

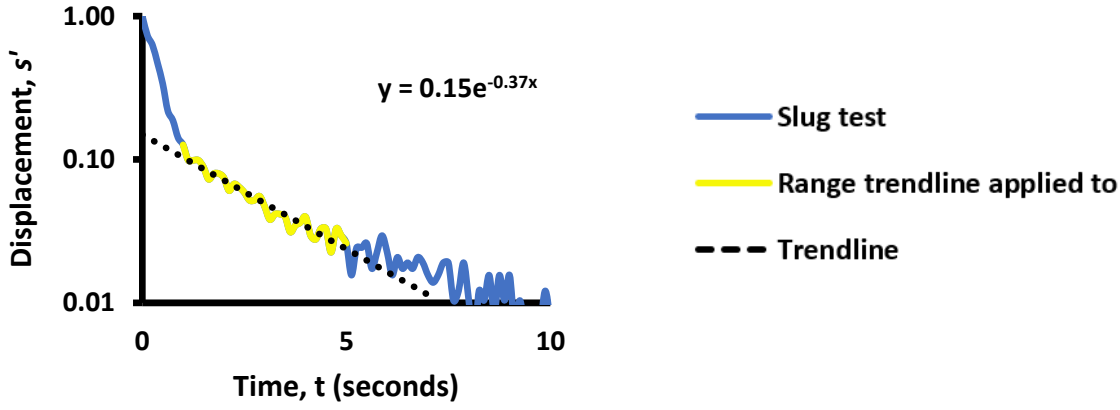

Figure C-5. NB3 trendline fitting (test 5)

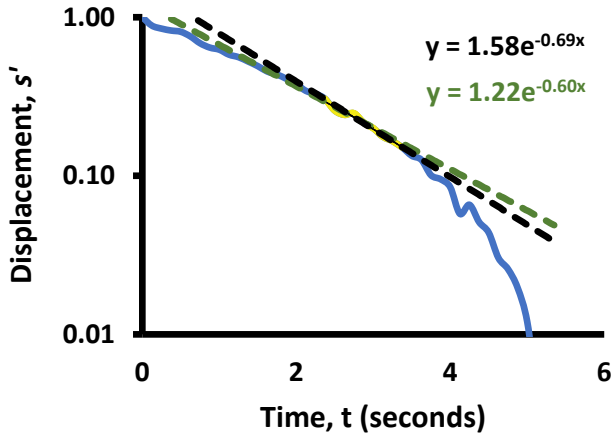

Figure C-6. NB2 trendline fitting (test 1)

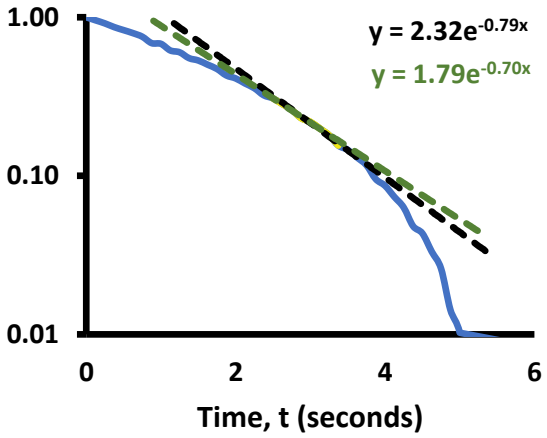

Figure C-7. NB2 trendline fitting (test 2)

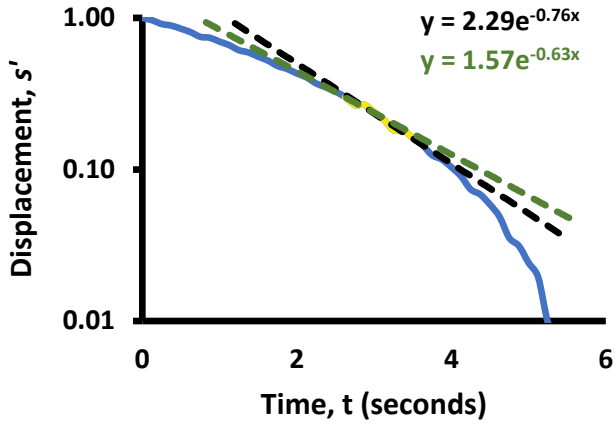

Figure C-8. NB2 trendline fitting (test 3)

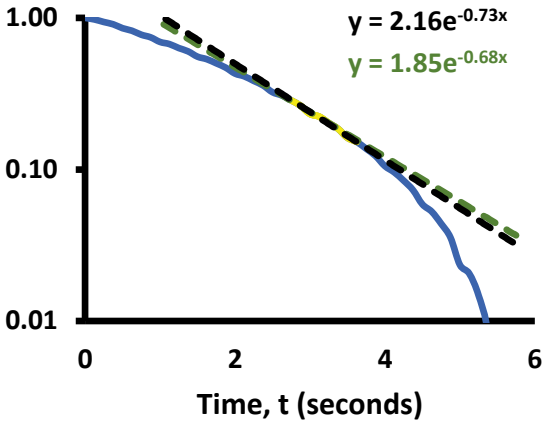

Figure C-9. NB2 trendline fitting (test4)

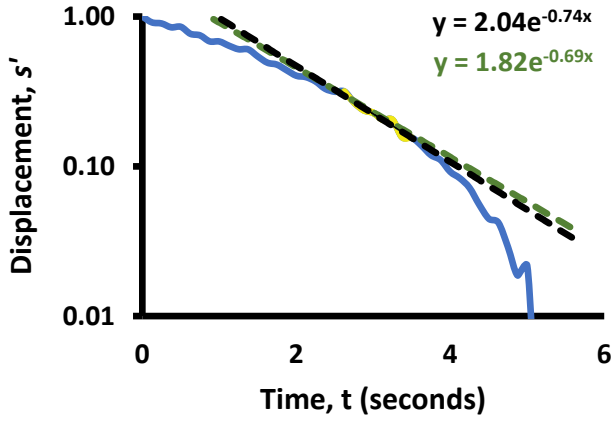

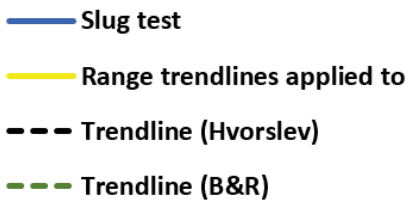

Figure C-10. NB2 trendline fitting (test 5)

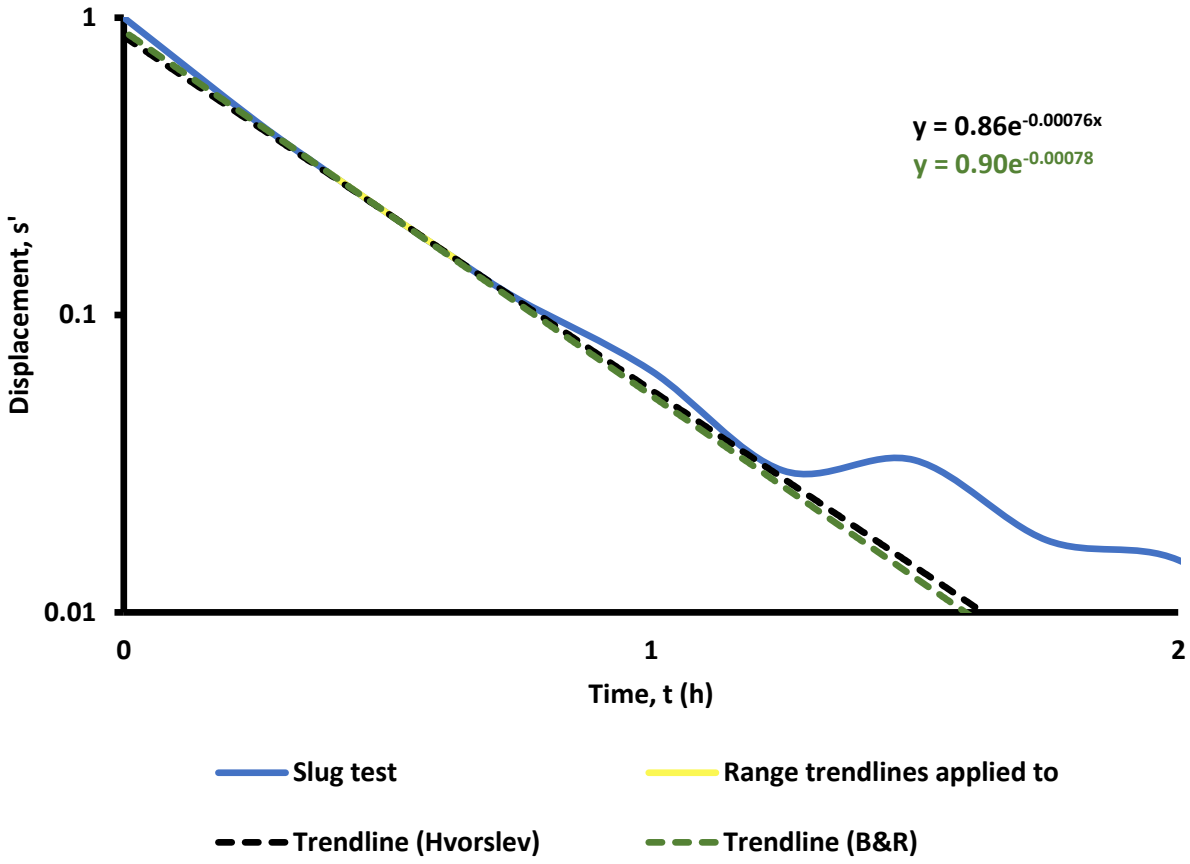

Figure C-11. NB5 trendline fitting (only test)

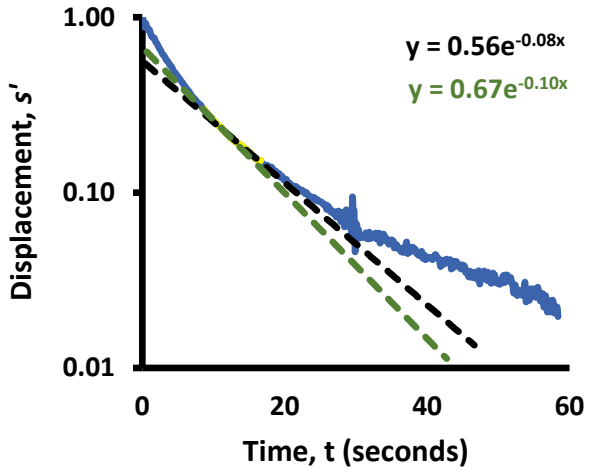

Figure C-12. NB1 trendline fitting (test 1)

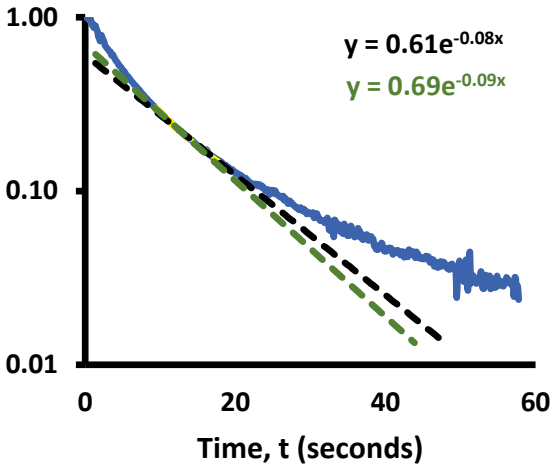

Figure C-13. NB1 trendline fitting (test 2)

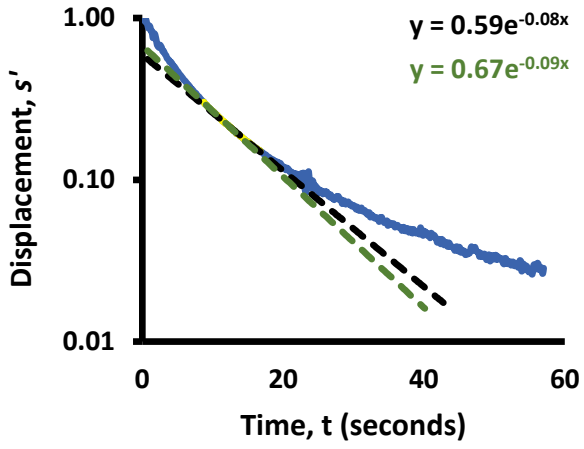

Figure C-14. NB1 trendline fitting (test 3)

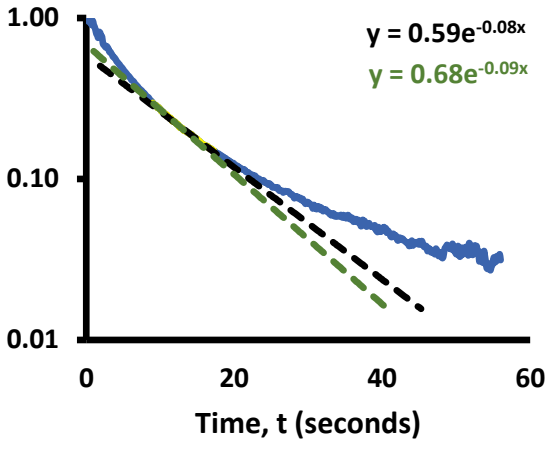

Figure C-15. NB1 trendline fitting (test 4)

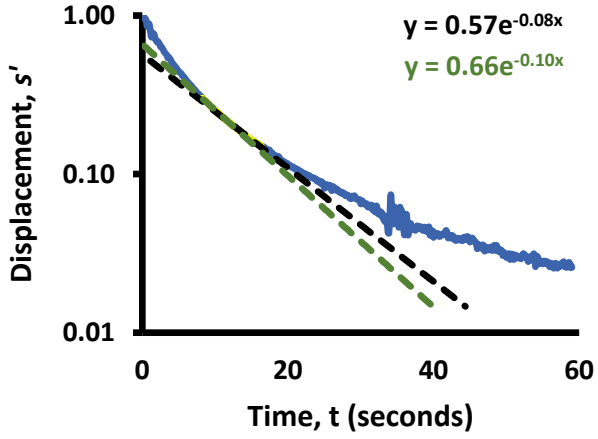

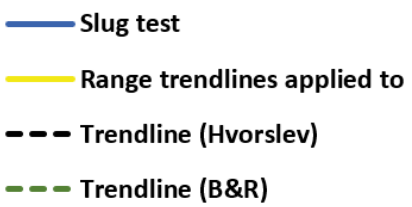

Figure C-16. NB1 trendline fitting (test 5)

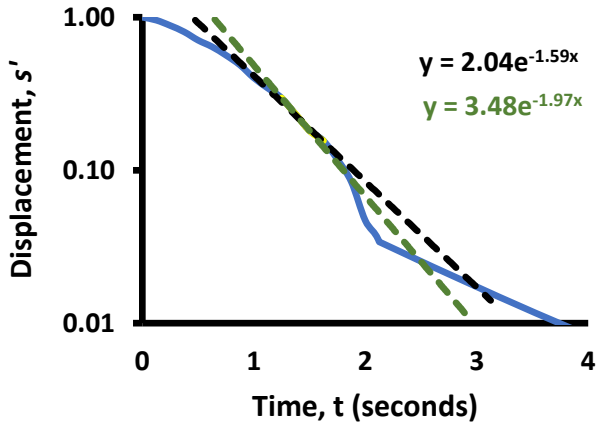

Figure C-17. AT4 trendline fitting (test 1)

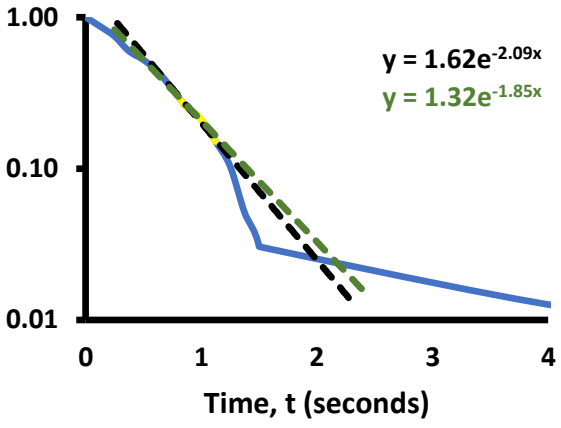

Figure C-18. AT4 trendline fitting (test 2)

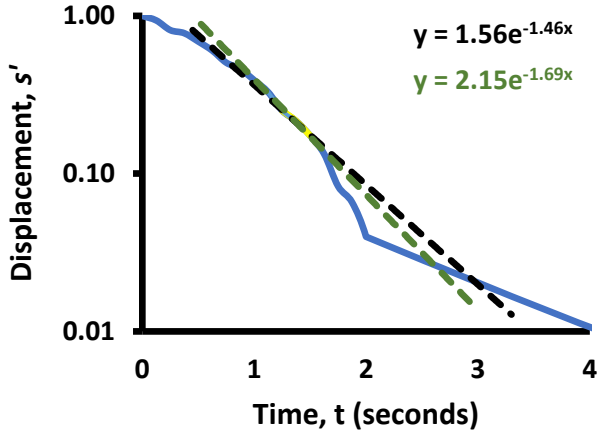

Figure C-19. AT4 trendline fitting (test 3)

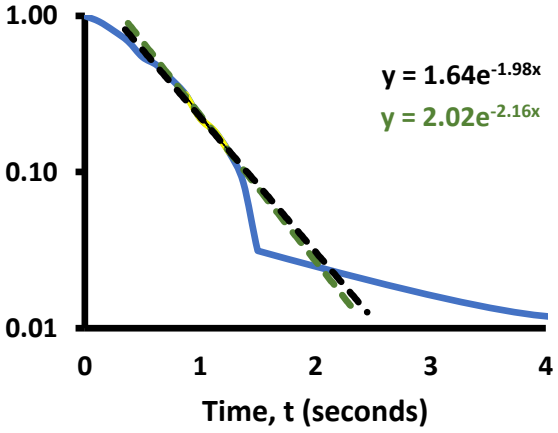

Figure C-20. AT4 trendline fitting (test 4)

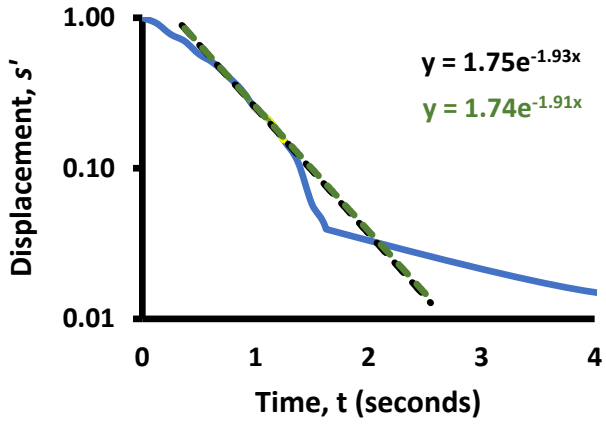

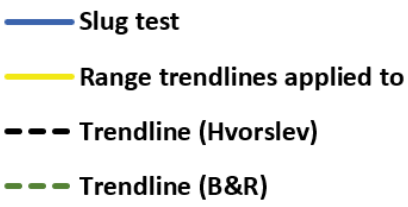

Figure C-21. AT4 trendline fitting (test 5)

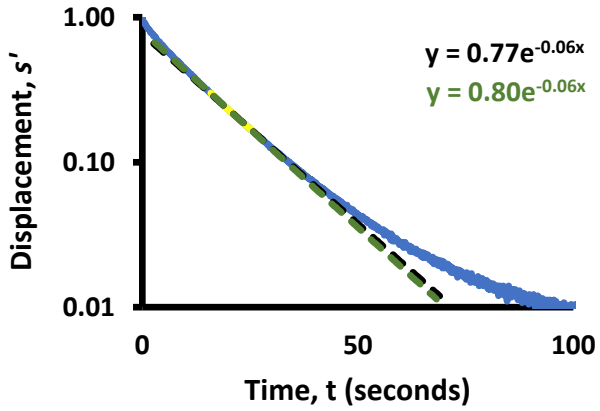

Figure C-22. AT3 trendline fitting (test 1)

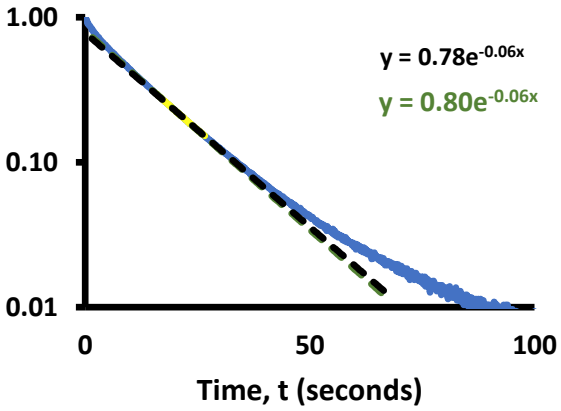

Figure C-23. AT3 trendline fitting (test 2)

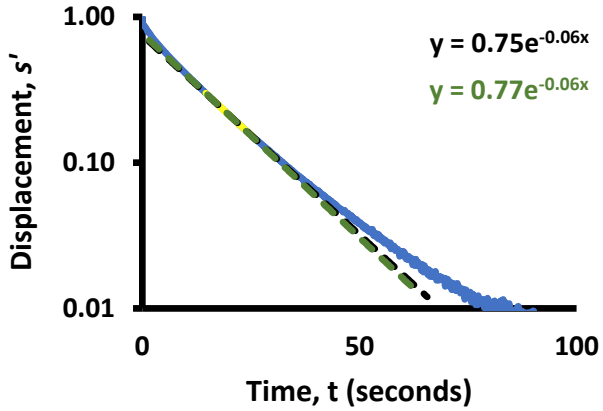

Figure C-24. AT3 trendline fitting (test 3)

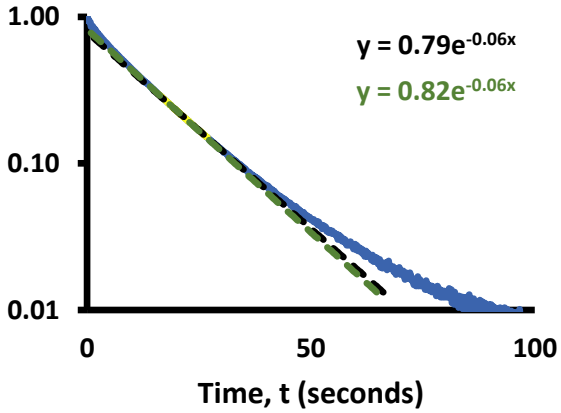

Figure C-25. AT3 trendline fitting (test 4)

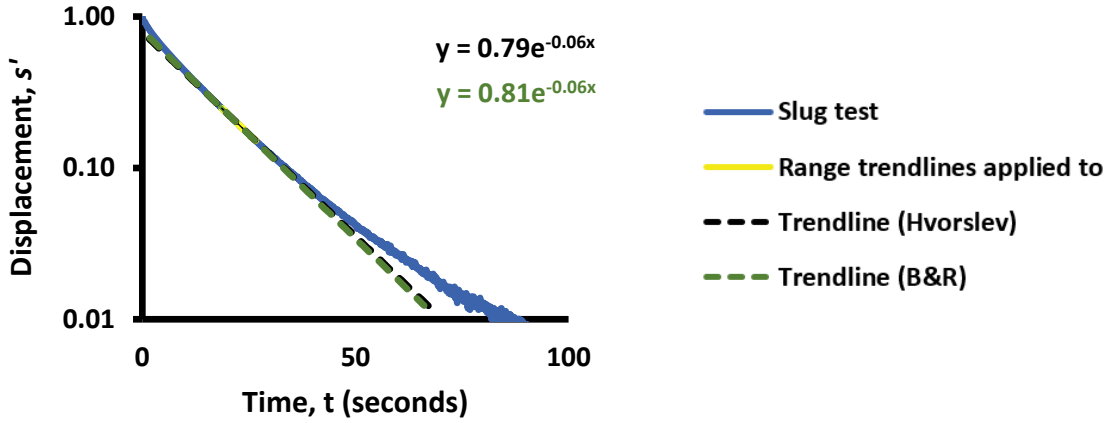

Figure C-26. AT3 trendline fitting (test 5)

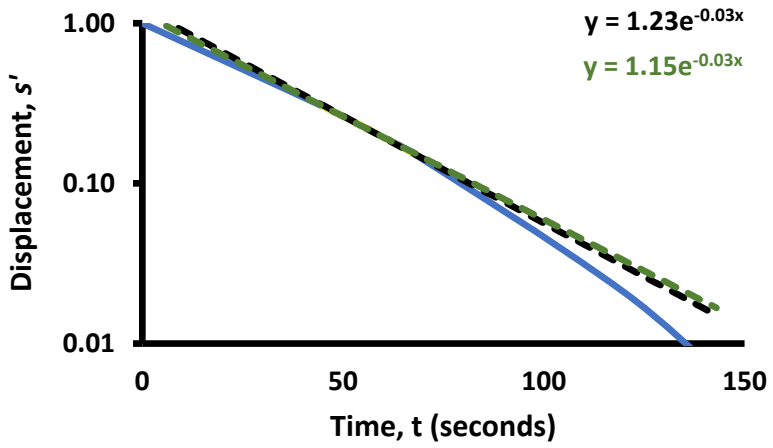

Figure C-27. AT2 trendline fitting (test 1)

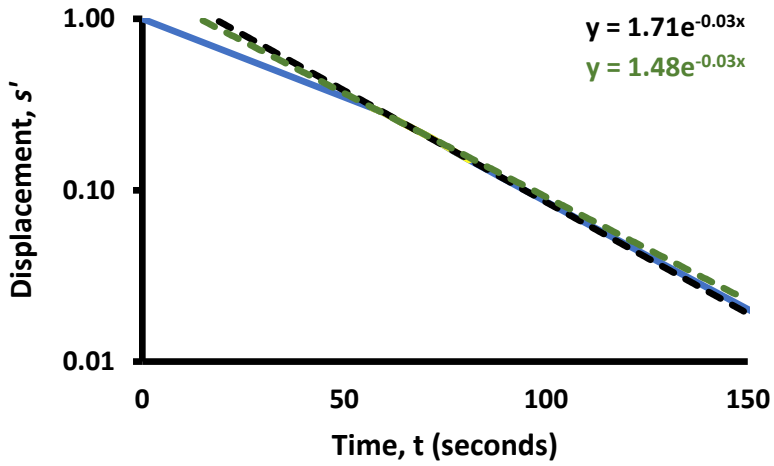

Figure C-28. AT2 trendline fitting (test 2)

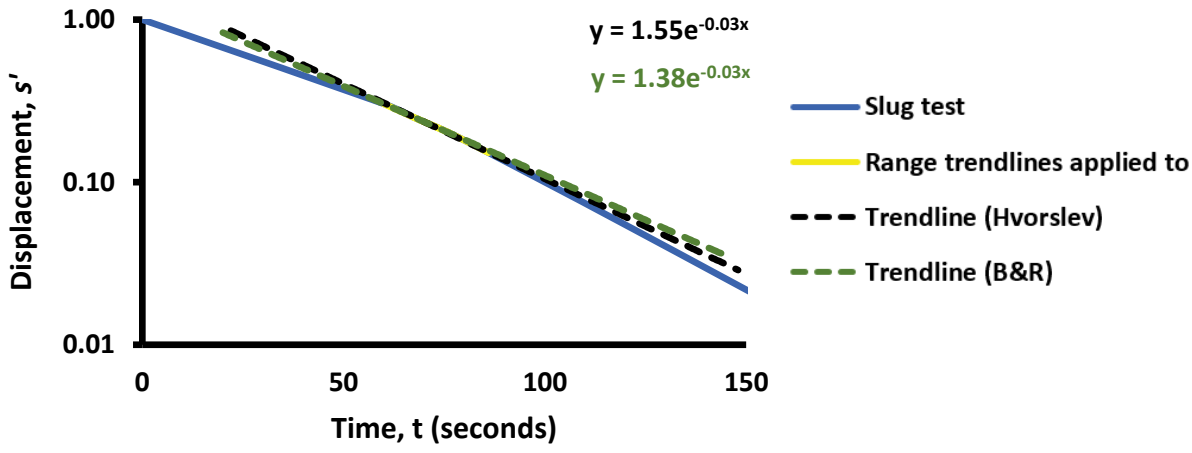

Figure C-29. AT2 trendline fitting (test 3)

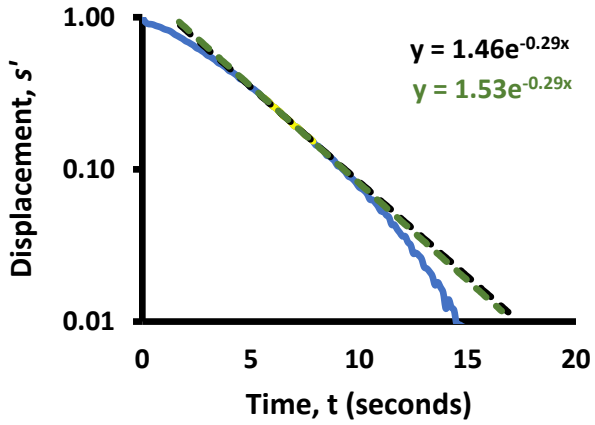

Figure C-30. AT1 trendline fitting (test 1)

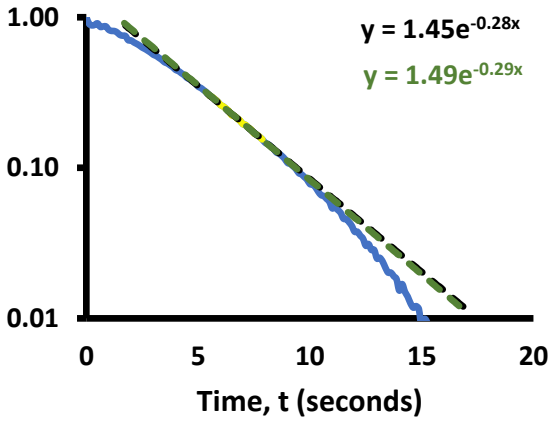

Figure C-31. AT1 trendline fitting (test 2)

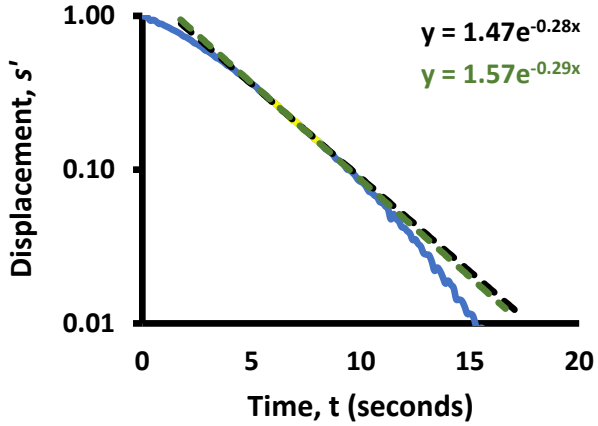

Figure C-32. AT1 trendline fitting (test 3)

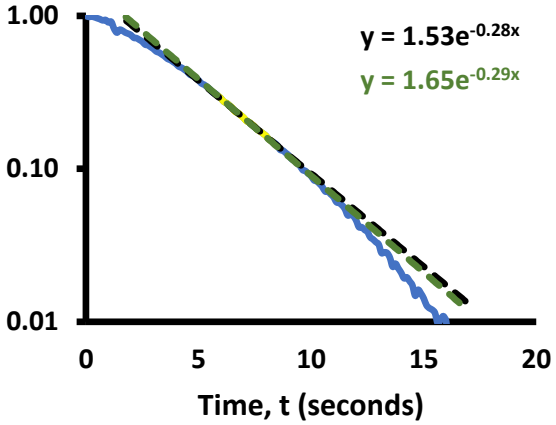

Figure C-33. AT1 trendline fitting (test 4)

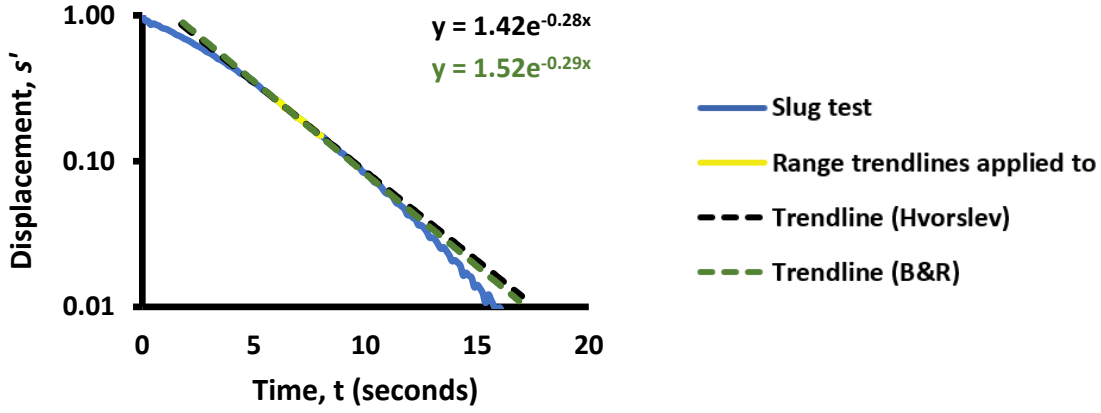

Figure C-34. AT1 trendline fitting (test 5)

Appendix D: Numerical model inverse matching

Tram Road wells

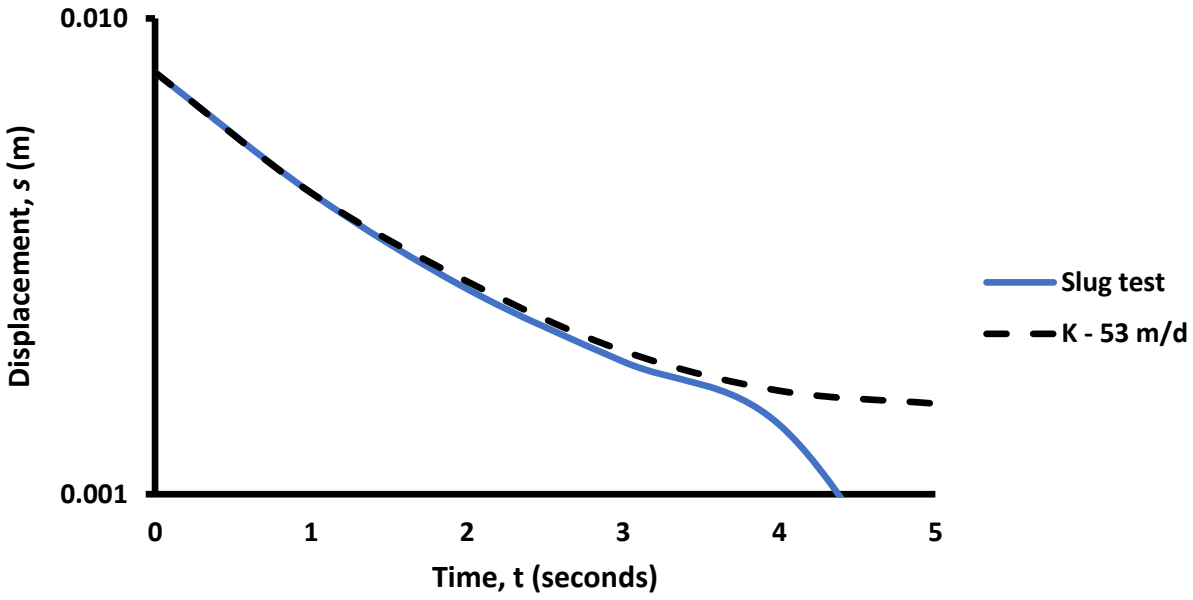

Figure D-1. NB3 curve matching

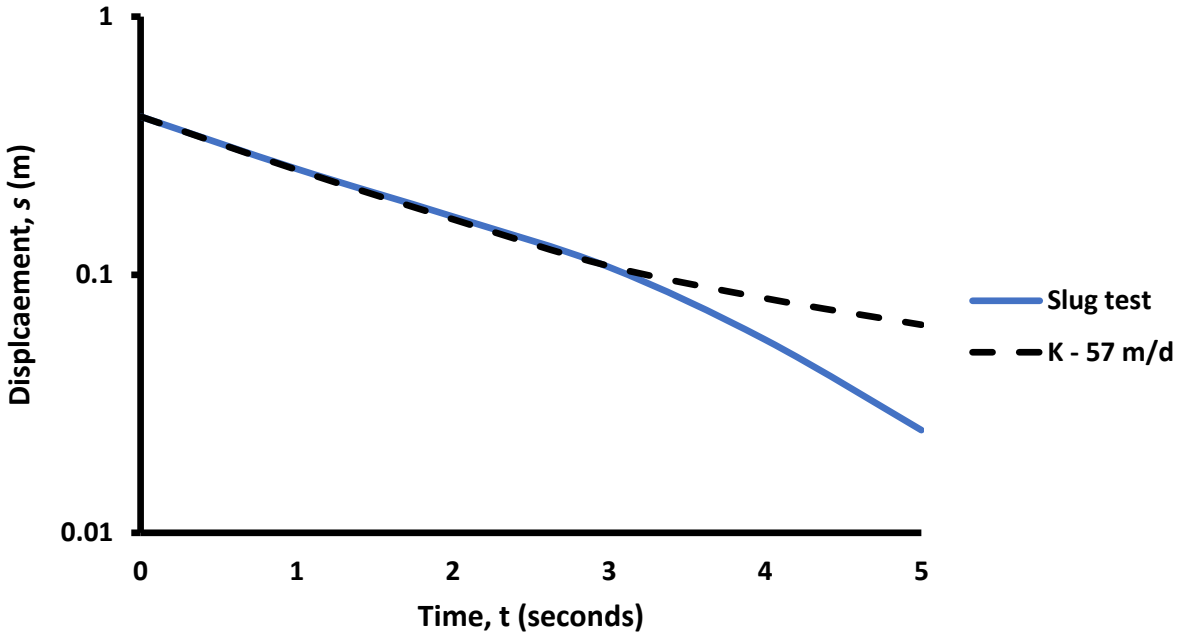

Figure D-2. NB2 curve matching

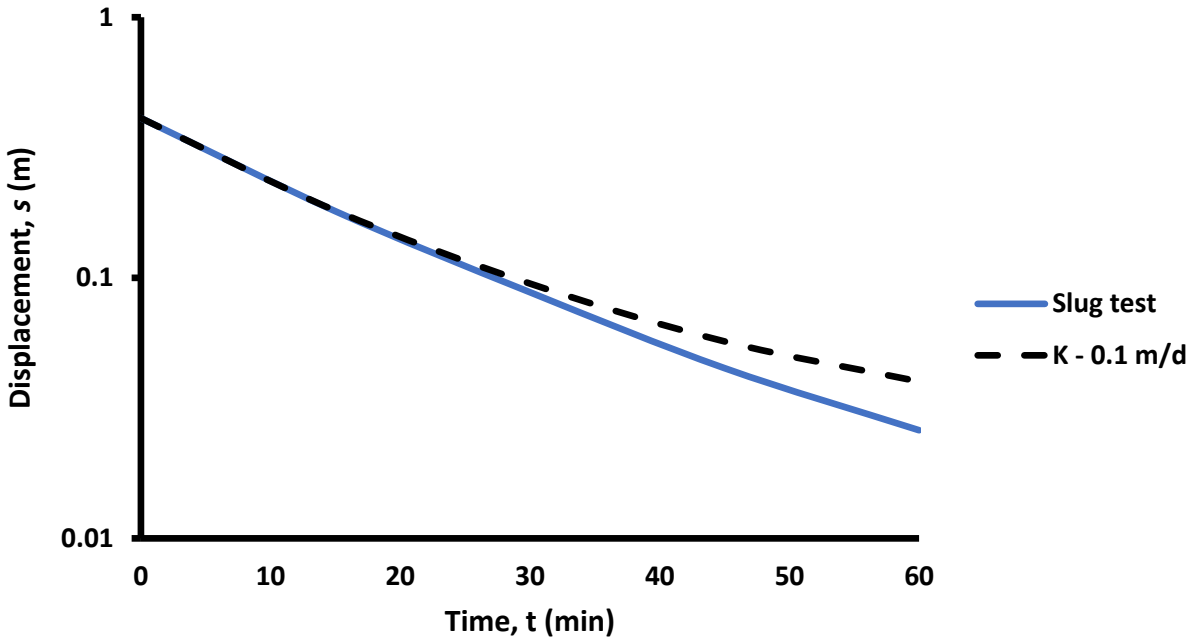

Figure D-3. NB5 curve matching

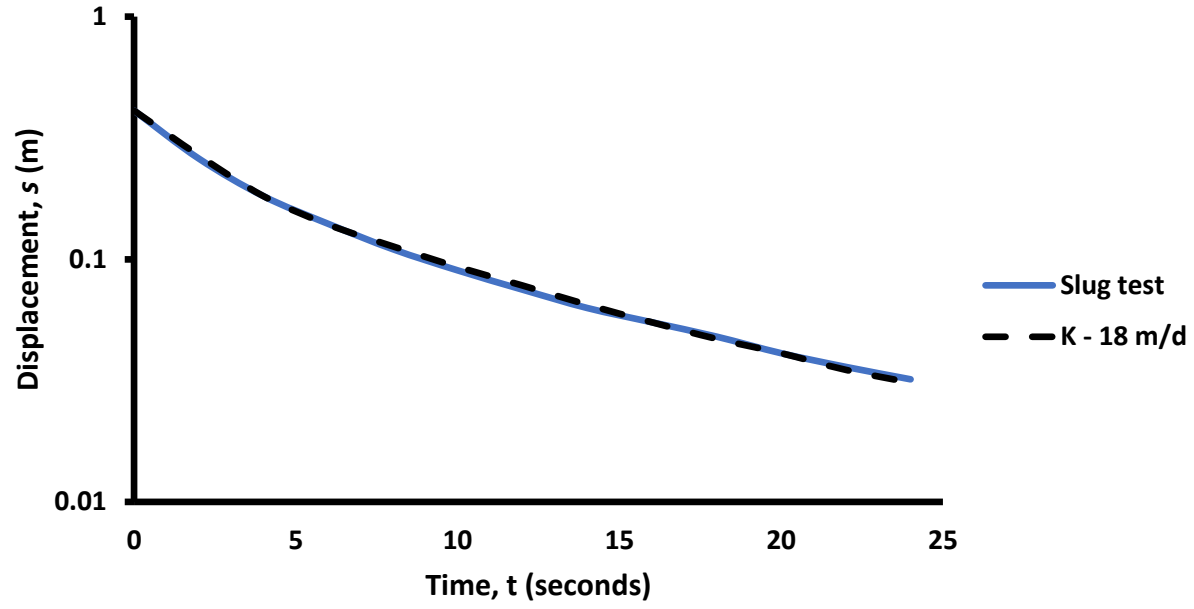

Figure D-4. NB1 curve matching

Adderley Terrace wells

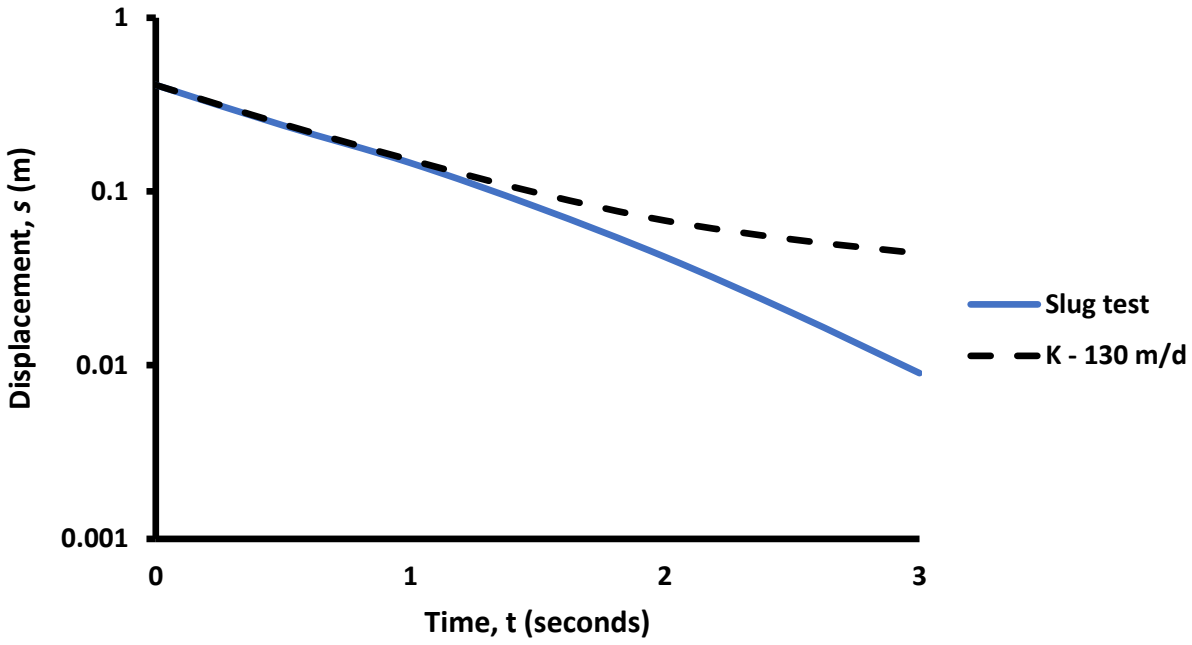

Figure D-5. AT4 curve matching

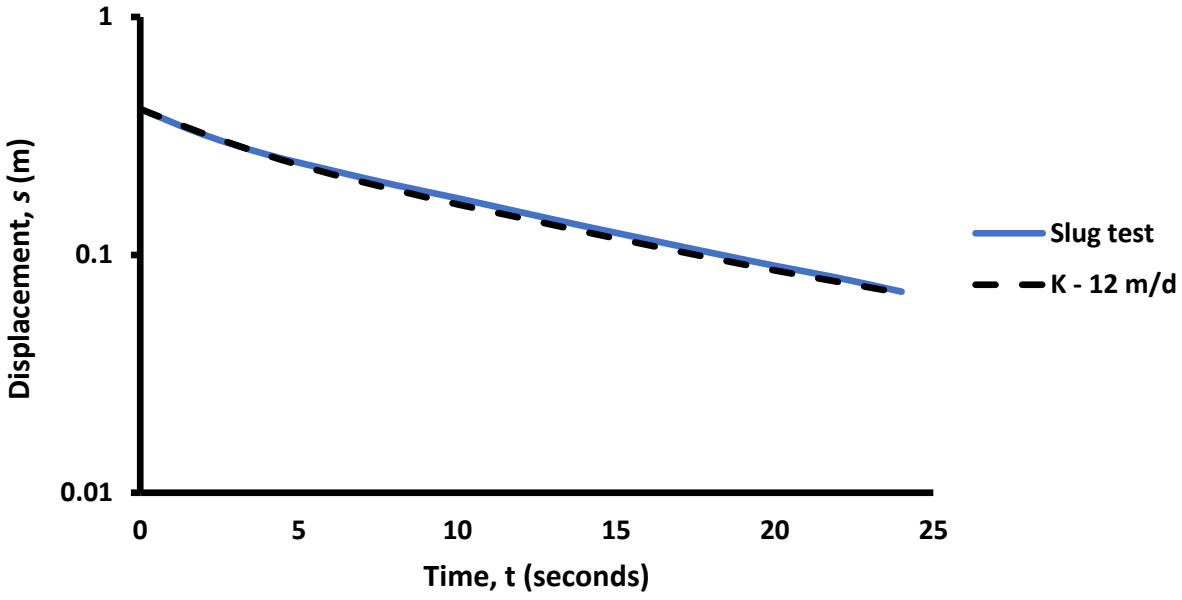

Figure D-6. AT3 curve matching

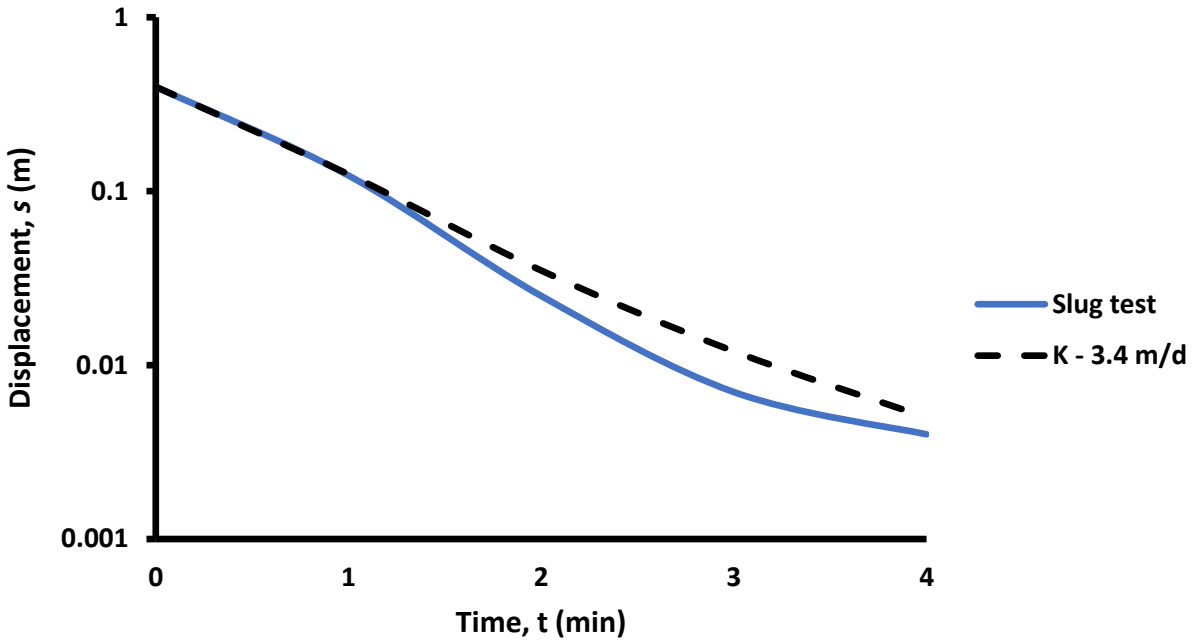

Figure D-7. AT2 curve matching

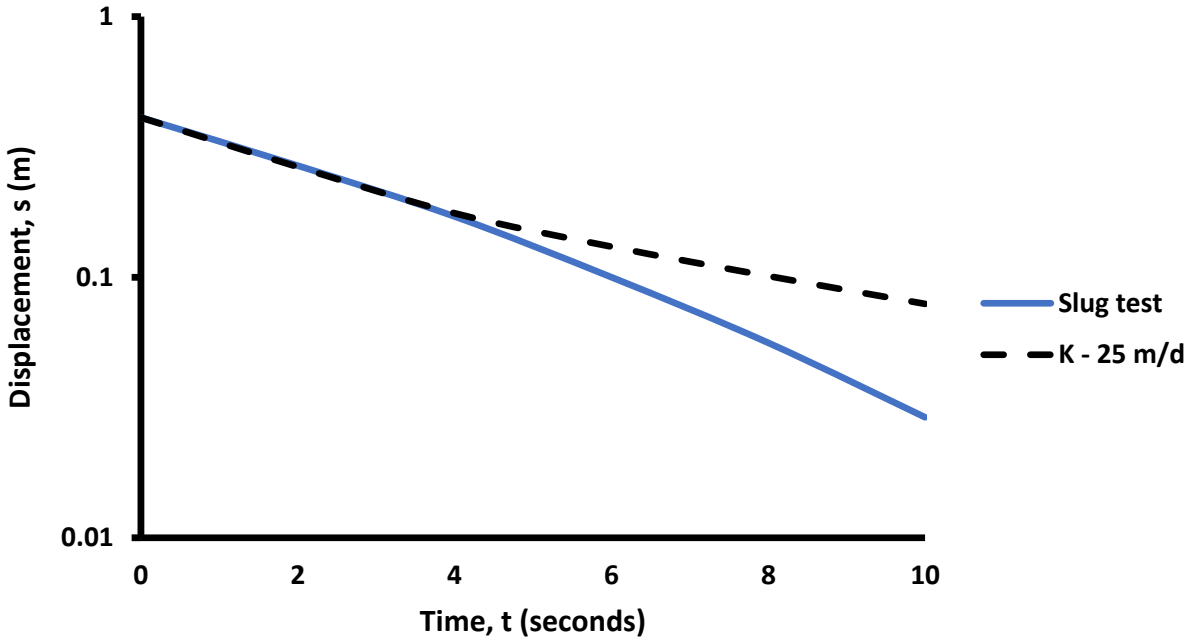

Figure D-8. AT1 curve matching